EMU Notes in Mineralogy, Vol. 1 (1997), Chapter 5, 373–429

Structural aspects of oxide and oxysalt minerals

Frank C. Hawthorne*

Department of Geological Sciences, University of Manitoba,
Winnipeg, Manitoba, Canada R3T 2N2

Introduction

The structures and chemistry of the oxide and oxysalt minerals are impressive in both their complexity and diversity, and it can be reasonably asserted that our understanding of these aspects lags far behind our experimental capabilities for their characterization. Nevertheless, there are some empirical rules that (sometimes weakly) govern the constitution of these minerals, rules that date back to early work on the modern electronic theory of valence (Lewis, 1923) and the structure of crystals. The most rigorous rule is that of electroneutrality: the sum of the formal charges of all the ions in a crystal is zero. Other rules grew out of observations on a few mineral and inorganic structures, and various ideas emerged during the 1920s: that atoms have a specific size, tables of atomic and ionic radii, the idea of coordination number, considering structures as polymerizations of coordination polyhedra. These ideas were refined by Pauling (1929, 1960) who synthesized them into his well-known rules for the behaviour of 'complex ionic crystals.' Some aspects of these ideas have been extensively developed up to the present time. There are now available tables of accurate empirical 'ionic' radii (Shannon, 1976) whereby mean interatomic distances for specific coordinations can be predicted typically to within ~0.01 Å. Individual bond lengths can be predicted *via* various developments of Pauling's second rule (*e.g.*, Baur, 1970, 1971), and the relative strengths of bonds can be calculated (Brown & Shannon, 1973) given the observed bond lengths in a structure. Thus we can currently predict various geometrical aspects of a crystal structure quite accurately, provided that we know the connectivity (often called the topology) of the chemical bonds. This particular statement brings into focus our principal area of ignorance concerning crystals, particularly the ~2000 oxide and oxysalt minerals: *we still have very little understanding of the bond topology of crystals*, as distinct from their geometrical features which we can usually predict with reasonable accuracy.

Crystal structures as graphs

Crystal structures are usually represented in the following ways:

(1) unit cell and symmetry information, plus a table of atom coordinates;
(2) a structure drawing that is usually based on assumptions as to which atoms are bonded together.

---

* E-mail address: frank_hawthorne@umanitoba.ca

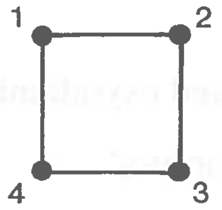

GRAPH

$$\begin{array}{c|cccc} & 1 & 2 & 3 & 4 \\ \hline 1 & - & 1 & 0 & 1 \\ 2 & 1 & - & 1 & 0 \\ 3 & 0 & 1 & - & 1 \\ 4 & 1 & 0 & 1 & - \end{array}$$

ADJACENCY MATRIX

Fig. 1. A hypothetical molecule consisting of four atoms (●) joined by chemical bonds (—); as drawn, this is a labelled graph (left). An algebraic representation of this graph is the adjacency matrix (right).

The numerical information contained in (1) can be used for various structure-property calculations, provided that we have sufficient computing power and appropriate potentials or wave functions; the problem is that this representation offers little intuitive feel for the factors controlling structural stability. The graphical representation of (2) can be used to make qualitative arguments (*e.g. à la* Pauling's rules), but we do not have a quantitative expression of the important features of a structure. Graph theory offers a potential solution to some of these problems.

A graphical representation of a simple structure is shown in Fig. 1. The black circles represent four atoms and the lines represent chemical bonds between these atoms. This representation, a set of points joined by lines, is the visual representation of a graph. Formally, we may define a *graph* as a non-empty set of elements, $V(G)$, called vertices, and a non-empty set of unordered pairs of these vertices, $E(G)$, called edges. If we let the vertices of the graph represent atoms (as in Fig. 1) or groups of atoms, and the edges of the graph represent chemical bonds (or linkages between groups of atoms), then our graph may represent a molecule. We can introduce an algebraic representation of this graph in the form of a matrix (Fig. 1). Each column and row of the matrix is associated with a specific (labelled) vertex, and the corresponding matrix entries denote whether or not two vertices are adjacent, *i.e.* joined by an edge. If the edges of the graph are weighted in some form such that the matrix elements denote this weighting, then this matrix is called the *adjacency matrix*. The adjacency matrix is thus a digital representation of the graph, which is in turn an analogue representation of the structure. The adjacency matrix does not preserve the geometrical features of the structure; information such as bond angles is lost. However, it does preserve information concerning the *topological* features of the bond network, with the possibility of carrying additional information concerning the strengths (or orders) of the chemical bonds.

The argument developed above has introduced a way of quantifying the topological aspects of the bond network of a group of atoms. It remains to determine the significance of this information. To do this, we now examine some of the connections that have recently developed between contemporary theories of chemical bonding and topological (or graphical) aspects of structure. I shall only sketch the outlines of the arguments, except where they serve to emphasize the equivalence or similarity between energetics of bonding and topological aspects of structure. Excellent reviews are given by Burdett (1980), Albright *et al.* (1985) and Hoffmann (1988).

Topological aspects of molecular-orbital theory

Molecules

A simple approach to the electronic structure and properties of molecules is to consider a molecule as the sum of the electronic properties of its constituent atoms, as modified by the interaction between these atoms. The most straightforward way of doing this is to construct the molecular-orbital wave-function from a *L*inear *C*ombination of *A*tomic *O*rbitals, the LCAO method of the chemist and the tight-binding method of the physicist. These wave-functions are eigenstates of some (unspecified) effective one-electron Hamiltonian, H^{eff}, that we may write as

$$H^{eff}\psi = E\psi \tag{1}$$

where E is the energy (eigenvalue) associated with ψ, and the LCAO molecular-orbital wave function is written as

$$\psi = \sum_i c_i \phi_i \tag{2}$$

where $\{\phi_i\}$ are the valence orbitals of the atoms of the molecule, and c_i is the contribution of a particular atomic orbital to a particular molecular orbital.

The total electron-energy of the state described by this wave function may be written as

$$E = \frac{\int \psi^* H^{eff} \psi dT}{\int \psi^* \psi dT} = \frac{< \psi | H^{eff} | \psi >}{< \psi | \psi >} \tag{3}$$

in which the integration is over all space. Substitution of (2) into (3) gives

$$E = \frac{\sum_i \sum_j c_i c_j \phi_i < H^{eff} \phi >}{\sum_i \sum_j c_i c_j < \phi_i | \phi_j >} \tag{4}$$

This equation may be simplified by the following substitutions and approximations:

(a) $<\phi_i|\phi_j>$ is the overlap integral between atomic orbitals on different atoms; we will denote this as S_{ij}, and note that it is always ≤ 1; when $i = j$, $<\phi i|\phi j> = 1$ for a normalized (atomic) basis-set of orbitals;

(b) we write $<\phi_i|H^{eff}|\phi_i> = H_{ii}$; this is the Coulomb integral, and represents the energy of an electron in orbital ϕ_i; it can be approximated by the orbital ionization potential;

(c) we write $<\phi_i|H^{eff}|\phi_j> = H_{ij}$; it represents the interaction between orbitals ϕ_i and ϕ_j, and is the resonance integral; it can be approximated by the Wolfsberg-Helmholz relationship $H_{ij} = KS_{ij}(H_{ii} + H_{jj})/2$ (Gibbs *et al.*, 1972).

The molecular-orbital energies may be obtained from equation (4) *via* the variational theorem, minimizing the energy with respect to the coefficients c_i. The most

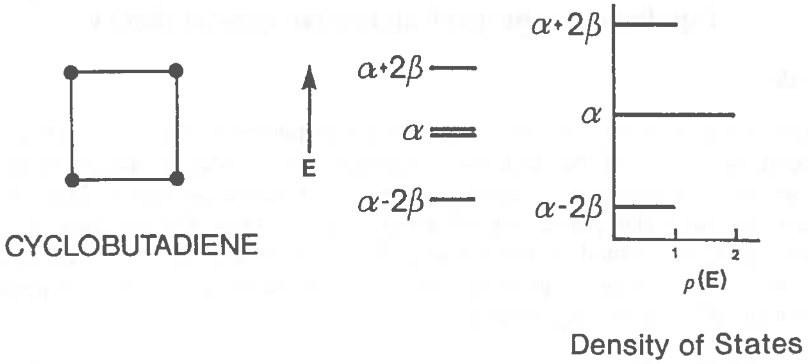

Fig. 2. The cyclobutadiene molecule (left); to the right are the four roots of equation (6), the electron energy levels expressed in the usual form (centre) and in a density-of-states form (right).

familiar form is the following *secular determinant* equation, the eigenvalues (roots) of which give the molecular-orbital energy-levels:

$$|H_{ij} - S_{ij}E| = 0 \qquad (5).$$

The Hückel approximation (Trinajstic, 1983) most directly shows the topological content of this approach. In the Hückel approximation, all H_{ii} values for the pπ orbitals are set equal to α, all H_{ij} are set equal to β, and all S_{ij} $(i \neq j)$ are set equal to zero. As an example, consider cyclobutadiene (Fig. 2). Writing out the secular determinant equation in full, we get

$$\begin{vmatrix} \alpha - E & \beta & 0 & \beta \\ \beta & \alpha - E & \beta & 0 \\ 0 & \beta & \alpha - E & \beta \\ \beta & 0 & \beta & \alpha - E \end{vmatrix} = 0 \qquad (6).$$

The matrix entries in equation (6) may be compared with the cyclobutadiene structure of Fig. 2. The diagonal terms (α – E) can be thought of as the 'self-interaction' terms; in the absence of any off-diagonal β terms, there are no chemical bonds formed, and the roots of the equation are the energies of the electrons in the atomic orbitals themselves. When chemical bonding occurs, these energies are modified by the off-diagonal β terms. Thus when two atoms are bonded together (*i.e.*, atoms 1 and 2 in Fig. 1), there is a non-zero value at this particular (1,2) entry in the secular determinant; when two atoms are not bonded together (*i.e.* atoms 1 and 3 in Fig. 2), then the corresponding determinant entry {1,3} is zero. Referring to Fig. 1, we see that this description is very similar to the adjacency matrix of the corresponding graph. If we use the normalized form of Hückel theory, in which β is taken as the energy unit, and α is taken as the zero-energy reference point (Trinajstic, 1983), then the determinant of equation (6) becomes identical to the corresponding adjacency matrix. The eigenvectors of the adjacency matrix are identical to the Hückel molecular-orbitals. Hence *it is the* *topological (graphical) characteristics of a molecule, rather than any geometrical details, that determine the form of the Hückel molecular-orbitals.* For cyclobutadiene, the orbital energies found from the secular determinant (*i.e.*, the four roots of equation 6) are $E = \alpha + 2\beta$, α (×2) and $\alpha - 2\beta$. These are shown in Fig. 2, both in a conventional energy representation, and as a *density-of-states* diagram.

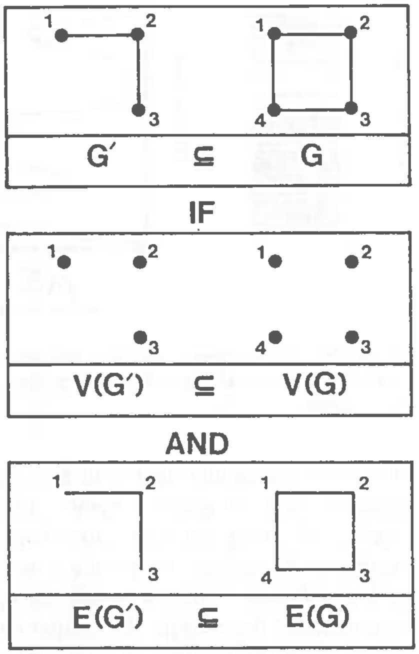

Fig. 3. The relationship between a graph G and a subgraph G′ expressed in terms of the relevant vertex- and edge-sets.

Molecular building blocks

We often resolve complicated systems into simple (usually additive or weakly interacting) components that are easier to handle. Molecular and crystal structures are no exception; we recognize structural building-blocks, and build hierarchies of structures using these 'molecular bricks'. Let us consider this from a graph theoretic point of view.

A graph G' is a subgraph of a graph G if the vertex- and edge-sets $V(G')$ and $E(G')$ are subsets of the vertex- and edge-sets $V(G)$ and $E(G)$; this is illustrated in Fig. 3. We may express any graph as the sum of a set of subgraphs. The eigenvalues of each subgraph G' are a subset of the eigenvalues of the main graph G, and the eigenvalues of the main graph are the sum of the eigenvalues of all the subgraphs. In the last section, we saw that the eigenvalues of an adjacency matrix are identical to the Hückel molecular-orbitals. Now let us consider the construction of large molecules from smaller building-blocks. This provides us with a convenient visual way of analyzing the connectivity of our molecule, and of relating molecules together. But this is not all. The fact that the eigenvalues of the graphs of our building blocks are contained in the eigenvalues of the graph of the complete molecule indicates that we may consider our building blocks as *orbital* or *energetic building-blocks.* Thus *there is an energetic basis for the use of fundamental building blocks (FBBs) in the representation and hierarchical analysis of complex structures.*

Crystals

We can conceive of constructing a crystal from constituent molecular building-blocks, in this way considering the crystal as a giant molecule. However, it is not clear what influence translational periodicity will have on the energetics of this conceptual building process. To try to clarify this problem, we will now examine the energetic differences between a molecule and a crystal.

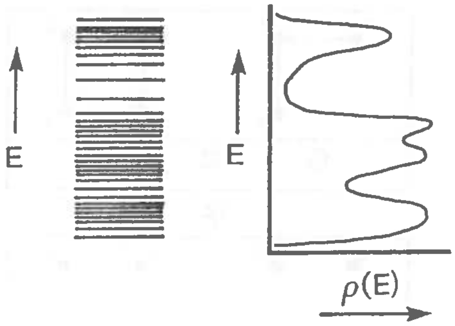

Fig. 4. The electron energy levels for a giant molecule expressed in the usual way (left) and as a density of states (right).

Let us imagine being able to solve equation (6) for a giant molecule. The results are sketched diagrammatically in Fig. 4. Solution of the secular determinant will give a very large number of molecular-orbital energies, and obviously their conventional representation solely as a function of energy is not very useful; such results are better expressed as a density-of-states diagram (Fig. 4), in which the electron occupation of a specific energy-interval (band) is expressed as a function of orbital energy.

What effect does translational symmetry have on this conceptual process? Obviously we cannot deal with a crystal using the same sort of calculation, as there are approximately Avogadro's number of atoms in a (macroscopic) crystal, far beyond any foreseeable computational capability. Instead, we must make use of the translational symmetry to reduce the problem to a manageable size. We do this by using *Bloch orbitals* (Ziman, 1965), in which the orbital content of the unit cell is constrained to the periodicity of the crystal. The secular determinant is solved at a representative set of points within the Brillouin zone (the *special-points method*), giving a (hopefully) representative sampling of the orbital energy-levels that may be smoothed to give the usual density-of-states representation. The total orbital-energy can then be calculated by integrating the electronic energy density-of-states up to the Fermi level.

The differences between a molecule and a crystal may thus be summarized as follows: in a molecule, there is a discrete set of orbital energy-levels; in a crystal, these levels broaden into bands whose occupancies as a function of energy is represented by the corresponding electronic energy density-of-states.

The method of moments

The usual method for deriving the electronic energy density-of-states has little intuitive connection to what we usually think of as the essential features of a crystal structure, the relative positions of the atoms and the disposition of the chemical bonds. In this regard, Burdett *et al.* (1984) have come up with a very important method of deriving the electronic energy density-of-states using the *method of moments*. I will give only a brief outline of the method; interested readers should consult the original paper for mathematical details, and are also referred to Burdett (1986, 1987) for further applications in solid-state chemistry.

To solve the secular determinant (equation 7), we diagonalize the Hamiltonian matrix. The trace of this matrix may be expressed as follows:

$$Tr(H^n) = \sum_i \sum_{j,k\ldots n} H_{ij} H_{jk} \ldots H_{ni} \qquad (7).$$

A topological (graphical) interpretation of one term in this sum is shown in Fig. 5. Each H_{ij} term is the interaction integral between orbitals i and j, and hence is equal to β (if the atoms are bonded) or zero (if the atoms are not bonded, or if $i = j$ when $\alpha = 0$). Thus a single term $\{H_{ij} H_{ik} \ldots H_{ln}\}$ in equation 8 is non-zero only if all H_{ij} terms are non-zero. As the last H_{ij} term is the interaction between the n^{th} orbital and the first orbital, the $\{H_{ij} H_{jk} \ldots H_{ni}\}$ term represents a closed path of length n in the graph of the orbitals (molecule). In Fig. 5, the term $\{H_{ij} H_{jk} H_{kl} H_{li}\}$ represents the clockwise path of length 4 around the cyclobutadiene $p\pi$ orbitals. Thus the complete sum of Equation 7 represents all circuits of length n through the graph of the (orbital structure of) the molecule.

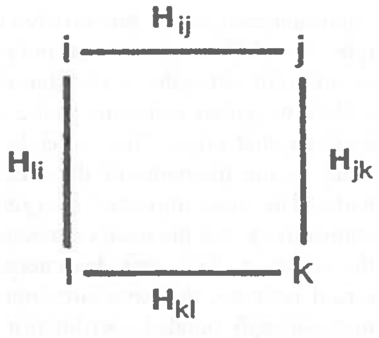

Fig. 5. Topological interpretation of a single term in the sum of equation 6; for each orbital i, the non-zero terms are a series of circuits of length n with orbital i as the origin; the term shown here has n = 4 (for cyclobutadiene).

The trace of the Hückel matrix remains invariant under diagonalization, and thus

$$Tr(H^n) = Tr(E^n) = \mu_n \qquad (8).$$

where E is the diagonal matrix of eigenvalues (energy levels) and μ_n is the n^{th} *moment* of E, formally denoted by

$$\mu_n = \sum_i E_i^n \qquad (9)$$

The collection of moments $\{\mu_n\}$ may be inverted (see Burdett *et al.*, 1984 for mathematical details) to give the density-of-states. As we can evaluate $Tr(H^n)$ directly from the topology of the orbital interactions (bond topology), we thus derive the electronic energy density-of-states *directly* from the bond topology. Of course, we have already shown that this is the case by demonstrating the equivalence of the secular determinant and the adjacency matrix of the molecule. However, the method of moments generalizes quite readily to infinite systems (*i.e.* crystals).

For an infinite system, we can define the n^{th} moment of E as

$$\mu_n = \int E^n \rho(E) dE \qquad (10)$$

where $\rho(E)$ is the density of states. In principle, the moments may be evaluated as before, and inverted to give the electronic energy density-of-states. Thus we see, in principle, the topological content of the electronic energy density-of-states in an infinite system, which in turn emphasizes the energetic content of a topological (graphical) representation of periodic structure. However, we can go further than this. Burdett (1986) has shown that the energy difference between two structures can be expressed in terms of the first few disparate moments of their respective electronic energy density-of-states. Thus when comparing two structures, *the important energetic terms are the most local topological differences between the structures*. Putting this in structural terms, the important energetic terms involve differences in coordination number (including ligand type) and differences in local polyhedral linkage. Furthermore, in structures with bonds of different strengths, each edge of each path (walk) that contributes to each moment will be weighted according to the value of the strength (resonance integral) of the bond defining that edge. Thus strongly bonded paths through the structure will contribute more to the moments of the electronic energy density-of-states than weakly bonded paths. The most important energetic features of a structure are thus not only the local connectivity, but the local connectivity of the strongly bonded coordination polyhedra in the structure. This provides energetic justification for a hypothesis that will be introduced later on, that structures may be ordered according to the polymerization of the more strongly bonded coordination polyhedra (Hawthorne, 1983a).

Topological aspects of crystal chemistry

We are all familiar with the rules that govern (sometimes weakly) the stability and structure of inorganic crystals. The most rigorous rule is that of electroneutrality: *the sum of the formal charges of all the ions in a crystal is zero.* Although we tend to take this rule for granted, it is an extremely powerful constraint on possible chemical variations in crystals. Other rules grew out of observations on a few mineral and inorganic structures. Barlow (as described by Bragg, 1955, p. 270–271) predicted the structure of NaCl on the basis of sphere-packing arguments long before the discovery of X-ray diffraction. Bragg's (1913) solution of the structure of halite vindicated Barlow's arguments, and the idea of structures as close packings of spheres became useful in the solution of crystal structures. Bragg also introduced the idea that atoms have a certain size, introduced the idea of coordination number, and considered silicate minerals as polymerizations of coordination polyhedra. These ideas were refined by Pauling (1929, 1960), who systematized them into his well-known rules for the behaviour of 'complex ionic crystals':

(1) a coordination polyhedron of anions is formed about each cation, the cation-anion distance being determined by the radius sum, and the ligancy (coordination number) of the cation being determined by the radius ratio.

(2) the strength of a bond from a cation to an anion is equal to the cation charge divided by the cation coordination number; in a stable (ionic) structure, the formal valence of each anion is approximately equal to the sum of the incident bond-strengths.

(3) the presence of shared faces and edges between coordination polyhedra decreases the stability of a structure; this effect is large for cations of large valence and small ligancy.

(4) in a crystal containing different cations, those with large valence and small coordination-number tend not to share polyhedral elements with each other.

These rules put some less rigorous constraints on the behaviour of structures, constraints that are traditionally associated with the ionic model of the chemical bond; they allow us to make the following type of statements about the structure and chemistry of inorganic crystals:

(a) the formula is electrically neutral;
(b) we may make (weak) predictions of likely coordination numbers from the radius-ratio rules;
(c) we can make fairly good (< 0.02 Å) predictions of mean bond-lengths by summing ionic radii.

There is an enormous amount of structural and chemical data available, and yet our predictive capabilities concerning this information is limited in the extreme. The following questions are pertinent in this regard:

(a) within the constraint of electroneutrality, why do some stoichiometries occur whereas others do not?
(b) given a specific stoichiometry, what is its bond connectivity (bond topology)?
(c) given a specific stoichiometry and bond connectivity, what controls the site occupancies?

These are some of the questions that need answering if we are going to understand and be able to predict the stability of inorganic atomic arrangements in general, and minerals in particular.

Pauling's rules

How do Pauling's rules relate to the topology of the bond connectivity in crystals? This is considered for each rule in turn, below:

Rule (1): The mean interatomic-distance in a coordination polyhedron can be determined by the sum of the radii of the constituent ions. This point has been extensively developed up to the present (Shannon, 1976; Baur, 1987; O'Keeffe & Brese, 1991), together with consideration of additional factors that also affect mean bond-lengths in crystals (Shannon, 1975; Baur, 1981). The first rule also states that the coordination number is determined by the radius ratio. This works reasonably well for small high-valence cations, but does not work well for large low-valence cations. For example, inspection of Shannon's (1976) table of ionic radii shows Na radii listed for coordination numbers from [4] to [12] with oxygen ligands, whereas a radius-ratio criterion would indicate that any cation can have (at most) only two coordination numbers for a specific anion. It is important to note that the coordination number of an atom is one of the lowest moments of the electronic energy density-of-states.

Rule (2): This is also known as the electrostatic-valence rule. It has been further extended by Baur (1970, 1971), who developed a scheme for predicting individual bond-lengths in crystals, given the bond connectivity, and by Brown & Shannon (1973), who quantitatively related the length of a bond to its strength (bond valence). The latter scheme has proved a powerful *a posteriori* method of examining crystal structures for crystal-chemical purposes. This rule relates strongly to the local connectivity of strong bonds in a structure, and again involves significant low-order moments of the electronic energy density-of-states.

Rules (3) and (4): Both of these rules again relate to the local connectivity in a structure, and strongly affect the important low-order moments, both by different short paths resulting from different local bond-topologies, and from differences in *anion* coordination numbers.

These arguments show that Pauling's rules can all be intuitively related to bond topology and its effect on the low-order moments of the electronic energy density-of-states.

Ionicity and covalency

Pauling (1929) presented his rules as *ad hoc* generalizations, rationalized by qualitative arguments based on an electrostatic model of the chemical bond. This led to an association of these rules with the ionic model, and there has been considerable criticism of the second rule as an 'unrealistic' model for bonding in most solids. Nevertheless, these rules have been too useful to discard, and in various modifications, continue to be used to the present day. Clearly, their proof is in their applicability to real structures rather than in the details of somewhat vague ionic arguments (Burdett & McLarnan, 1984).

In the last 20 years, there has been significant progress in rationalizing and predicting geometrical aspects of structures from a molecular-orbital viewpoint (Burdett, 1980; Gibbs, 1982; Tossell & Gibbs, 1977). In particular, it has been shown that many of the geometrical predictions of Pauling's rules can also be rationalized by molecular-orbital calculations on small structural fragments. Burdett & McLarnan (1984) show how the same predictions from Pauling's rules can be rationalized in terms of band-structure calculations, again focusing on the covalent interactions, but doing so for an infinite structure. It is interesting to note how these two approaches parallel the arguments given previously concerning the relationship between bond topology and energetics:

(1) the energy of a molecular fragment is a function of its topological characteristics *via* the form of the secular determinant;

(2) the electronic energy density-of-states of a continuous structure can be expressed in terms of the sum of the moments of the energy density-of-states, which is related to the topological properties of its bond network.

The thread that links these ideas together is the topology of the bond network *via* its effect on the energy of the system. This also parallels our earlier conclusion that all of Pauling's rules relate to the topological characteristics of the bond network of a crystal.

Let us consider two (dimorphic) structures of the same stoichiometry but different atomic arrangement. As the chemical formulae of the two structures are the same, the *atomic* components of the energy of each structure must be the same, and the difference in energy between the two structures must relate *completely* to the difference in bond connectivity. This 'general principles' argument emphasizes the importance of bond topology in structural stability, and finds more specific expression in the method of moments developed by Burdett *et al.* (1984). Thus we come to the general conclusion that *arguments of ionicity and/or covalency in structure are secondary to the overriding influence of bond topology on the stability and energetics of structure.*

Bond-valence theory

In the early 1970s, several workers (Donnay & Allmann, 1970; Baur, 1971; Brown & Shannon, 1973; Ferguson, 1974; Pyatenko, 1973) developed extensions of Pauling's second rule, and the term 'bond-valence' evolved as a measure of the strength of a chemical bond. Based on this approach, Brown (1981, 1992) and O'Keeffe (1989, 1990) have developed a simple yet coherent picture of chemical bonding in inorganic structures. Although empirical bond-valence curves are now widely used (Brown & Altermatt, 1985), the general ideas of bond-valence theory have not yet seen the use that they deserve. I shall briefly review these ideas as they can be developed further to deal in a very simple way with many aspects of complex inorganic structures that cannot be approached by other methods.

Bond-valence relationships

According to Pauling's second rule (Pauling, 1960), bond-strength, p, is defined as

$$p = \text{cation valence/cation coordination number} = Z/cn \qquad (11).$$

Summing the bond-strengths around the anions, the second rule states that the sum should be approximately equal to the magnitude of the anion valence:

$$\sum_{anion} p \approx |Z_{anion}| \qquad (12).$$

Correlations between deviations from Pauling's second rule and bond-length variations in crystals have been parameterized for specific cation-anion bonds. For such schemes, I use the term *bond valence*, in contrast to the Pauling scheme for which I use the term *bond strength*; this is merely a convenient nomenclature without any other significance.

Bond valence, s, may be expressed as a function of bond length, R, in the following way:

$$s = s_o|R/R_o|^{-N} \text{ or } s = |R/R_1|^{-n} \qquad (13)$$

where s_o, R_o, N, R_1 and n are constants characteristic of cation-anion pairs, and were derived by fitting such equations to a large number of well-refined crystal structures under the constraint that the valence-sum rule work as closely as possible (Brown & Shannon, 1973). In equation 13, R_o is nominally a refined parameter, but is obviously equal to the grand mean bond-length for the particular bond-pair and cation coordination-number under consideration; s_o is equal to the Pauling bond-strength. Thus $(R/R_o) \approx 1$, and s_o is actually a scaling factor that ensures that the sum of the bond valences around an atom is approximately equal to the magnitude of its valence.

We may consider covalence in the following way. Suppose that there is a delocalization of charge into the bonds, together with a reduction in the charge on each atom. For an A–B bond, let the residual charges change by Z_Ap_A and Z_Bp_B, respectively. The (Pauling) bond-strength [= scaling constant s_o in eqn 14] is given by Z_Ap_A/cn, where cn is the coordination number of atom A. Inserting these values into equation 14 and summing over the bonds around B gives

$$\sum_B = p_A \sum s_o |R/R_o|^{-N} = p_B|Z_B| \qquad (14).$$

If $p_A \approx p_B$, these terms cancel and the bond-valence equation works, provided the relative delocalization of charge from each formally ionized atom is not radically different. Thus the bond-valence equation can apply from 'very ionic' to 'very covalent' situations.

Bond-valence theory as a molecular-orbital model

Pauling (1929) couched his original arguments in the vocabulary of an ionic-bonding model, and there has been considerable criticism of his second rule and its more recent extensions, based on its perception as a description of ionic bonding. In this regard, Bragg (1930) produced an interesting argument to justify Pauling's second rule. He considered the (nearest-neighbour) forces that bond atoms together into coordination polyhedra, conceptually modelling the interactions by "lines of force". He noted that atoms that are closer together will have more lines of force between them, atoms that are further apart will have less lines of force, and that next-nearest-neighbours can interact only through their nearest-neighbours. The 'charge' of the bond strength was associated with the bond between two atoms, and the amount of charge was inversely related to the bond length. This sounds much more like a molecular-orbital description of bonding than an ionic description, allowing for the unconventional vocabulary used in the argument.

Brown & Shannon (1973) emphasized the difference between bond-valence theory and the ionic model. In bond-valence theory, the structure consists of a series of atomic cores held together by valence electrons that are associated with the chemical bonds between atoms; they also explicitly state that the valence electrons may be associated with chemical bonds in a symmetric (covalent) or asymmetric (ionic) manner. However, *a priori* knowledge of the electron distribution is not necessary, as it is quantitatively derived from the application of the bond-valence curves to the observed structure. Indeed, Burdett & Hawthorne (1993) show how the bond-valence bond-length relation may be derived algebraically from a molecular-orbital description of a solid in which there is a significant energy-gap between the interacting orbitals on adjacent atoms. *Thus we may consider bond-valence theory as a very simple form of molecular-orbital theory, parameterized via interatomic distance rather than electronegativity or ionization potential*, and (arbitrarily) scaled *via* the valence-sum rule.

Network solids

Let us define a crystal, liquid or molecule as a network of atoms connected by chemical bonds. For the materials in which we are interested, any path through this network contains alternating cations and anions, and the total network is subject to the *law of electroneutrality*: the total valence of the cations is equal to the total valence of the anions. A bond valence can be assigned to each bond such that the *valence-sum rule* is obeyed: *the sum of the bond valences at each atom is equal to the magnitude of the atomic valence*. If the interatomic distances are known, then the bond valences can be calculated from the curves of Brown (1981); if the interatomic distances are not known, then the bond valences can be approximated by Pauling bond-strengths.

Characteristic bond-valences

Although the ideas discussed above are important, they are *a posteriori* analysis: the structure must be known in detail before we can apply these ideas. This is obviously not satisfactory. We need an *a priori* approach to structure stability if we are to develop any predictive capability. In this regard, Brown (1981) introduced a very important idea. If we examine the bond valences around a specific cation in a wide range of crystal structures, we find that the values lie within ~20% of the mean value; this mean value is thus characteristic of that particular cation. If the cation only occurs in one type of coordination, then the mean bond-valence for that cation will be equal to the Pauling bond-strength; thus P (phosphorus) always occurs in tetrahedral coordination to oxygen, and will hence have a mean bond-valence of $5/4 = 1.25$ *vu*. If the cation has more than one coordination number, then the mean bond-valence will be equal to the weighted mean of the bond valences in all the observed structures. Thus Fe^{2+} occurs in various coordinations from [4] to [8]; the tendency is for [4]- and [5]-coordinations to be more common than [7]- and [8]-coordinations, and hence the mean bond-valence is 0.40 *vu*.

The mean bond-valence correlates with formal charge and cation size, and hence it should vary systematically through the periodic table; this is in fact the case. Table 1 shows these values, smoothed across the periods and down the groups of the periodic table.

Lewis acid and base strengths

The concept of bond valence can be generalized in the following way. The mean bond-valence of a cation correlates strongly with its *electronegativity* (Fig. 6). Electronegativity is a measure of the electrophilic strength (electron-accepting capacity) of the cation, and the correlation with the characteristic bond-valence (Fig. 6) indicates that the latter is a measure of the *Lewis acid strength* of the cation (see also O'Keeffe & Brese, 1991). Thus we have the following definition (Brown, 1981):

The Lewis acid strength of a cation may be defined as the characteristic bond-valence = atomic (formal)valence/mean-coordination-number.

Table 1. Lewis acid strengths (*vu*) for cations

Li	0.22	Sc	0.50	Cu^{2+}	0.45
Be	0.50	Ti^{3+}	0.50	Zn	0.36
B	0.88	Ti^{4+}	0.75	Ga	0.50
C	1.30	V^{3+}	0.50	Ge	0.75
N	1.75	V^{5+}	1.20	As	1.02
Na	0.16	Cr^{3+}	0.50	Se	1.30
Mg	0.36	Cr^{6+}	1.50	Rb	0.10
Al	0.63	Mn^{2+}	0.36	Sr	0.24
Si	0.95	Mn^{3+}	0.50	Sn	0.66
P	1.30	Mn^{4+}	0.67	Sb	0.86
S	1.65	Fe^{2+}	0.36	Te	1.06
Cl	2.00	Fe^{3+}	0.50	Cs	0.08
K	0.13	Co^{2+}	0.40	Ba	0.20
Ca	0.27	Ni^{2+}	0.50	Pb^{2+}	0.20

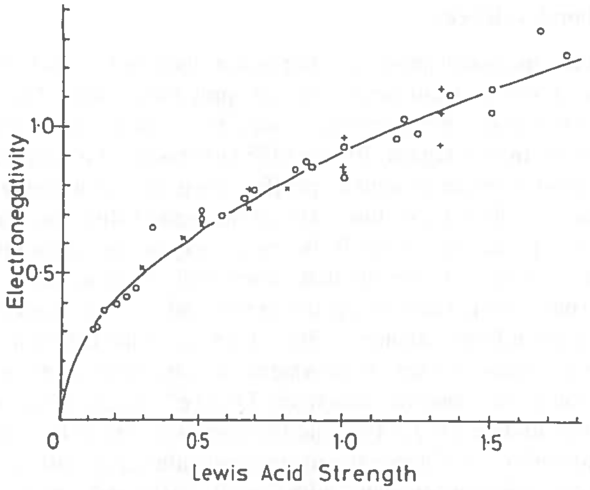

Fig. 6. Lewis acid strength (mean bond-valence for a specific cation) as a function of cation electronegativity (from Brown, 1981); circles are main-group elements in their highest oxidation state, crosses (×, +) are the same elements in lower oxidation states.

The Lewis base strength of an anion can be defined in exactly the same way, as the characteristic valence of the bonds formed by the anion. However, bond-valence variations around anions are much greater than those around cations. For example, the valences of the bonds to O^{2-} vary between nearly zero and 2.0 *vu*; thus in $Na[Al(SO_4)_2(H_2O)_6](H_2O)_6$ (Cromer *et al.*, 1967), Na is in [12]-coordination, and the oxygen to which it is bonded receives 0.08 *vu* from the Na–O bond; conversely in CrO_3 (Stephens & Cruickshank, 1970), one oxygen is bonded only to Cr^{6+} and receives 2.00 *vu* from the Cr–O bond. With this kind of variation, it is not particularly useful to define a Lewis base strength for a simple anion such as O^{2-}.

The situation is entirely different for *complex oxyanions*. Consider the $(SO_4)^{2-}$ oxyanion shown in Fig. 7. Each oxygen receives 1.5 *vu* from the central S^{6+} cation, and hence each oxygen of the group needs an additional 0.5 *vu* to be supplied by additional cations. If the oxygen coordination number is [n], then the average valence of the bonds to O^{2-} (exclusive of the S–O bond) is 0.5/(n – 1) *vu*; thus if n = 2, 3, 4 or 5, then the mean bond-valences to the oxygen are 0.50, 0.25, 0.17 or 0.11 *vu*, respectively. As all of the oxygen atoms in the $(SO_4)^{2-}$ oxyanion have the same environment, then the average bond-valence received by the oxyanion is the same as the average bond-valence received by the individual oxygen atoms. In this way, we can define the Lewis basicity of an oxyanion. Note that

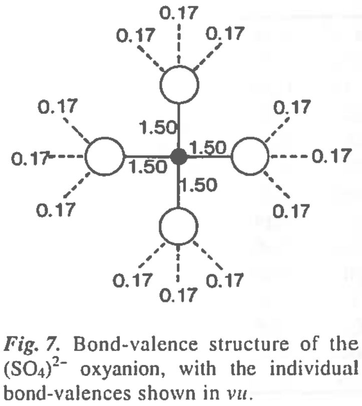

Fig. 7. Bond-valence structure of the $(SO_4)^{2-}$ oxyanion, with the individual bond-valences shown in *vu*.
● = sulphur, ○ = oxygen.

for the $(SO_4)^{2-}$ oxyanion discussed above, the possible average bond-valences are quite tightly constrained (0.50–0.11 *vu*), and we can easily calculate a useful Lewis basicity. Table 2 lists Lewis basicities for some common inorganic oxyanions.

Table 2. Lewis basicities (*vu*) for selected oxyanions

$(BO_3)^{3-}$	0.33	$(CO_3)^{2-}$	0.25
$(SiO_4)^{4-}$	0.33	$(NO_3)^{3-}$	0.12
$(AlO_4)^{3-}$	0.42	$(VO_4)^{3-}$	0.25
$(PO_4)^{3-}$	0.25	$(SO_4)^{2-}$	0.17
$(AsO_4)^{3-}$	0.25	$(CrO_4)^{2-}$	0.17

The valence-matching principle

The definitions of Lewis acid and base strengths lead to a specific criterion for chemical bonding, the *valence-matching principle*:

The most stable structures will form when the Lewis acid-strength of the cation closely matches the Lewis base-strength of the anion.

This is the chemical analogue of the handshaking principle in combinatorial mathematics, and the 'kissing' principle in social relationships. As a chemical bond contains two constituents, then the properties of the constituents must match for a stable configuration to form.

Simple applications of the valence-matching principle

Thenardite, Na_2SO_4 (Hawthorne & Ferguson, 1975a), illustrates both the utility of defining a Lewis base strength for an oxyanion, and the working of the valence-matching principle (Fig. 7). As outlined above, the bond-valences to O^{2-} vary between 0.17 and 1.50 *vu*. Assuming a mean oxygen coordination number of [4], the Lewis basicity of the $(SO_4)^{2-}$ oxyanion is 0.17 *vu*, which matches up very well with the Lewis acidity of 0.16 *vu* for Na given in Table 1. Thus the Na–(SO_4) bond accords with the valence-matching principle, and thenardite is a stable mineral.

Consider the formula Na_4SiO_4. The Lewis basicity of the $(SiO_4)^{4-}$ oxyanion is 0.33 *vu* (Table 2); the Lewis acidity of Na is 0.17 *vu*. These values do not match up, and thus a stable bond cannot form; consequently Na_4SiO_4 is not a very stable material and is not found as a mineral.

Consider the formula Ca_2SiO_4. The Lewis basicity of $(SiO_4)^{4-}$ is 0.33 *vu* and the Lewis acidity of Ca is 0.29 *vu*; these values match up reasonably well, and Ca_2SiO_4 is stable as the mineral larnite.

Consider the formula $CaSO_4$. The relevant Lewis basicity and acidity are 0.17 and 0.29 *vu*, respectively; according to the valence-matching principle, we do not expect a stable structure to form. However, the mineral anhydrite is stable, the cation and anion coordination numbers both reducing to allow the structure to satisfy the valence-sum rule (Hawthorne & Ferguson, 1975b). However, anhydrite hydrates readily in the presence of water to produce gypsum, $CaSO_4(H_2O)_2$; this instability is suggested by the violation of the valence-matching principle.

These simple examples illustrate the power of the valence-matching principle as a simple way in which we can consider the possibility of cation-anion interactions of interest. It is important to recognize that this is *a priori* analysis, rather than the *a posteriori* analysis of Pauling's second rule and its various modifications.

A hierarchical approach to structure

Bragg (1930) classified the silicate minerals according to the way in which the (SiO_4) tetrahedra polymerize, and this scheme was generalized to polymerized tetrahedral structures by Zoltai (1960) and Liebau (1985). Further developments along similar lines were the classifications of the aluminium hexafluoride minerals (Pabst, 1950; Hawthorne, 1984a) and the borate minerals (Christ, 1960; Christ & Clark, 1977; Burns *et al.*, 1995; Hawthorne *et al.*, 1996). Such an approach to hierarchical organization is of little use in such chemical groups as the phosphates or the sulphates, in which the principal oxyanion does not self-polymerize. Moore (1984) developed a classification of phosphate minerals, based on the polymerization of divalent and trivalent metal octahedra. However, all these hierarchical schemes focus on specific chemical classes of compounds, and are not easily adapted to other classes.

This general problem may be considered within the framework of bond-valence theory. First let us consider the cations in a structure. The cation bond-valence requirements are satisfied by the formation of anion coordination polyhedra around them. Thus we can think of a structure as an array of complex anions that polymerize in order to satisfy their (simple) anion bond-valence requirements according to the valence-sum rule. Let the bond-valences in an array of coordination polyhedra be represented by s_0^i (i = 1,n) where $s_0^i > s_0^{i+1}$.

A general hypothesis

Hawthorne (1983a) has proposed the following hypothesis:

Structures may be hierarchically ordered according to the polymerization of coordination polyhedra with higher bond-valences.

There are two important points to be made with regard to this idea:

(1) we define the structural elements by bond valences rather than by chemistry; consequently, there is no division of structures into different chemical groups except as occurs naturally *via* the different 'strengths' of the chemical bonds.

(2) Earlier, we argued that the topology of the bond network is a major feature controlling the energy of a structure. The polymerization of the principal coordination polyhedra is merely another way of expressing the topology of the bond network. Thus at the intuitive level, we can recognize an energetic basis for the hierarchical organization of structures according to the details of their polyhedral polymerization.

Dimensional polymerization

Families of complex structures are often based on different arrangements of a *fundamental building block* (FBB), a tightly-bonded unit within the structure that can be envisaged as the inorganic analogue of a molecule in an organic structure. The FBB is usually a *homo-* or *heteropolyhedral cluster* of coordination polyhedra with the strongest bond-valence linkages in the structure. The FBB is repeated, usually polymerized, to form the *structural unit*, a complex anionic polyhedral array whose charge is balanced by the

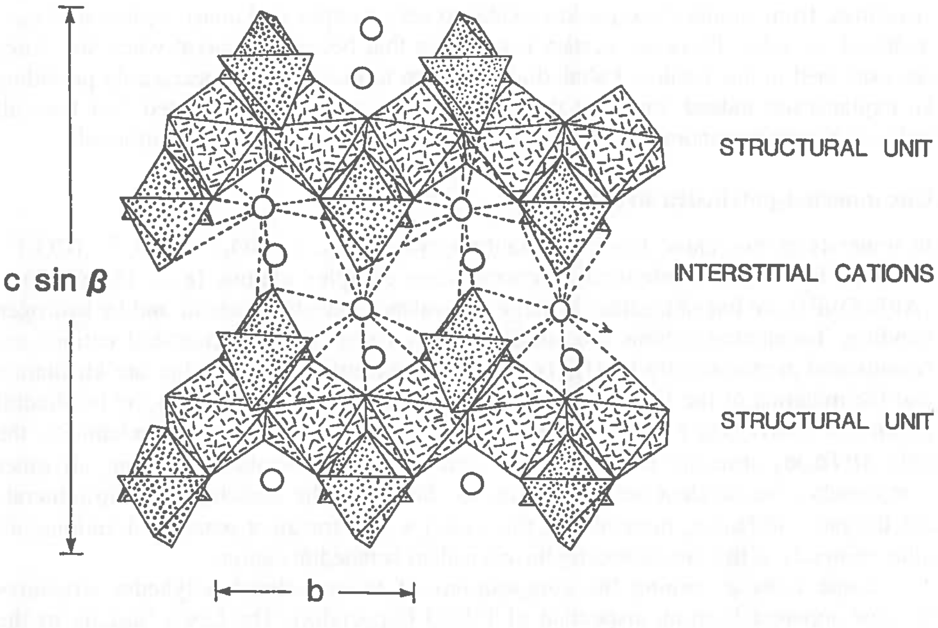

Fig. 8. The structural unit and the interstitial species in törnebohmite.

presence of large low-valence *interstitial* cations (usually alkalis or alkaline earths). These definitions are illustrated for the mineral törnebohmite in Fig. 8. The following nomenclature is used here: $M \geq [5]$-coordinated, $T = [3]$- or $[4]$-coordinated, ϕ = unspecified anion.

The various structural units can be arranged according to the mode of polymerization:

(a) unconnected polyhedra
(b) finite clusters
(c) infinite chains
(d) infinite sheets
(e) infinite frameworks

As discussed later, hydrogen-containing groups (*e.g.* $(OH)^-$, $(H_2O)^0$) often exert a major control on the dimensional character of the structural unit (Hawthorne, 1992). Most work has focused on structures with triangles, tetrahedra and octahedra as principal coordination components of the structural unit (Hawthorne, 1979, 1984a, 1985a, 1986, 1990; Eby & Hawthorne, 1993; Moore, 1970a,b, 1973, 1974, 1975a, 1982, 1984; Lima-de-Faria, 1983; Lima-de-Faria & Figueiredo, 1976), although there has been some notable work (Moore, 1981) on structures with important higher coordination numbers. The following outline cannot, of course, be comprehensive, but it is hopefully representative of the diversity shown by these types of structures. I shall focus on the structures of minerals for several reasons. First, much work of this type has involved mineral structures. Second, this restriction provides a reasonable sampling of inorganic oxysalt structures, from simple close-packed oxides to very complicated quasi-zeolitic hydroxy-hydrated oxysalts. There are certain regularities that become apparent when structures are examined in this fashion. I shall draw attention to these without necessarily providing an explanation; indeed, many of these features are, as yet, unexplained, but they all indicate Nature's economy of effort when it comes to structural design in minerals.

Unconnected-polyhedra structures

In minerals of this class, low-coordination oxyanions [*e.g.*, $(SO_4)^{2-}$, $(PO_4)^{3-}$, $(CO_3)^{2-}$, $(NO_3)^{-}$, $(TeO_4)^{2-}$] and intermediate-coordination complex cations [*e.g.*, $\{Mg(H_2O)_6\}$, $\{Al(H_2O)_5F\}$] are linked together by large low-valence interstitial cations and by hydrogen bonding. Tetrahedral cations are coordinated by oxygens, and octahedral cations are coordinated predominantly by (H_2O) groups; the exceptions to the latter are khademite and the minerals of the fleischerite group (Appendix, Table I), in which the octahedral groups are $(Al(H_2O)_5F)$ and $(Ge(OH)_6)$, respectively. It is notable that khademite is the only $M(T\phi_4)\phi_n$ structure (in this class) with a trivalent octahedral cation; all other compounds have divalent octahedral cations. Similarly, the fleischerite-group minerals are the only $M(T\phi_4)_2\phi_n$ minerals (in this class) with tetravalent octahedral cations; all other minerals of this stoichiometry have trivalent octahedral cations.

Some rules governing the compositions of these isolated polyhedra structures become apparent from an inspection of Table I (Appendix). The Lewis basicity of the $(T\phi_4)$ group must be low (*i.e.*, <0.20 *vu*), otherwise the valence-matching principle forces it to bond to a strong Lewis acid and form a polymerized structural unit. Thus these compounds are dominantly sulphates (or other hexavalent TO_4 salts). When a pentavalent T cation (such as P or As) occurs, it does so as an acid (PO_3OH) group; it is notable that such acid pentavalent-cation groups have a Lewis basicity of 0.18 *vu* (very similar to the value of 0.17 *vu* for the hexavalent (TO_4) groups, and significantly different from the Lewis basicity of 0.25 *vu* for the (PO_4) group). The only exception is struvite which has a (PO_4) group (Appendix, Table I). However, struvite has $(NH_4)^+$ as the interstitial complex-cation species, and $(NH_4)^+$ has a Lewis acidity of 0.25 *vu* (Table 1); thus solely because of the nature of the interstitial cation in struvite, this mineral can have an isolated (PO_4) group. Hence bond-valence considerations seem to account quite nicely for the compositional characteristics of these isolated-polyhedra structures.

Finite-cluster structures

Selected compounds of this class are given in Appendix, Table II, and the different types of clusters found in these minerals are illustrated in Fig. 9.

In jurbanite (Sabelli, 1985a), the cluster consists of an octahedral edge-sharing dimer of the form $[Al_2(OH)_2(H_2O)_8]$ and an isolated (SO_4) tetrahedron (Fig. 9a). These two fragments are bound together by hydrogen bonding from the octahedral dimer (donor) to the tetrahedron (acceptor), and hence jurbanite is actually transitional between the unconnected-polyhedra structures and the finite-cluster structures.

In the $M(T\phi_4)\phi_n$ minerals, the structures of the members of the rozenite group are based on the $[M_2(T\phi_4)_2\phi_8]$ cluster (Fig. 9b), linked solely by hydrogen bonding between

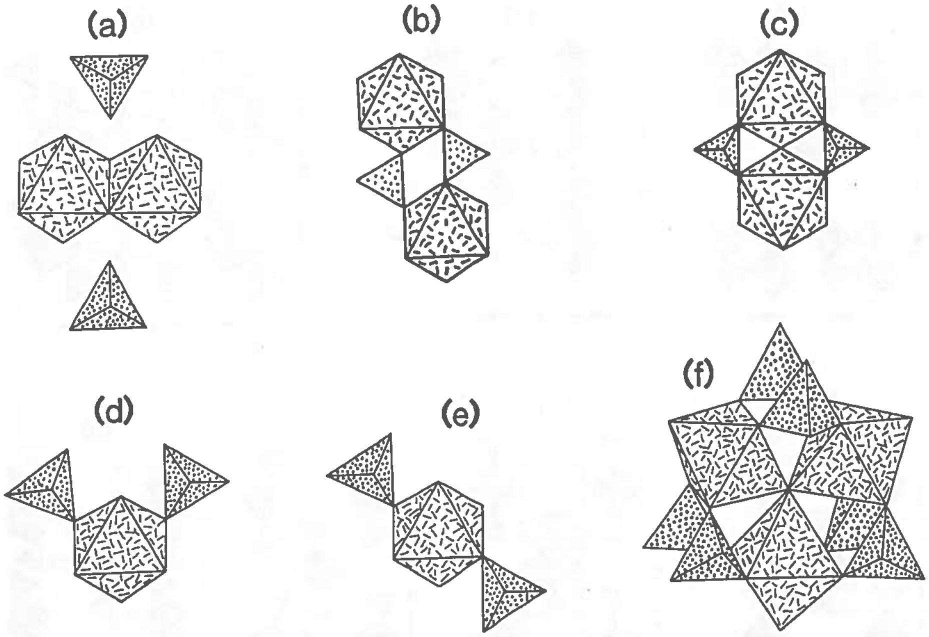

Fig. 9. Finite polyhedral clusters in $[M(T\phi_4)\phi_n]$ and $[M(T\phi_4)_2\ \phi_n]$ structures: (a) the $[M_2(T\phi_4)_2\phi_{10}]$ cluster in jurbanite; (b) the $[M_2(T\phi_4)_2\phi_8]$ cluster in the rozenite group minerals; (c) the $[M_2(T\phi_4)_2\phi_7]$ cluster in morinite; (d) the *cis* $[M(T\phi_4)_2\phi_4]$ cluster in römerite; (c) the *trans* $[M(T\phi_4)_2\phi_4]$ cluster in anapaite, blödite, leonite and schertelite; (f) the $[M_3(T\phi_4)_6\phi_4]$ cluster in metavoltine.

adjacent clusters. The morinite structure (Hawthorne, 1979) is based on the $[M_2(T\phi_4)_2\phi_7]$ cluster (Fig. 9c), linked by interstitial cations as well as inter-unit hydrogen bonds. Hawthorne (1983a) derived all possible finite clusters of the form $[M_2(T\phi_4)_2\phi_n]$ with no linkage between tetrahedra and with only corner-sharing between tetrahedra and octahedra. Based on the conjecture that the more stable clusters are those in which the maximum number of anions have their bond-valences most nearly satisfied, four clusters were predicted to be the most stable; two of these are the clusters of Figs. 9b,c.

There is far more structural variety in the $M(T\phi_4)_2\phi_n$ minerals (Appendix, Table II). Anapaite, blödite, leonite and schertelite are based on the simple *trans* $[M(T\phi_4)_2\phi_4]$ cluster of Fig. 9e, linked by a variety of interstitial cations and hydrogen-bond arrangements (Hawthorne, 1985c). Römerite (Fanfani *et al.*, 1970a) is also based on an $[M(T\phi_4)_2\phi_4]$ cluster, but in the *cis* rather than in the *trans* arrangement (Fig. 9d). Metavoltine (Giacovazzo *et al.*, 1976b) is built from a complex but elegant $[M_3(T\phi_4)_6\phi_4]$ cluster (Fig. 9f) that is also found in a series of synthetic compounds investigated by Scordari (1980, 1981b). Again it is notable that the $M(T\phi_4)_2\phi_n$ minerals in this class are characterized by interstitial cations, whereas the bulk of the $M(T\phi_4)\phi_n$ minerals are not, as was the case for the unconnected-polyhedra structures.

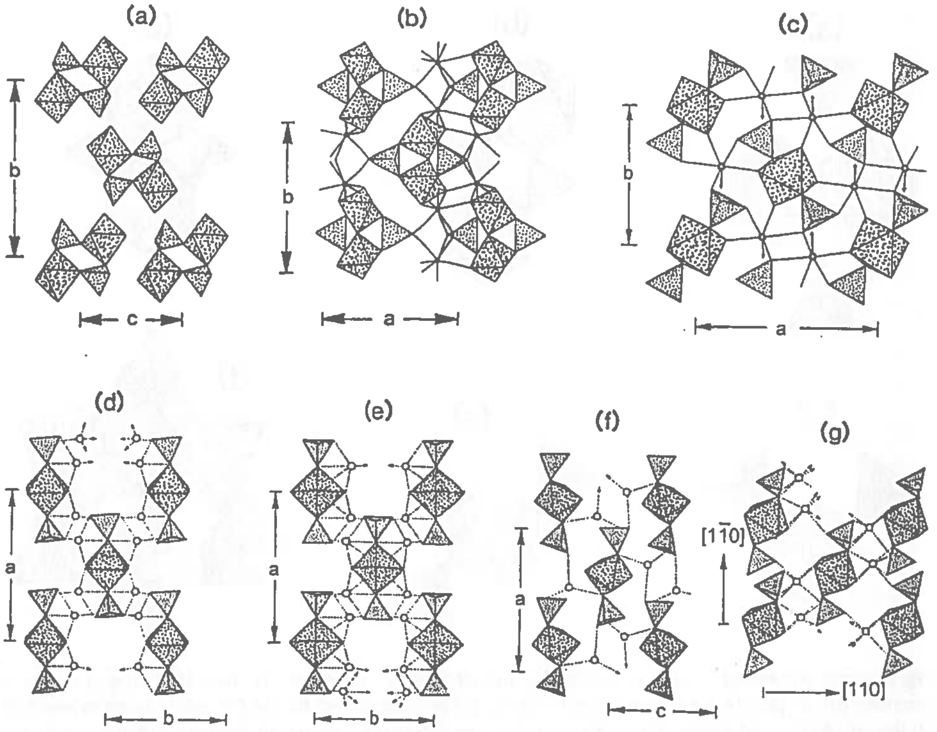

Fig. 10. Selected finite cluster structures of [$M(T\phi_4)\phi_n$] and [$M(T\phi_4)_2\phi_n$] stoichiometry: (a) rozenite; (b) morinite; (c) blödite; (d),(e) leonite; (f) schertelite; (g) anapaite.

The energetic considerations discussed previously suggest that the stability of these finite-cluster structures will be dominated by the topological aspects of their connectivity. Nevertheless, it is apparent from the structures of Table II (Appendix) that this is not the only significant aspect of their stability. Fig. 10 shows the structures of most of the minerals of Table II. It is very striking that these clusters pack in essentially the same fashion, irrespective of their nature, and irrespective of their interstitial species. Although a more detailed examination of this point is desirable, its very observation indicates that not only does Nature choose a very small number of fundamental building blocks, but She also is very economical in Her ways of linking them together.

Infinite-chain structures

There are large number of possible [$M_x(T\phi_4)_y\phi_z$] chains that can be constructed from fundamental building blocks involving one or two octahedra and one, two or four tetrahedra. Only a few of these possible chains have actually been found in inorganic oxysalt structures, and a cross-section of these is shown in Fig. 11; selected structures based on these chains are listed in Table III (Appendix).

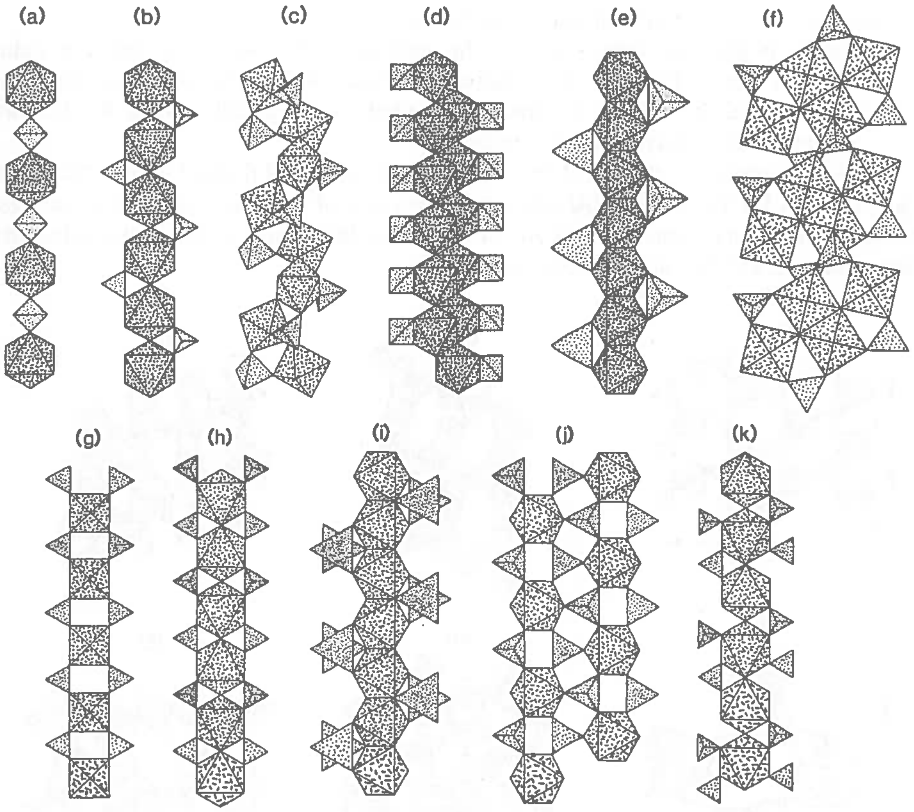

Fig. 11. Infinite chains in $[M(T\phi_4)\phi_n]$ and $[M(T\phi_4)_2\phi_n]$ structures: (a) the $[M(T\phi_4)\phi_4]$ chain in the chalcanthite-group minerals, liroconite and brassite; (b) the $[M(T\phi_4)\phi_3]$ chain in butlerite, parabutlerite, the childrenite group and uklonskovite; (c) the $[M(T\phi_4)\phi_3]$ chain in fibroferrite; (d) the $[M(T\phi_4)\phi]$ chain in chlorotionite; (e) the $[M(T\phi_4)\phi_2]$ chain in the linarite-group minerals; (f) the $[M_2(T\phi_4)_4\phi_5]$ chain in amarantite and hohmannite; (g) the $[M(T\phi_4)_2\phi_2]$ chain in the kröhnkite, talmessite and fairfieldite groups; (h) the $[M(T\phi_4)_2\phi]$ chain in tancoite, sideronatrite, the jahnsite and segelerite groups, guildite and yftisite; (i) the $[M(T\phi_4)_2\phi]$ chain in the brackebuschite, fornacite and vauquelinite groups; (j) the $[M(T\phi_4)_2\phi]$ chain in ransomite and krausite; (k) the $[M_2(T\phi_4)_4\phi_5]$ chain in botryogen.

The chains of Fig. 11 may be divided into two types: *common* [(a), (b), (c), (g), (h), (i)] and *rare* [(d), (e), (f), (j), (k)]. Structures based on these chains are listed in Table III. Minerals based on common chains are much more abundant than minerals based on rare chains, and also tend to show many more isostructural species than minerals based on rare chains.

Let us consider first the common chains of stoichiometry $[M(T\phi_4)\phi_n]$ (Figs. 11a–c). The first chain (Fig. 11a) has no linkage between octahedra, the second chain (Fig. 11b) has corner linkage between octahedra, and the third chain (Fig. 11c) has edge linkage between octahedra. These are the more important of the chains in this group, and it is notable that

(a) they all have a fairly simple connectivity;
(b) there is just one particular chain for each type of connectivity between octahedra; thus in the first chain, there is no direct linkage between octahedra; in the second chain, there is corner-sharing between octahedra; in the third chain, there is edge-sharing between octahedra.

Graph-theoretic arguments show that there are 200–300 distinct chains based on repeat units of $[M(T\phi_4)\phi_n]$ and $[M_2(T\phi_4)_2\phi_{2n}]$. Very few of these are found in structures, and by far the most common chains are the three simplest chains in which the octahedra share none, one and two anions, respectively.

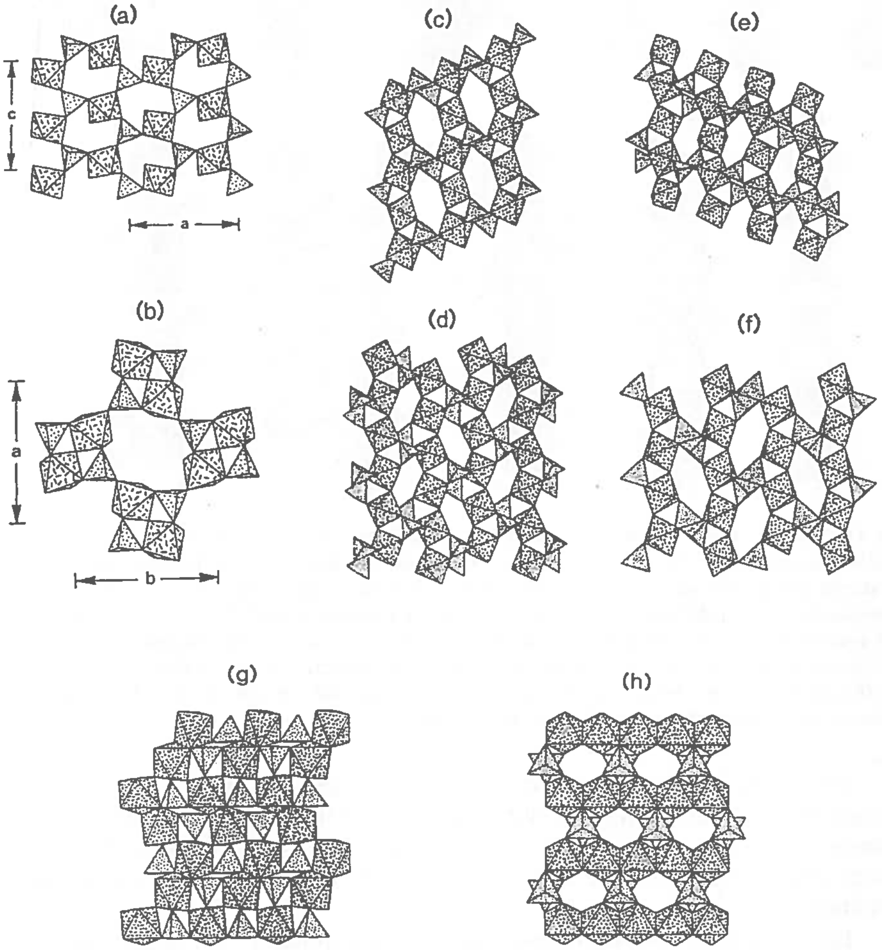

Fig. 12. Selected infinite sheets in $[M(T\phi_4)\phi_n]$ structures: (a) the $[M(T\phi_4)\phi_3]$ sheet in newberyite; (b) the $[M_2(T\phi_4)_2\phi_5]$ sheet in minyulite; (c) the $[M(T\phi_4)\phi_2]$ sheet in the laueite-group minerals; (d) the $[M(T\phi_4)\phi_2]$ sheet in pseudolaueite; (e) the $[M(T\phi_4)\phi_2]$ sheet in stewartite; (f) the $[M(T\phi_4)\phi_2]$ sheet in metavauxite; (g) the $[M_2(T\phi_4)_2\phi_7]$ sheet in whitmoreite; (h) the $[M(T\phi_4)\phi]$ sheet in tsumcorite and bermanite.

Let us consider next the common chains of stoichiometry $[M(T\phi_4)_2\phi_n]$ (Figs. 11g–i). Again, these chains have no linkage, corner linkage and edge linkage, respectively, between adjacent octahedra, and are the three simplest possible chains of $[M(T\phi_4)_2\phi_n]$ stoichiometry. The parallel behaviour of the $[M(T\phi_4)\phi_n]$ and $[M(T\phi_4)_2\phi_n]$ chain structures is striking, to say the least. The more complex chains of Figs. 11d–f are found in a smaller number of (far less common) minerals. In addition, it seems that the more complex structural units tend to occur in the ferric-iron sulphates.

Infinite-sheet structures

Minerals of this class are given in Table IV (Appendix). As the degree of polymerization of the structural unit increases, the number of possible bond-connectivities becomes enormous. However, Nature still seems to favour only a fairly small number of them; these are illustrated in Figs. 12 and 13.

The sheet structures of the $M(T\phi_4)\phi_n$ minerals show considerable variety in terms of the type of linkage between the FBBs. Notable in the less-connected structural units is that of minyulite (Fig. 12b), which is built by condensation (*via* corner linkage between octahedra and tetrahedra) of $[M_2(T\phi_4)_2\phi_7]$ clusters (Kampf, 1977) that are the structural unit in morinite (Fig. 9c). The structures of the laueite, stewartite, pseudolaueite, strunzite and metavauxite groups (Figs. 12c–f) are based on sheets formed from condensation of the vertex-sharing octahedral-tetrahedral chains of the sort shown in Fig. 11b. The tetrahedra cross-link the chains into sheets, and there is much possible variation in this type of linkage; for more details on this isomerism, see Moore (1975a). The five structural groups of these minerals are based on the four sheets of Figs. 12c–f. These sheets are linked through insular divalent-metal octahedra, either by direct corner-linkage to phosphate tetrahedra plus hydrogen bonding, or by hydrogen bonding alone. There is great potential for stereoisomerism in the ligand arrangement of these linking octahedra, but only the *trans* corner-linkages occur in these groups. In the whitmoreite sheet (Moore *et al.*, 1974) (Fig. 12g), we can see both the $[M_2(T\phi_4)_2\phi_7]$ cluster of the morinite structure and the $[M_2(T\phi_4)_2\phi_8]$ cluster of the rozenite-group structures (Figs. 9c,b). Similarly, in the $[M(T\phi_4)\phi]$ sheet of the bermanite (Kampf & Moore, 1976) and tsumcorite (Tillmanns & Gebert, 1973) structures (Fig. 12h), we can see the $[M(T\phi_4)\phi_2]$ chain that is the structural unit in the minerals of the linarite group (Fig. 11e).

The sheet units found in the $M(T\phi_4)_2\phi_n$ and $M_x(T\phi_3)_y\phi_n$ minerals are shown in Fig. 13. Again we see this structural building process, whereby structural units of more primitive connectivities act as fundamental building blocks for the more condensed structural units of corresponding composition. Thus the $[M(T\phi_4)_2\phi_2]$ sheet in rhomboclase (Mereiter, 1974) (Fig. 13a) is constructed from the *cis* $[M(T\phi_4)_2\phi_4]$ cluster that is the structural unit of römerite (Fig. 9d). Similarly, the $[M(T\phi_4)_2\phi_2]$ sheet of olmsteadite (Moore *et al.*, 1976) (Fig. 13b) is based on the *trans* $[M(T\phi_4)_2\phi_4]$ cluster (Fig. 9e) found in anapaite, blödite, leonite and schertelite (Figs. 10c–g). Note that the rhomboclase and olmsteadite sheets are actually *geometrical isomers* (Hawthorne, 1983a). Analogous relationships are obvious for the $[M(T\phi_4)_2]$ merwinite-type sheet and the $[M(T_2\phi_7)\phi_2]$ bafertisite-type sheet (Figs 13c,d). Both are based on the $[M(T\phi_4)_2\phi_2]$ kröhnkite chain of Fig. 11g, but in each sheet, the chains are cross-linked in a different fashion. In the

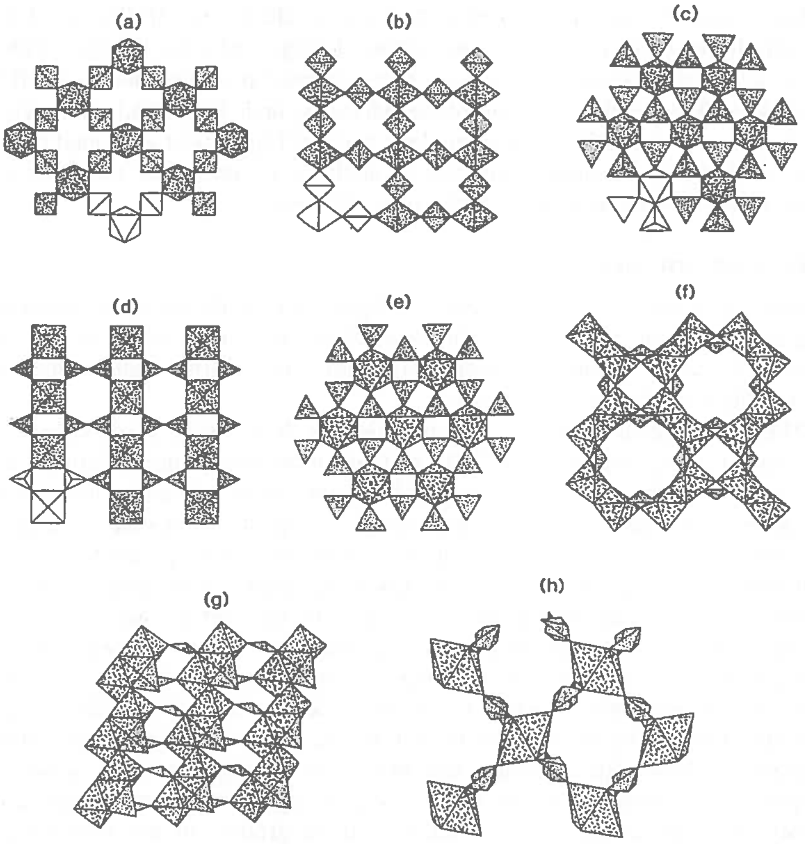

Fig. 13. Selected infinite sheets in $[M(T\phi_4)_2\phi_n]$ and $[M_x(T\phi_3)_y\phi_n]$ structures: (a) the $[M(T\phi_4)_2\phi_2]$ sheet in rhomboclase; (b) the $[M(T\phi_4)_2\phi_2]$ sheet in olmsteadite; (c) the $[M(T\phi_4)_2]$ sheet in the merwinite-group minerals and yavapaiite; (d) the $[M(T_2\phi_7)\phi_2]$ sheet in bafertisite; (e) the $[M(T\phi_3)_2]$ sheet in the eitelite-group minerals; (f) the $[M(T\phi_3)\phi_2]$ sheet in tunisite; (g) the $[M_2(T\phi_3)\phi_4]$ sheet in rodalquilarite; (h) the $[M(T_2\phi_5)_2]$ sheet in denningite.

merwinite sheet (Moore & Araki, 1972), tetrahedra from one chain share corners with octahedra of adjacent chains, and neighbouring tetrahedra point in opposite directions relative to the plane of the sheet. In the bafertisite sheet (Ya-hsien *et al.*, 1963), the $[M(T\phi_4)_2\phi_2]$ chains link by sharing corners between tetrahedra. Thus both sheets are 'built' from the same more primitive structural unit, and these two sheets are in fact *graphical isomers* (Hawthorne, 1983a).

Framework structures

Selected minerals of this class are listed in Table V (Appendix). Unfortunately, the topological aspects of the framework structures cannot be easily summarized in a concise graphical fashion, partly because of their large number, and partly because of the complexity that results from polymerization in all three spatial dimensions. Consequently, we will consider just a few examples that show particularly clearly the different types of linkages that can occur.

The structure of bonattite (Zahrobsky & Baur, 1968) is shown in Fig. 14a. Now bonattite is quite hydrated (Appendix, Table V), and comparison with the minerals of Table IV (Appendix) suggests that it should be a sheet structure (*cf.* newberyite, Table IV). Prominent in the structure are the $[M(T\phi_4)\phi_4]$ chains (Fig. 11a) that also occur as fragments of the newberyite sheet (Fig. 12a). In bonattite, adjacent chains are skew and link to form a framework; in newberyite (Sutor, 1967), the chains are parallel, and with the same number of inter-chain linkages, they link to form sheets rather than a framework. Thus bonattite and newberyite are *graphical isomers*, and provide a good illustration of how different modes of linking the same fundamental building block can lead to structures of very different connectivities and properties.

The structure of titanite is shown in Fig. 14b; this basic arrangement is found in a considerable number of minerals (Appendix, Table V) of widely differing chemistry (Hawthorne *et al.*, 1987). The $[M(T\phi_4)\phi]$ framework can be constructed from $[M(T\phi_4)\phi]$ vertex-sharing chains of the sort found in butlerite (Fanfani *et al.*, 1971), parabutlerite (Borene, 1970), the childrenite group (Giuseppetti & Tadini, 1984) and uklonskovite (Sabelli, 1985b) (Fig. 11b; Appendix, Table III). The chains pack in a C-centered array and cross-link by sharing corners between octahedra and tetrahedra of adjacent chains. It is notable that this chain is also a fundamental building block of the sheets (Figs. 12c–f) in the laueite, stewartite, pseudolaueite, strunzite and metavauxite groups (Table IV).

The structure of descloizite (Hawthorne & Faggiani, 1979) is shown in Fig. 14c; again this is a popular structural arrangement (Appendix, Table V). Prominent features of the tetrahedral-octahedral framework are the edge-sharing chains of octahedra flanked by staggered tetrahedra that link along the chain. This $[M(T\phi_4)\phi]$ chain is found in the structures of the linarite-group minerals (Fig. 11e), and is also a fundamental building block for the $[M(T\phi_4)\phi]$ sheet (Fig. 12h) that is the structural unit in tsumcorite and bermanite (Appendix, Table IV).

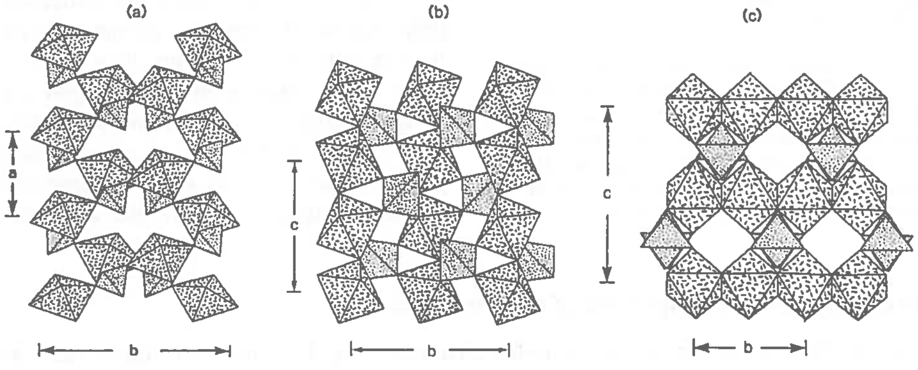

Fig. 14. Selected framework structures in $[M(T\phi_4)\phi_n]$ and $[M(T\phi_4)_2\phi_n]$ minerals: (a) the $[M(T\phi_4)\phi_3]$ framework structure of bonattite; (b) the $[M(T\phi_4)\phi]$ framework structure of titanite; (c) the $[M(T\phi_4)\phi]$ framework structure of descloizite.

These three examples show the type of structural variability we find in the framework structures, and also the small number of polyhedral linkage patterns (fundamental building blocks) that occur and seem common to a wide range of structural types. This suggests that these patterns of bond connectivity are very stable, and hence tend to persist from one structure-type to another. In addition, the incorporation of relatively primitive fragments into more highly-condensed structural units tends to support the conceptual approach of considering a large structure both topologically and energetically as an assemblage of smaller structural fragments.

(OH) and (H_2O) in oxysalt structures

Hydrogen has unusual stereochemical propensities and as a result, it has a unique role in controlling or moderating many aspects of structure and properties in inorganic crystals. The hydrogen cation H^+ commonly has a coordination number of [2] in inorganic structures; higher coordination numbers are not rare, but for simplicity we will consider the former, as the arguments presented here can easily be generalized to higher coordination numbers. There is usually a spontaneous distortion, with the hydrogen ion moving off-centre towards one of the two coordinating anions. The geometry of this arrangement has been well-characterized by neutron diffraction (Ferraris & Franchini-Angela, 1972); the typical arrangement is shown in Fig. 15. Brown (1976) has shown that the most common bond-valence distribution is about 0.80 *vu* to the closer oxygen, and approximately 0.20 *vu* to the further oxygen. This generally leads to the stronger bond being included in $(H_2O)^0$ or $(OH)^-$ groups that now become complex anions; the longer (weaker) bond is referred to as a *hydrogen bond*. The oxygen closer to the hydrogen is called the (hydrogen-bond) *donor*, and the oxygen further from the hydrogen is called the (hydrogen-bond) *acceptor* (Fig. 15).

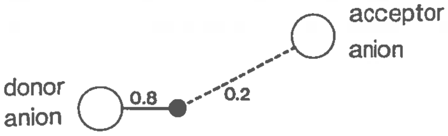

Fig. 15. Typical geometry of hydrogen coordination: the hydrogen is [2]-coordinated, and spontaneously moves off-centre to form two bonds of the approximate valence shown, and a bent O–H–O angle; the anion closer to the hydrogen is called the 'donor' anion, and the anion further from the hydrogen is called the 'acceptor' anion.

The $(OH)^-$ and $(H_2O)^0$ groups play a very important role in oxysalt structures, particularly with regard to the topological properties of their bond networks. The reason for this stems from the extremely polar nature of these two groups. On the oxygen side of each group, they function as an anion, whereas on the hydrogen side of each group, they function as a cation (Fig. 16); it is because of this unusual property that they play such a unique role in controlling the structure and chemistry of oxysalts.

(OH) and (H_2O) as components of the structural unit

Both of these groups have strong polar character (Fig. 16), and this allows them to control the character of the structural unit. On the Lewis-base side of each group, the bond valence is relatively strong, approximately 1.2 *vu* for (OH) and 0.4 *vu* for (H_2O); the remainder of the bond-valence requirements of the central oxygen is satisfied by the

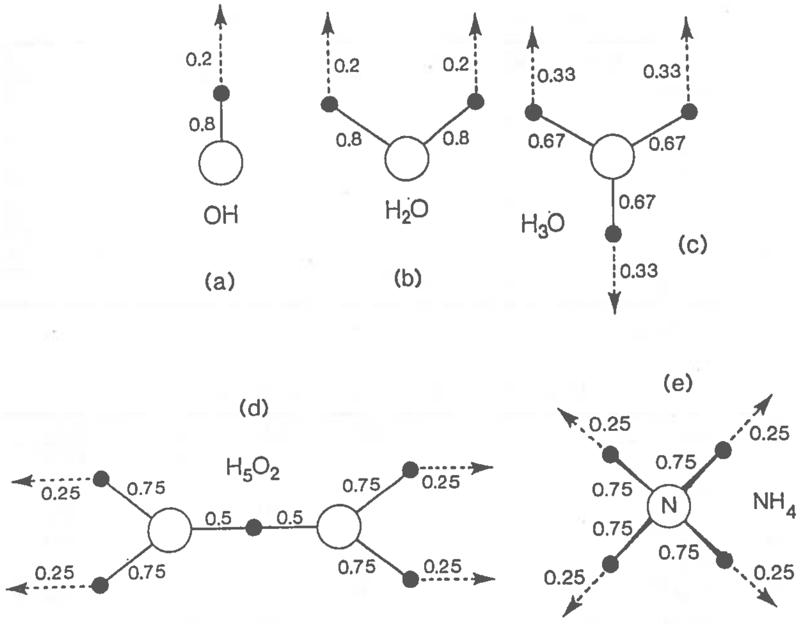

Fig. 16. Typical bond-valence distributions for the hydrogen-bearing groups found in minerals: (a) $(OH)^-$; (b) $(H_2O)^0$; (c) $(H_3O)^+$; (d) $(H_5O_2)^+$; (e) $(NH_4)^+$.

hydrogen atom(s). On the Lewis-acid side of the group, the bond-valence is relatively weak, about 0.2 *vu* for each group (Fig. 16). Thus on the Lewis-base (or anionic) side of the group, the strong bond constitutes part of the bonding network of the structural unit; conversely, on the Lewis-acid (or cationic) side of the group, the hydrogen bond is too weak to form part of the bonding network of the structural unit. Hence *the role of both (OH) and (H_2O) is to prevent the polymerization of the structural unit in specific directions.* Consequently, these groups play a crucial role in controlling the class of polymerization of the structural unit (Hawthorne, 1992).

The role of H as a control on structural polymerization is illustrated very well in the structure of newberyite [$Mg(PO_3OH)(H_2O)_3$], (Sutor, 1967). The structural unit is a sheet of corner-sharing (MgO_6) octahedra and (PO_4) tetrahedra, with the polyhedra arranged at the vertices of a 6^3 net (Fig. 12a); the bond-valence structure is shown in Table 3. In the (PO_4) tetrahedra, three of the ligands link to (MgO_6) octahedra within the sheet. The other ligand is 'tied off' orthogonal to the sheet by the fact that the oxygen is strongly bonded to a hydrogen atom (*i.e.*, it is a hydroxyl group). The long P–O bond of 1.59 Å contributes a bond-valence of 1.10 *vu* to the oxygen, and the remaining 0.90 *vu* is contributed by the hydrogen atom which then weakly hydrogen-bonds (bond valence of about 0.10 *vu*) to the neighbouring sheet in the *Y*-direction. In the (MgO_6) octahedra, three of the ligands link to (PO_4) tetrahedra within the sheets. The other ligands are 'tied off' by the fact that they are (H_2O) groups; the Mg–O bonds of 2.11, 2.12 and 2.13 Å contribute a bond-valence of approximately 0.32 *vu* to each oxygen, and the remaining 1.68 *vu* is contributed by the two hydrogen atoms which then weakly hydrogen-bond

Table 3. Bond-valence table (*vu*) for newberyite*

	Mg	P	H(6)	H(71)	H(72)	H(81)	H(82)	H(91)	H(92)	Sum
O(3)	0.389	1.399								1.788
O(4)	0.349	1.242	0.20	0.20						1.891
O(5)	0.364	1.232			0.20	0.20				1.996
O(6)		1.095	0.80				0.20			2.095
O(7)	0.326			0.80	0.80			0.20		2.126
O(8)	0.316					0.80	0.80		0.20	2.116
O(9)	0.313							0.80	0.80	1.913
Sum	2.057	4.968	1.0	1.0	1.0	1.0	1.0	1.0	1.0	

* calculated from the parameters of Brown & Altermatt (1985)

Table 4. Bond-valence table (*vu*) for artinite

	Mg	C	H(1)	H(2)	H(3)	H(4)	Sum
**O(1)	0.391		0.08			$0.80^{x2}\rightarrow$	2.071
**O(1)´	0.391	1.678	0.08				2.149
O(2)		$1.264^{x2}\downarrow$		0.30	0.30		1.864
OH	$0.372^{x2}\rightarrow$		0.92				2.014
	0.350						
OW	$0.283^{x2}\downarrow\rightarrow 2$			0.70	0.70		1.966
	2.051	4.206	1.00	1.00	1.00	1.00	

** O(1) and O(1)´ are disordered, and are both half-occupied

(~0.16 *vu* for each bond) to the neighbouring sheets in the Y-direction. The chemical formula of the structural unit is also the chemical formula of the mineral, and the sheet-like nature of the structural unit is controlled by the number and distribution of hydrogen atoms in the structure.

All intra-unit linkage stops at the (OH) and (H_2O) groups in newberyite. This is not necessarily the case in all structures; both (OH) and (H_2O) can allow intra-unit linkage in some directions and prevent it in others. A good example of this is artinite, $[Mg_2(CO_3)(OH)_2(H_2O)_3]$, (Akao & Iwai, 1977), (Fig. 17 and Table 4). The structural unit is a ribbon (chain) of edge-sharing (MgO_6) octahedra, flanked by (CO_3) triangles linked to alternate outer octahedral vertices of the ribbon in a staggered arrangement on either side of the ribbon. The anions down the centre of the ribbon are bonded to three Mg cations; they receive about $0.36 \times 3 = 1.08$ *vu* from the Mg cations, and thus receive 0.92 *vu* from their associated hydrogen atoms which then weakly hydrogen-bond (bond-valence approximately 0.08 *vu*) to an adjacent ribbon. The (OH) group thus *allows* linkage in the *X*- and *Y*-directions, but *prevents* linkage in the *Z*-direction. The anions bonded to Mg along the edge of the ribbon are bonded to either one Mg, two Mg, or one Mg and one C, with incident bond-valence contributions of about 0.3, 0.6, and 1.7 *vu*, respectively. The former two ligands must be (H_2O) groups which hydrogen-bond fairly strongly to anions in the same structural unit and in adjacent structural units. Thus the (H_2O) group bonded to one Mg prevents further unit polymerization in all three directions, whereas the (H_2O) group bonded to two Mg atoms allows polymerization in the *Y*-direction but prevents polymerization in the other two directions. The bond-valence

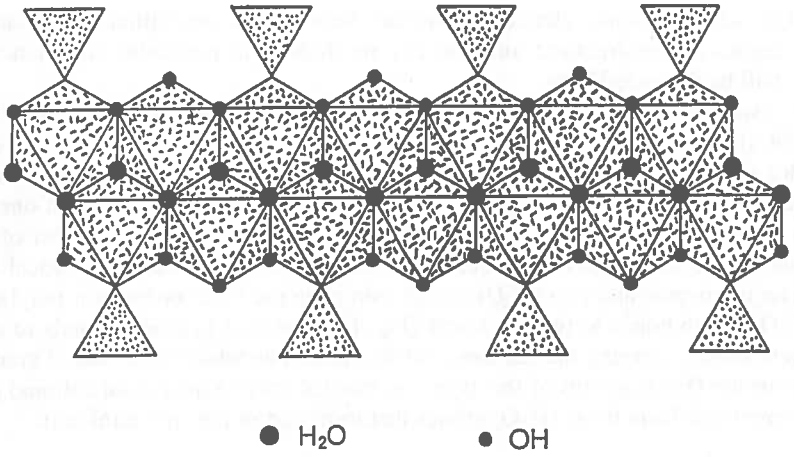

Fig. 17. The structural unit in artinite, a ribbon of ($Mg\phi_6$) octahedra and (CO_3) triangles; all simple anions not bonded to carbon are either (OH) or (H_2O).

requirements of the two anions bonded only to C are satisfied by hydrogen bonding involving donor atoms both in the same structural unit and in different structural units. Thus in artinite, all linkage between structural units is through hydrogen bonding *via* (OH) and (H_2O) groups of the structural units. In addition, the (OH) groups allow polymerization in two directions within the structural unit, whereas the two types of (H_2O) groups allow polymerization in one and no directions, respectively, within the structural unit.

Thus H, in the form of (OH) and (H_2O) groups, plays an important role in controlling the polymerization of the structural unit in oxysalt structures. Because of its very asymmetric distribution of bond-valences, the hydrogen atom can link to any strongly bonded unit, essentially preventing any further polymerization in that direction. Thus *the dimensionality of the structural unit is controlled primarily by the amount and role of hydrogen in the structure.*

(H_2O) groups bonded to interstitial cations

Iinterstitial cations are usually large and of low charge (Lima-de-Faria *et al.*, 1990); they are usually alkali or alkaline-earth cations with Lewis acidities significantly less than the cations belonging to the structural unit. Consequently, (H_2O) can function as a ligand for these cations whereas (OH) usually cannot, as the cation to which it must bond cannot contribute enough bond-valence (*i.e.* about 1.0 *vu*) for its bond-valence requirements to be satisfied. There are (at least) three possible reasons for (H_2O) groups to act as ligands for interstitial cations:

(a) to satisfy the bond-valence requirements around the interstitial cation in cases where there are insufficient anions available from adjacent structural units;

(b) to carry the bond-valence from the interstitial cation to a distant unsatisfied anion of an adjacent structural unit;

(c) to act as a bond-valence transformer between the interstitial cation and the anions of the structural unit; this is a mechanism of particular importance, and will be discussed later.

An example of (H_2O) of this type occurs in stringhamite (Hawthorne, 1985b) $[CaCu(SiO_4)](H_2O)$ (Fig. 18). The structural unit is a sheet of corner-sharing (SiO_4) tetrahedra and square-planar (CuO_4) polyhedra, arranged parallel to (010). These sheets are linked together by interstitial Ca atoms; each Ca links to four anions from one sheet and one anion from the adjacent sheet. Presumably the Ca coordination number of [5], a value that is rare for Ca, is not adequate with regard to the satisfaction of local bond-valence requirements, and two (H_2O) groups complete the Ca coordination polyhedron. Each (H_2O) group bonds to two Ca atoms (Fig. 18), and also hydrogen bonds to anions in adjacent sheets, carrying the Ca bond-valence to anions which otherwise it could not reach. Thus the (H_2O) groups of this type (*i.e.* bonded only to interstitial cations) play a very different role from those (H_2O) groups that form part of the structural unit.

Hydrogen-bonded interstitial (H_2O) groups

There are many structures in which interstitial (H_2O) groups are not bonded to any interstitial cations and yet occupy well-defined positions within a structure and participate in a hydrogen-bonding network. The (H_2O) groups of this sort act as both hydrogen-bond donors and hydrogen-bond acceptors. Any hydrogen-containing group (both (OH) and (H_2O) of the structural unit, interstitial (H_2O) bonded to interstitial cations, and inter-

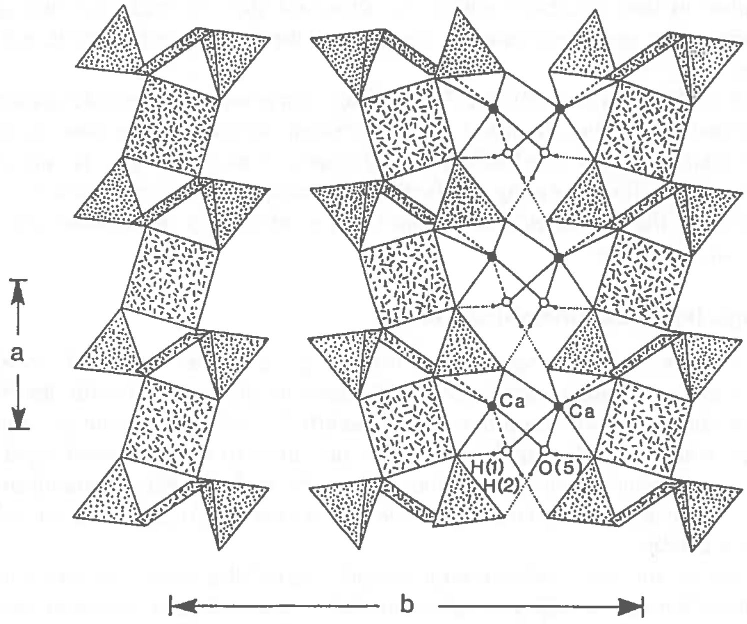

Fig. 18. The crystal structure of stringhamite projected on to (001); interstitial species are omitted on the left of the figure to emphasize the sheet-like nature of the structural unit.

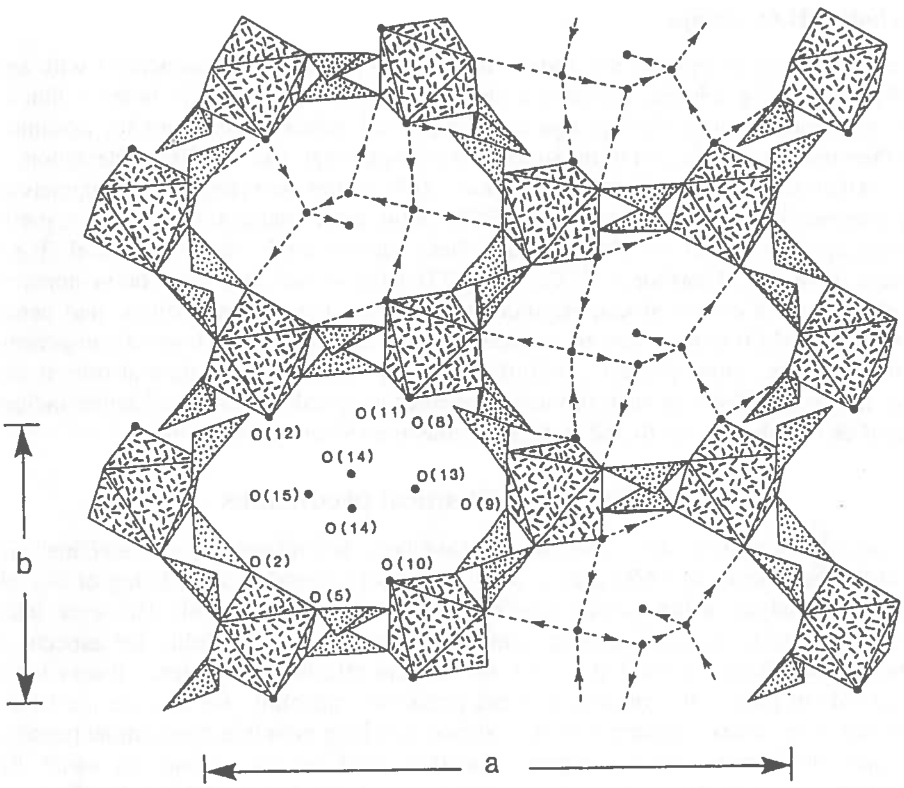

Fig. 19. The crystal structure of mandarinoite projected on to (001); note the two different types of (H_2O) groups, one bonded to cations of the structural unit, and the other held in the structure by hydrogen-bonding only.

stitial (H_2O) groups not bonded to the structural unit or interstitial cations) can act as a hydrogen-bond donor to (H_2O) groups of this sort, and any anion or (H_2O) group can act as hydrogen-bond acceptor for such (H_2O) groups. Crystals with such hydrogen-bonding networks can be thought of as intermediate between anhydrous structures and clathrate structures. The clathrate-like fragments that constitute these hydrogen-bonded networks have been designated as large examples of H–O groups (Emsley *et al.*, 1981). However, for the reasons cited above, I consider them not as single groups but as part of the interstitial structure.

The structure of mandarinoite, $[Fe_2^{3+}(SeO_3)_3(H_2O)_3](H_2O)_3$, shows such interstitial (H_2O) groups (Hawthorne, 1984b). The structural unit is a heteropolyhedral framework of corner-linked (SeO_3) triangular pyramids and (FeO_6) octahedra, with large cavities that are occupied by hydrogen-bonded (H_2O) groups in well-defined positions (Fig. 19). Thus of the six (H_2O) groups in the formula unit, three are bonded to Fe^{3+} and are part of the structural unit; the three remaining (H_2O) groups are interstitial and not bonded to any cation at all, but are held in place solely by a network of hydrogen bonds.

Occluded (H_2O) groups

Occluded (H_2O) groups are not bonded to any cation and are not associated with any hydrogen-bonding scheme; normally such (H_2O) groups are located in holes within or between structural units. Such groups can occupy well-defined crystallographic positions, but their linkage with the rest of the structure is solely through Van der Waals interaction.

Alkali-free beryl can have non-bonded (H_2O) groups occurring in the channels of the framework structure (Gibbs *et al.*, 1968). Most beryl contains alkali cations partly occupying sites within the channels, and these cations are bonded to channel (H_2O) groups. However, Hawthorne & Černý (1977) have shown that most beryl contains (H_2O) groups in excess of that required to coordinate the channel cations, and hence some of the (H_2O) groups must be occluded rather than occurring as bonded components of the structure. Although such (H_2O) does not play a significant structural role, it can have important effects on such physical properties as specific gravity, refractive indices (Černý & Hawthorne, 1976) and dielectric behaviour (Shannon *et al.*, 1992).

Structural and chemical predictions

The arguments we have developed thus far have been dealing with *a posteriori* analysis: bond-valence theory as a MO theory, development of a hierarchical ordering of oxysalt structures, analysis of the various roles of hydrogen in oxysalt crystals. However, what we really need to do is to develop some kind of predictive capability for aspects of structure and chemistry that have so far resisted our efforts. Bond-valence theory has a major role to play in this regard, as it has predictive capability; we can use the Lewis acid and base values, together with the valence-matching principle, to examine possible chemical interactions without requiring detailed structural information. By using this approach, we can begin to examine several aspects of structure and chemistry that have hitherto resisted our efforts.

Binary structural representation

One of the problems in dealing with inorganic structures is the complexity of the atom interactions; there are a large number of them, and their spatial characteristics are important. However, the same situation applies to an atom: there is a nucleus and numerous electrons, all interacting in a very complex manner; nevertheless, we can still usefully consider an atom as a single unit with simple properties such as size, charge and electronegativity. Why not take the same approach to the structural unit – consider it as a very complex oxyanion with intrinsic characteristic properties? When this is done (*e.g.*, Hawthorne, 1985a, 1986, 1990), we can define a Lewis basicity for the structural unit in exactly the same way that we do for a more conventional oxyanion.

The interstitial components may be cations (*e.g.*, alkalis or alkaline earths) and (H_2O) groups. As discussed above, (H_2O) groups may bond to interstitial cations; we may consider these as *complex cations* (*e.g.* $[Ca(H_2O)_7]^{2+}$ groups) which then have properties (*e.g.* Lewis acidities) very different from their constituent simple cations. The interstitial components of a structure can usually be considered in a simple additive fashion to produce an aggregate set of properties (*e.g.*, charge, Lewis acidity).

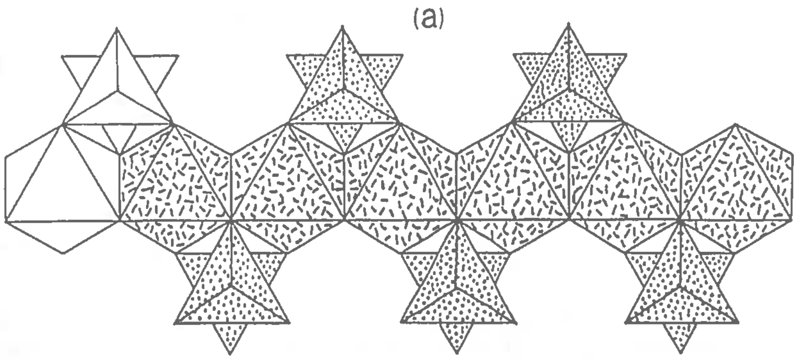

Fig. 20. The bond network in the structural unit of goedkenite.

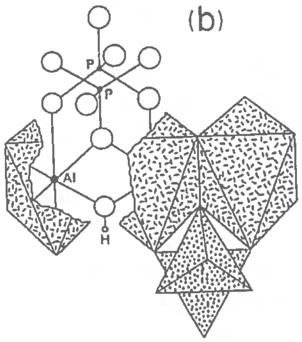

We have essentially factored the structure into two components, and this enables us to use the valence-matching principle to examine the interaction of the structural unit with the interstitial species. It is worth emphasizing here that we have developed a *binary representation* that gives us a simple quantitative model of even the most complicated structure, and allows us quantitative insight into the weak bonding between interstitial species and the structural unit.

This procedure may be illustrated using the structure of goedkenite (Moore *et al.*, 1975), $Sr_2[Al(PO_4)_2(OH)]$, the bond network of which is shown in Fig. 20. There are 9 oxygens in this fragment (as indicated by the general $[M(T\phi_4)_2\phi]$ form of the structural unit), and the residual anionic charge is 4^-. In order to calculate the basicity of this structural unit, we must assign simple anion coordination numbers to the unit. Obviously, there must be an objective process for doing this, as the calculation of structural-unit basicity hinges on this assignment. Fortunately, this assignment is fairly well-constrained by the general observation that most oxysalts of interest have oxygen in [3]- or [4]-coordination; of course, it is easy to think of exceptions, quartz (SiO_2) for example, but the fact that these exceptions are few 'proves the rule'. Normally, it is adequate to use the coordination number [4]; however, there are the following exceptions: (i) compounds with $M = 3^+$ and $T = 6^+$, for which the coordination number [3] is more appropriate; (ii) a coordination number of [3] (including H atoms) is more appropriate for (H_2O), and is also used for (OH) when it is bonded to M^{3+} cations. To attain an oxygen coordination number of [4], the cluster shown in Fig. 20 needs an additional number of bonds from the interstitial cations. From the connectivity of the structural unit, the cluster of Fig. 20 needs an additional 20 bonds; however, it will receive one (hydrogen) bond from an adjacent chain, which leaves 19 bonds to be received from the interstitial cations. These 19 bonds must come from 4^+ charges, and thus the average bond-valence required by the cluster is $4/19 = 0.22$ *vu*; this is the basicity of the structural unit in

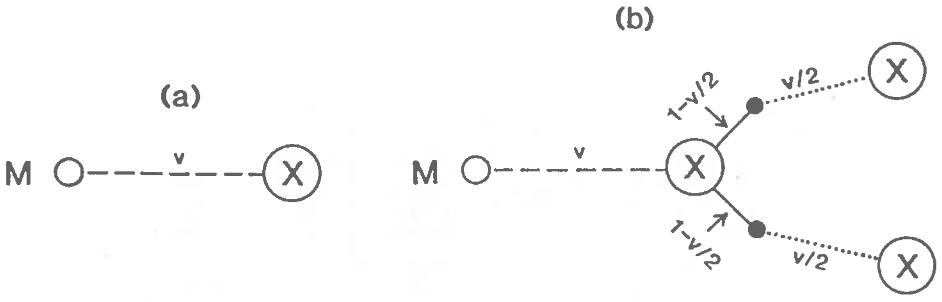

Fig. 21. The transformer effect of (H_2O) groups: (a) a cation, *M*, bonds to an oxygen *X* with bond valence v; (b) a cation, *M*, bonds to an oxygen *X* of an (H_2O) group, and the strong bond is split into two weaker bonds (hydrogen bonds) *via* the bond-valence requirements of the constituent H^+ and O^{2-} ions; ● = hydrogen atom.

goedkenite. Examination of the table of Lewis acid strengths (Table 1) shows that the cations of appropriate Lewis acidity are Pb(0.20 *vu*), Sr(0.24 *vu*) and Ba(0.20 *vu*); in agreement with this, Sr is the interstitial cation in goedkenite.

(H_2O) as a bond-valence transformer

Let a cation, *M*, bond to an anion *X* (Fig. 21a); the anion *X* receives a bond-valence of v valence units from the cation *M*. Consider a cation, *M*, that bonds to an (H_2O) group which in turn bonds to an anion *X* (Fig. 21b). In the second case, the oxygen receives a bond-valence of v valence units from the cation *M*, and its bond-valence requirements are satisfied by two short O–H bonds of valence (1–v/2) valence units. To satisfy the bond-valence requirements around each hydrogen atom, each hydrogen forms at least one hydrogen-bond with its neighbouring anions. In Fig. 21b, one of these hydrogen bonds is to the *X* anion which thus receives a bond-valence of one half what it received when it was bonded directly to the *M* cation. Thus the (H_2O) group acts as a *bond-valence transformer*, causing one bond (bond valence = v *vu*) to be split into two weaker bonds (bond valence = v/2 *vu*). *It is this transformer effect that is the key to understanding the role of interstitial* (H_2O) *in crystals.*

Interstitial (H_2O)

Interstitial (H_2O) may coordinate interstitial cations or it may occur solely as a component of a hydrogen-bonded network. Whichever is the case, the (H_2O) occupies fixed atomic positions and must play a role in the stability of the structure. The key to understanding this role is found in two distinct ideas of bond-valence theory:

(a) (H_2O) as a bond-valence transformer
(b) application of the valence-matching principle to the interaction between the structural unit and the interstitial cations.

Ideally, the valence of the bonds from the interstitial cations to the structural unit must match the Lewis basicity of that structural unit; if they do not match, then there cannot be a stable interaction and that particular structural arrangement will not occur. However, if the Lewis acidity of the interstitial cation is too large, the cation may bond

Table 5. Details of H_2O 'of hydration' in botryogen

Botryogen: $Mg_2[Fe^{3+}_2(SO_4)_4(OH)_2(H_2O)_2](H_2O)_{10}$

Bonded atoms	Number of anions	Ideal coordination number	Bonds needed for ideal coordination
S	10	3	2 x 10
S + Fe^{3+}	6	3	1 x 6
$2Fe^{3+}$ + H	2	3	0
Fe^{3+} + 2H	2	3	0

Bonds needed to structural unit = $2 \times 10 + 1 \times 6 = 26$
No. of H bonds to structural unit = $2 \times 2 + 2 \times 1 = 6$
No. of additional bonds needed = $26 - 6 = 20$
Charge on structural unit = 4^-
Lewis basicity of structural unit = 4/20 = 0.20 *vu*

Interstitial cation(s) is Mg
Mg coordination = $\{5H_2O + O\}$
Bonds from Mg to structural unit = $5 \times 2 + 1 = 11$
Effective Lewis acidity of Mg = $2/\{5 \times 2 + 1\} = 0.19$ *vu*
The interstitial (H_2O) has moderated the Lewis acidity of the interstitial cation such that the valence-matching principle is satisfied.

to an interstitial (H_2O) group which acts as a bond-valence transformer, taking the strong bond and transforming it into two weaker bonds (Fig. 21). In this way, *incorporation of interstitial (H_2O) into the structure can moderate the Lewis acidity of the interstitial cations such that the valence-matching principle is satisfied.*

Let us consider the hydroxy-hydrated ferric-iron sulphate mineral botryogen (Süsse, 1968b), $Mg_2[Fe^{3+}_2(SO_4)_4(OH)_2(H_2O)_2](H_2O)_{10}$; why does this mineral have 10 interstitial (H_2O) groups per structural formula? The coordinations of the various anions in the structural unit are shown in Table 5. Using the ideal coordination numbers discussed earlier (= [3] for all the simple anions in botryogen), the structural unit needs an additional 26 bonds to achieve ideal coordination of all its simple anions. Six of these bonds will be hydrogen bonds from (OH) and (H_2O) groups within the structural unit or in adjacent structural units, leaving 20 bonds needed from interstitial cations. Thus the Lewis basicity of the structural unit in botryogen is the charge divided by the number of required bonds: 4/20 = 0.20 *vu*. he interstitial cations in botryogen are Mg, with a Lewis acidity of 0.36 *vu*. The valence-matching principle is violated, and a stable structure should not form. However, the interstitial Mg atoms are coordinated by $\{5(H_2O)+O\}$, and this will moderate the effective Lewis acidity of the cation *via* the transformer effect of (H_2O). The effective Lewis acidity of the 'complex cation' $\{Mg(H_2O)_5O\}$ is the charge divided by the number of bonds: $2 / (5 \times 2 + 1) = 0.19$ *vu*. The moderated Lewis acidity of the complex interstitial cation matches the Lewis basicity of the structural unit, and a stable structure is formed.

Bond-valence controls on interstitial cations

Apart from the requirement of electroneutrality, the factors that govern the identity of the interstitial cations are obscure. In synthetic crystals, this point is less obvious than in minerals. When synthesizing crystals, we select the chemical systems used, thereby

Table 6. Minerals with chain units of stoichiometry $[M^{2+}(T^{5+}O_4)_2(H_2O)_2]$ and $[M^{2+}(T^{5+,6+}O_4)_2(H_2O,OH)]$

$[M^{2+}(T^{5+}O_4)_2(H_2O)_2]$		$[M^{2+}(T^{5+,6+}O_4)_2(H_2O,OH)]$	
Brandtite	$Ca_2[Mn(AsO_4)_2(H_2O)_2]$	Arsenbrackebuschite	$Pb_2[Fe^{2+}(AsO_4)_2(H_2O)]$
*Kröhnkite	$Na_2[Cu(SO_4)_2(H_2O)_2]$	Arsentsumebite	$Pb_2[Cu(SO_4)(AsO_4)(OH)]$
Roselite	$Ca_2[Co(AsO_4)_2(H_2O)_2]$	Brackebuschite	$Pb_2[Mn(VO_4)_2(H_2O)]$
		Gamagarite	$Ba_2[(Fe^{3+},Mn)(VO_4)_2(OH,H_2O)]$
Cassidyite	$Ca_2[Ni(PO_4)_2(H_2O)_2]$	Goedkenite	$Sr_2[Al(PO_4)_2(OH)]$
Collinsite	$Ca_2[Mg(PO_4)_2(H_2O)_2]$	Tsumebite	$Pb_2[Cu(PO_4)(SO_4)(OH)]$
Gaitite	$Ca_2[Zn(AsO_4)_2(H_2O)_2]$		
Roselite-beta	$Ca_2[Co(AsO_4)_2(H_2O)_2]$	Fornacite	$Pb_2[Cu(AsO_4)(CrO_4)(OH)]$
Talmessite	$Ca_2[Mg(AsO_4)_2(H_2O)_2]$	Molybdofornacite	$Pb_2[Cu(AsO_4)(MoO_4)(OH)]$
		*Törnebohmite	$(RE)_2[Al(SiO_4)_2(OH)]$
Fairfieldite	$Ca_2[Mn(PO_4)_2(H_2O)_2]$		
Messelite	$Ca_2[Fe^{2+}(PO_4)_2(H_2O)_2]$	Vauquelinite	$Pb_2[Cu(PO_4)(CrO_4)(OH)]$

* The different-valence cations in the structural units of kröhnkite and törnebohmite force different-valence interstitial cations for these two minerals.

excluding other components from the crystal. This is not the case for minerals. Here, the chemical system is often extremely large, and the crystallizing structure has access to a large variety of possible constituents. However, inspection of mineral compositions from a wide variety of chemical environments and geographical locations shows that a specific structure-type can have extreme selectivity in the incorporation of interstitial cations. Table 6 shows minerals of general stoichiometries $[M^{2+}(T^{5+}O_4)_2(H_2O)_2]$ and $[M^{2+}(T^{5+}O_4)_2(H_2O)]$. Both contain interstitial divalent (M^{2+}) cations, and yet the interstitial cations seem mutually exclusive between the two groups (it should be emphasized that this is *not* a geochemical feature; both sets of cations were often available for incorporation into these structures). The analogous situation in synthetic materials is the non-isostructural nature of analogous isochemical $Ca–(Sr,Ba,Pb^{2+})$ compounds.

What makes the nature of the interstitial species so sensitive to the character of the structural unit? We find the answer to this problem in the application of the valence-matching principle to our binary representation of structure. The Lewis acidity of the interstitial cation must match with the basicity of the structural unit. It is not enough that the interstitial cation have the correct valence, it must also have the correct Lewis acidity. Let us examine the example outlined in the previous paragraph, that is the identity of the interstitial cations in the $[M^{2+}(T^{5+}O_4)_2(H_2O)_2]$ and $[M^{2+}(T^{5+}O_4)_2(H_2O)]$ structures, using brandtite and brackebuschite as examples.

For brandtite (Hawthorne & Ferguson, 1977; $Ca_2[Mn^{2+}(AsO_4)_2(H_2O)_2]$), the situation is shown in Table 7; counting the bonds within the structural unit indicates that an additional 20 bonds to the structural unit are needed to attain the requisite simple-anion coordination numbers. Four of these bonds are hydrogen bonds from other structural units, leaving 16 bonds to be contributed by the interstitial cations. The residual charge on the structural unit is 4^- (per $[Mn^{2+}(AsO_4)_2(H_2O)_2]$ unit), and hence the basicity of the structural unit is $4/16 = 0.25$ *vu*. Inspection of the Lewis acidity table (Table 1) shows that Ca has a Lewis acidity of 0.27 *vu*, matching up with the Lewis basicity of the structural unit. Hence the valence-matching principle is satisfied, and brandtite, $Ca_2[Mn^{2+}(AsO_4)_2(H_2O)_2]$ is a stable structure.

Table 7. Calculation of structural-unit basicity for brandtite and brackebuschite

Brandtite = $Ca_2[Mn^{2+}(AsO_4)_2(H_2O)_2]$ Structural unit = $[Mn^{[6]}(As^{[4]}O_4)_2(H_2^{[2]}O)_2]$
Number of bonds in structural unit = 1 × [6] + 2 × [4] + 2 × [2] = 18
Number of bonds needed for [4]-coordination of all simple anions (except (H_2O) for which [3]-coordination is assigned) = 8 × [4] + 2 × [3] = 38
Number of additional bonds to structural unit to achieve this coordination = 20
Number of hydrogen bonds to structural unit = 2 × 2 = 4
Therefore the number of bonds required from interstitial cations = 20 4 = 16
Charge on the structural unit $[Mn^{2+}(AsO_4)_2(H_2O)_2]$ in brandtite = 4^-
Lewis basicity of structural unit = charge/bonds = 4/16 = 0.25 *vu*
This basicity matches most closely with the Lewis acidity of Ca at 0.27 *vu*
Thus the formula of brandtite is $Ca_2[Mn(AsO_4)_2(H_2O)_2]$

Brackebuschite = $Pb_2[Mn^{2+}(VO_4)_2(H_2O)]$ Structural unit = $[Mn^{[6]}(V^{[4]}O_4)_2(H^{[2]}{}_2O)]$
Number of bonds in structural unit = 1 × [6] + 2 × [4] + 2 × [1] = 16
Number of bonds needed for [4]-coordination of all simple anions (including (H_2O) which is [4]-coordinated in this structural unit) = 9 × [4] = 36
Number of additional bonds to structural unit to achieve this coordination = 20
Number of hydrogen bonds to structural unit = 2
Number of bonds required from interstitial cations = 18
Charge on the structural unit $[Mn^{2+}(VO_4)_2(H_2O)]$ in brackebuschite = 4^-
Lewis basicity of structural unit = charge/bonds = 4/18 = 0.22 *vu*
This basicity matches most closely with the Lewis acidity of Pb at 0.20 *vu*
Thus the formula of brackebuschite is $Pb_2[Mn(VO_4)_2(H_2O)]$

For brackebuschite (Donaldson & Barnes, 1955; $Pb_2[Mn^{2+}(VO_4)_2(H_2O)]$), the situation is also shown in Table 7; an additional 20 bonds are needed to satisfy the requisite simple-anion coordination requirements. Two of these bonds are hydrogen bonds from adjacent structural units, leaving 18 bonds to be satisfied by interstitial cations. The residual charge on the structural unit is 4^-, and hence the basicity of the structural unit is 4/18 = 0.22 *vu*. This value matches up quite well with the Lewis basicity of Pb^{2+} (0.20 *vu*, see Table 1), the valence-matching principle is satisfied, and $Pb^{2+}[Mn^{2+}(V^{5+}O_4)_2(H_2O)]$ is a stable structure.

Some very interesting questions now become apparent concerning the nature of crystallization:

(1) Does the form of the structural unit dictate the identity of the interstitial cations, or does the availability of a particular interstitial cation dictate the form of the structural unit?
(2) Does the pH of the environment affect the form of the structural unit or the amount of interstitial (H_2O) incorporated into the structure?
(3) Are there synergetic interactions between these factors?

Using bond-valence theory in conjunction with the topological characteristics of the structural unit, we can begin to investigate some of these questions.

Summary

Bond topology has a major effect on the energetics of a structure, suggesting that major trends in structure stability, properties and behaviour should be systematically related to the coordination geometry and polyhedral linkage of a structure. Combination of these ideas with bond-valence theory (a very simple form of molecular-orbital theory) allows simple binary representation of even the most complex structure: a (usually anionic) structural unit that interacts with (usually cationic or neutral) interstitial species to form the complete structure. This interaction can be quantitatively examined in terms of the Lewis basicities and acidities of the binary components; such features as interstitial-cation chemistry and 'water' of hydration can be explained and quantitative predictions can be made.

The principal idea here is to develop an approach that is reasonably transparent to chemical and physical intuition, and that can be applied to large numbers of very complex structures. There is need for a simple approach that addresses the more global aspects of complex oxysalt structures. These ideas tend to be intuitive and semi-quantitative, but are capable of organizing a large amount of information into a coherent framework, and also provide a basis for thinking about many questions that were intractable to previous approaches.

Acknowledgements

This work was supported by the Natural Sciences and Engineering Council of Canada in the form of an Operating Grant to the author.

References

Abbona, F., Calleri, M. & Ivaldi, G.(1984): Synthetic struvite, $MgNH_4PO_4 \cdot 6H_2O$: correct polarity and surface features of some complementary forms. *Acta Crystallogr.*, **B40**:223–227.

Akao, M. & Iwai, S. (1977): The hydrogen bonding of artinite. *Acta Crystallogr.*, **B33**:3951–3953.

Albright, T.A., Burdett, J.K. & Whangbo, M.H. (1985): *Orbital interactions in chemistry*. New York: Wiley Interscience.

Allman, R. & Donnay, G. (1973): The crystal structure of julgoldite. *Mineral. Mag.*, **38**:271–281.

Bachet, B., Cesbron, F. & Chevalier, R.L (1981): Structure cristalline de la khademite $Al(SO_4)F \cdot 5H_2O$. *Bull. Minéral.*, **104**:19–22.

Bachmann, H.G. & Zemann, J. (1961): Die Kristallstruktur von Linarit, $PbCuSO_4(OH)_2$. *Acta Crystallogr.*, **14**:747–753.

Bacon, D.E. & Curry, N.A. (1962): The water molecules in $CuSO_4 \cdot 5H_2O$. *Proc. R. Soc. London*, **266**:95–108.

Bailey, S.W. (1980): Structures of layer silicates. *In* Brindley, G.W. and Brown, G. (eds): *Crystal structures of clay minerals and their X-ray identification*. London: Mineral. Soc., 1–123.

Balko, V.P. & Bakakin, V.V. (1975): The crystal structure of the natural yttrium and rare-earth fluortitanosilicate $(Y,Tr)_4(F,OH)_6TiO(SiO_4)_2$ (Yftisite). *Zh. Strukt. Khim.*, **16**:837–842.

Baur, W.H. (1959): Die Kristallstruktur des Edelamblygonits $LiAlPO_4(OH,F)$. *Acta Crystallogr.*, **12**:988–994.

Baur, W.H. (1962): Zur Kristallchemie der Salzhydrate. Die Kristallstrukturen von $MgSO_4 \cdot 4H_2O$ (Leonhardtit) and $FeSO_4 \cdot 4H_2O$ (Rozenit). *Acta Crystallogr.*, **15**:815–826.

Baur, W.H. (1964a): On the crystal chemistry of salt hydrates. II. A neutron diffraction study of $MgSO_4.4H_2O$. *Acta Crystallogr.*, **17**:863–869.

Baur, W.H. (1964b): On the crystal chemistry of salt hydrates. III. The determination of the crystal structure of $FeSO_4.7H_2O$ (melanterite) *Acta Crystallogr.*, **17**:1167–1174.

Baur, W.H. (1969a): The crystal structure of paravauxite, $Fe^{2+}Al_2(PO_4)_2(OH)_2(OH_2)_6 \cdot 2H_2O$. *Neues Jahrb. Mineral. Monatsh.*, **1969**:430–433.

Baur, W.H. (1969b): A comparison of the crystal structures of pseudolaueite and laueite. *Am. Mineral.*, **54**:1312–1323.

Baur, W.H. (1970): Bond length variation and distorted coordination polyhedra in inorganic crystals. *Trans. Am. Crystallogr. Assn.*, **6**: 129–155.

Baur, W.H. (1971): The prediction of bond length variations in silicon-oxygen bonds. *Am. Mineral.*, **56**:1573 1599.

Baur, W.H. (1978): Crystal structure refinement of lawsonite. *Am. Mineral.*, **63**:311–315.

Baur, W.H. (1981): Interatomic distance predictions for computer simulations of crystal structures. *In* O'Keeffe, M. & Navrotsky, A: (eds.): *Structure and bonding in crystals*. New York: Academic Press, **2**:31–51.

Baur, W.H. (1987): Effective ionic radii in nitrides. *Crystallogr. Rep.*, **1**:59–83.

Baur, W.H. & Rama Rao, B. (1967): The crystal structure of metavauxite. *Naturwissenschaften*, **21**:561–562.

Baur, W.H. & Rolin, J.L. (1972): Salt hydrates. IX. The comparison of the crystal structure of magnesium sulfate pentahydrate with copper sulfate pentahydrate and magnesium chromate pentahydrate. *Acta Crystallogr.*, **B28**:1448–1455.

Beevers, C.A. & Lipson, H. (1932): The crystal structure of nickel sulphate hexahydrate, $NiSO_4{\cdot}6H_2O$. *Z. Kristallogr.*, **83**:123–135.

Bladh, K.W., Corbett, R.K., McLean, W.J. & Laughton, R.B. (1972): The crystal structure of tilasite. *Am. Mineral.*, **57**:1880–1884.

Blount, A.M., Threadgold, L.M. & Bailey, S.W. (1969): Refinement of the crystal structure of nacrite. *Clays and Clay Miner.*, **17**:185–194.

Borene, J. (1970): Structure cristalline de la parabutlerite. *Bull. Soc. Fr. Minéral. Crystallogr.*, **93**:185–189.

Bragg, W.L. (1913): The structure of some crystals as indicated by their diffraction of X-rays. *Proc. R. Soc. London*, **A89**:248–263.

Bragg, W.L. (1930): The structure of silicates. *Z. Kristallogr.*, **74**:237–305.

Bragg, W.L. (1955): *The crystalline state. A general survey.* London: Bell.

Brotherton, P.D., Maslen, E.N., Pryce, M.W. & White, A.H. (1974): Crystal structure of collinsite. *Aust. J. Chem.*, **27**:653–656.

Brown, I.D. (1976): On the geometry of O–H...O hydrogen bonds. *Acta Crystallogr.*, **A32**:24–31.

Brown, I.D. (1981): The bond-valence method; an empirical approach to chemical bonding and structure. *In* O'Keeffe, M. & Navrotsky, A: (eds.): *Structure and bonding in crystals*. New York: Academic Press, **2**:1–30.

Brown, I.D. (1992): Chemical and steric constraints in inorganic solids. *Acta Crystallogr.*, **B48**:553–572.

Brown, I.D. & Altermatt, D. (1985): Bond-valence parameters obtained from a systematic analysis of the inorganic crystal structure database. *Acta Crystallogr.*, **B41**:244–247.

Brown, I.D. & Shannon, R.D. (1973): Empirical bond-strength–bond-length curves for oxides. *Acta Crystallogr.*, **A29**:266–282.

Burdett, J.K. (1980): *Molecular shapes*. New York: Wiley.

Burdett, J.K. (1986): Structural-electronic relationships in the solid state. *In* Greenberg, A. & Leibman, J.F. (eds.): *Molecular structure and energetics*. Boca Raton: VCH Publishers, 209–275

Burdett, J.K. (1987): Some structural problems examined using the method of moments. *Struct. Bond. (Berlin)*, **65**:29–89.

Burdett, J.K. & Hawthorne, F.C. (1993): An orbital approach to the theory of bond-valence. *Am. Mineral.*, **78**:884–892.

Burdett, J.K., Lee, S. & Sha, W.C. (1984): The method of moments and the energy levels of molecules and solids. *Croat. Chem. Acta*, **57**:1193–1216.

Burdett, J.K. & McLarnan, T.J. (1984): An orbital interpretation of Pauling's rules. *Am. Mineral.*, **69**:601–621.

Burnham, C.W. (1966): Ferrosilite. *Carnegie Inst. Wash. Year Book*, **65**:285–290.

Burns, P.C., Eby, R.K. & Hawthorne, F.C. (1991): Liroconite, $Cu_2Al(AsO_4)(OH)_4(H_2O)_4$, a heteropolyhedral oxysalt mineral. *Acta Crystallogr.*, **C47**:916–919.

Burns, P.C., Grice, J.D. & Hawthorne, F.C. (1995): Borate minerals. I. Polyhedral clusters and fundamental building blocks. *Can. Mineral*, **33**:1131–1151.

Calleri, M., Gavetti, A., Ivaldi, G. & Rubbo, M. (1984): Synthetic epsomite, $MgSO_4{\cdot}7H_2O$: absolute configuration and surface features of the complementary {111} forms. *Acta Crystallogr.*, **B40**:218–222.

Cameron, M. & Papike, J.J. (1981): Structural and chemical variations in pyroxenes. *Am. Mineral.*, **66**:1–50.

Carapezza, M. & Riva di Sanseverino, L. (1968): Crystallography and genesis of double sulfates and their hydrates. II. Structure, powder pattern and thermoanalysis of cyanochroite, $K_2Cu(SO_4)_2{\cdot}6H_2O$. *Mineral. Petrol. Acta*, **14**:23–37.

Carapezza, M. & Riva di Sanseverino, L. (1970): Crystallography and genesis of double sulfates and their hydrates. III. Picromerite, $K_2Mg(SO_4)_2{\cdot}6H_2O$: a methodological check. *Mineral. Petrol. Acta.*, **16**:5–11.

Catti, M. & Franchini-Angela, M. (1979): Krautite, $Mn(H_2O)(AsO_3OH)$: crystal structure, hydrogen bonding and relations with haidingerite and pharmacolite. *Am. Mineral.*, **64**:1248–1254.

Catti, M., Ferraris, G. & Ivaldi, G. (1977): Hydrogen bonding in the crystalline state. Structure of talmessite, $Ca_2(Mg,Co)(AsO_4)_2{\cdot}2H_2O$ and crystal chemistry of related minerals. *Bull. Soc. Fr. Minéral. Cristallogr.*, **100**:230–236.

Catti, M., Ferraris, G. & Ivaldi, G. (1979): Refinement of the crystal structure of anapaite, $Ca_2Fe(PO_4)_2{\cdot}4H_2O$: hydrogen bonding and relationships with the bihydrated phase. *Bull. Soc. Fr. Minéral. Cristallogr.*, **102**:314–318.

Catti, M., Chiari, G. & Ferraris, G. (1980): Fluckite, $CaMn(HAsO_4)_2{\cdot}2H_2O$, a structure related by pseudo-polytypism to krautite $MnHAsO_4{\cdot}H_2O$. *Bull. Minéral.*, **103**:129–134.

Černý, P. & Hawthorne, F.C. (1976): Refractive indices versus alkali contents in beryl: general limitations and applications to some pegmatite types. *Can. Mineral.*, **14**:491–497.

Christ, C.L. (1960): Crystal chemistry and systematic classification of hydrated borate minerals. *Am. Mineral.*, **45**:334–340.

Christ, C.L. & Clark, J.R. (1977): A crystal-chemistry classification of borate structures with emphasis on hydrated borates. *Phys. Chem. Miner.*, **2**:59–87.

Cocco, G., Fanfani, L. & Zanazzi, P.F. (1967): The crystal structure of fornacite. *Z. Kristallogr.*, **124**:385–397.

Cromer, D.T., Kay, M.I. & Larsen, A.C. (1967): Refinement of the alum structures. II. X-ray and neutron diffraction of $NaAl(SO_4)_2{\cdot}12H_2O$, gamma-alum. *Acta Crystallogr.*, **22**:182–187.

Dollase, W.A. (1968): Refinement and comparison of the structures of zoisite and clinozoisite. *Am. Mineral.*, **53**:1882–1898.

Dollase, W.A. (1969): Crystal structure and cation ordering of piemontite. *Am. Mineral.*, **54**:710–717.

Dollase, W.A. (1971): Refinement of the crystal structure of epidote, allanite and hancockite. *Am. Mineral.*, **56**:447–464.

Donaldson, D.M. & Barnes, W.H. (1955): The structures of the minerals of the descloizite and adelite groups: III - brackebuschite. *Am. Mineral.*, **40**:597–613.

Donnay, G. & Allmann, R. (1968): Si_3O_{10} groups in the crystal structure of ardennite. *Acta Crystallogr.*, **B24**:845–855.

Donnay, G. & Allmann, R. (1970): How to recognize O^{2-}, OH^-, and H_2O in crystal structures determined by X-rays. *Am. Mineral.*, **55**:1003–1015.

Eby, R.K. & Hawthorne, F.C. (1993): Structural relations in copper oxysalt minerals. I. Structural hierarchy. *Acta Crystallogr.*, **B49**:28–56.

Emsley, J., Jones, D.H. & Lucas, J. (1981): Detecting and measuring strong hydrogen bonds: recent developments. *Rev. Inorg. Chem.*, **3**:105–140.

Evans, H.T. Jr. & Mrose, M.E. (1977): The crystal chemistry of the hydrous copper silicates, shattuckite and plancheite. *Am. Mineral.*, **62**:491–502.

Fanfani, L. & Zanazzi, P.F. (1968): The crystal structure of vauquelinite and the relationship to fornacite. *Z. Kristallogr.*, **126**:433–443.

Fanfani, L., Nunzi, A. & Zanazzi, P.F. (1970a): The crystal structure of roemerite. *Am. Mineral.*, **55**:78–89.

Fanfani, L., Nunzi, A. & Zanazzi, P.F. (1970b): The crystal structure of fairfieldite. *Acta Crystallogr.*, **B26**:640–645.

Fanfani, L., Nunzi, A. & Zanazzi, P.F. (1971): The crystal structure of butlerite. *Am. Mineral.*, **56**:751–757.

Fanfani, L., Tomassini, M., Zanazzi, P.F. & Zanzari, A.R. (1978): The crystal structure of strunzite, a contribution to the crystal chemistry of basic ferric-manganous hydrated phosphates. *Tschermaks Mineral. Petrogr. Mitt.*, **25**:77–87.

Fang, J.H. & Robinson, P.D. (1972): Crystal structures and mineral chemistry of double-salt hydrates: II. The crystal structure of mendozite, $NaAl(SO_4)_2{\cdot}11H_2O$. *Am. Mineral.*, **57**: 1081–1088.

Ferguson, R.B. (1974): A cation-anion distance-dependent method for evaluating valence-bond distributions in ionic structures and results for some olivines and pyroxenes. *Acta Crystallogr.*, **B30**:2527–2542.

Ferraris, G. & Franchini-Angela, M. (1972): Survey of the geometry and environment of water molecules in crystalline hydrates studied by neutron diffraction. *Acta Crystallogr.*, **B28**:3572–3583.

Ferraris, G. & Franchini-Angela, M. (1973): Hydrogen bonding in the crystalline state. Crystal structure of $MgHAsO_4.7H_2O$, roesslerite. *Acta Crystallogr.*, **B29**:286–292.

Ferraris, G., Jones, D.W. & Yerkess, J. (1973): Refinement of the crystal structure of magnesium sulphate heptahydrate (epsomite) by neutron diffraction. *J. Chem. Soc., Dalton Trans.*, 816–821.

Finney, J.J. (1963): The crystal structure of carminite. *Am. Mineral.*, **48**:1–13.

Galli, E. & Alberti, A. (1969): On the crystal structure of pumpellyite. *Acta Crystallogr.*, **B25**:2276–2281.

Ghose, S., Leo, S. & Wan, C. (1974): Structural chemistry of copper and zinc minerals. Part I. Veszelyite, $(Cu,Zn)_2ZnPO_4(OH)_3 \cdot 2H_2O$: a novel type of sheet structure and crystal chemistry of copper-zinc substitution. *Am. Mineral.*, **59**:573–581.

Ghose, S., Wan, C. & Okamura, F.P. (1975): Site preference and crystal chemistry of transition metal ions in pyroxenes and olivines. *Acta Crystallogr.*, **A31**:S76 (abstr.).

Giacovazzo, C., Scandale, E., & Scordari, F.(1976a): The crystal structure of chlorothionite, $CuK_2Cl_2SO_4$. *Z. Kristallogr.*, **144**:226–237.

Giacovazzo, G., Scordari, F., Todisco, A. & Menchetti, S. (1976b): Crystal structure model for metavoltine from Sierra Gorda. *Tschermaks Mineral. Petrogr. Mitt.*, **23**:155–165.

Gibbs, G.V. (1982): Molecules as models for bonding in silicates. *Am. Mineral.*, **67**:421–450.

Gibbs, G.V., Breck, D.W. & Meagher, E.P. (1968): Structural refinement of hydrous and anhydrous beryl, $Al_2(Be_3Si_6)_{18}$ and emerald, $Al_{1.9}Cr_{0.1}(Be_3Si_6)O_{18}$. *Lithos*, 1:275–285.

Gibbs, G.V., Hamil, M.M., Louisnathan, S.J., Bartell, L.S. & Yow, H. (1972): Correlations between Si–O bondlength, Si–O–Si angle and bond-overlap populations calculated using extended Hückel molecular orbital theory. *Am. Mineral.*, **57**:1578–1613.

Ginderow, D. & Cesbron, F. (1979): Structure cristalline de l'aubertite, $AlCuCl(SO_4)_2 \cdot 14H_2O$. *Acta Crystallogr.*, **B35**:2499–2502.

Giuseppetti, E. & Tadini, C. (1984): The crystal structure of childrenite from Tavistock (S.W. England), $Ch_{89}Eo_{11}$ term of childrenite-eosphorite series. *Neues Jahr. Mineral. Mon.*, 263–271.

Golovastikov, N.I. (1974): Crystal structure of the alkali titanosilicate labuntsovite. *Sov. Phys. Crystallogr.*, **18**:596–599.

Graeber, E.J. & Rosenzweig, A. (1971): The crystal structures of yavapaiite, $KFe(SO_4)_2$, and goldichite, $KFe(SO_4)_2 \cdot 4H_2O$. *Am. Mineral.*, **56**:1917–1933.

Graeber, E.J., Morosin, B. & Rosenzweig, A. (1965): The crystal structure of krausite, $KFe(SO_4)_2 \cdot H_2O$. *Am. Mineral.*, **50**:1929–1936.

Gramaccioli, C.M., Pilati, T. & Liborio, G. (1979): Structure of a manganese(II) arsenatotrisilicate, $Mn_4[AsSi_3O_{12}(OH)]$: the presence of a new tetrapolyphosphate-like anion. *Acta Crystallogr.*, **B25**:2287–2291.

Gramaccioli, C.M., Liborio, G. & Pilati, T. (1981): Structure of medaite, $Mn_6[VSi_5O_{18}(OH)]$: the presence of a new kind of heteropolysilicate anion. *Acta Crystallogr.*, **B37**:1972–1978.

Groat, L.A., Raudsepp, M., Hawthorne, F.C., Ercit, T.S., Sherriff, B.L. & Hartman, J.S. (1990): The amblygonite-montebrasite sieries: Characterization by single-crystal structure refinement, infrared spectroscopy and multinuclear MAS-NMR spectroscopy. *Am. Mineral.*, **75**:992–1008.

Hansen, A.W. (1960): The crystal structure of eosphorite. *Acta Crystallogr.*, **13**:384–387.

Hawthorne, F.C. (1976): The hydrogen positions in scorodite. *Acta Crystallogr.* **B22**:2891–2892.

Hawthorne, F.C. (1979): The crystal structure of morinite. *Can. Mineral.*, **17**:93–102.

Hawthorne, F.C. (1983a): Graphical enumeration of polyhedral clusters. *Acta Crystallogr.*, **A39**:724–736.

Hawthorne, F.C. (1983b): The crystal structure of tancoite. *Tschermaks Mineral. Petrogr. Mitt.*, **31**:121–135.

Hawthorne, F.C. (1984a): The crystal structure of stenonite, and the classification of the aluminofluoride minerals. *Can. Mineral.*, **22**:245–251.

Hawthorne, F.C. (1984b): The crystal structure of mandarinoite, $Fe^{3+}_2Se_3O_9 \cdot 6H_2O$ *Can. Mineral.*, **22**:475–480.

Hawthorne, F.C. (1985a): Towards a structural classification of minerals: the ${}^{vi}M^{iv}T_2O_n$ minerals. *Am. Mineral.*, **70**:455–473.

Hawthorne, F.C. (1985b): The crystal structure of stringhamite. *Tschermaks Mineral. Petrogr. Mitt.*, **34**:15–34.

Hawthorne, F.C. (1985c): Refinement of the crystal structure of blödite: structural similarities in the $[{}^{VI}M({}^{IV}T\phi_4)_2\phi_n]$ finite-cluster minerals. *Can. Mineral.*, **23**:669–674.

Hawthorne, F.C. (1986): Structural hierarchy in ${}^{iv}M^{iii}_x\,T_y\phi_z$ minerals. *Can. Mineral.*, **24**:625–642.

Hawthorne, F.C. (1988): Sigloite: The oxidation mechanism in $[M^{3+}_2(PO)_2(OH)_2(H_2O)_2]^{2-}$ structures. *Mineral. Petrol.*, **38**:201–211.

Hawthorne, F.C. (1990): Structural hierarchy in $M^{[6]}T^{[4]}\phi_n$ minerals. *Z. Kristallogr.*, **192**:1–52.

Hawthorne, F.C. (1992): The role of OH and H_2O in oxide and oxysalt minerals. *Z. Kristallogr.*, **201**:183–206.

Hawthorne, F.C. & Černý, P. (1977): The alkali-metal positions in Cs-Li beryl. *Can. Mineral.*, **15**:414–421.

Hawthorne, F.C. & Faggiani, R. (1979): Refinement of the structure of descloizite. *Acta Crystallogr.*, **B35**:717–720.

Hawthorne, F.C. & Ferguson, R.B. (1975a): Anhydrous sulphates: I. Refinement of the crystal structure of celestite, with an appendix on the structure of thenardite. *Can. Mineral.*, **13**:181–187.

Hawthorne, F.C. & Ferguson, R.B. (1975b): Refinement of the crystal structure of kröhnkite. *Acta Crystallogr.*, **B31**:1753–1755.

Hawthorne, F.C. & Ferguson, R.B. (1977): The crystal structure of roselite. *Can. Mineral.*, **15**:36–42.

Hawthorne, F.C. & Ito, J. (1977): Synthesis and characterization of transition metal orthopyroxenes: I. Orthoenstatite and Mg–Mn–Co orthopyroxene. *Can. Mineral.*, **15**:321–338.

Hawthorne, F.C., Groat, L.A., Raudsepp, M. & Ercit, T.S. (1987): Kieserite, a titanite-group mineral. *Neues Jahrb. Mineral. Abh.*, **157**:121–132.

Hawthorne, F.C., Groat, L.A., Raudsepp, M., Ball, N.A., Kimata, M., Spike, F.D., Halden, N.M., Lumpkin, G.R., Ewing, R.C., Greegor, R.B., Lytle, F.W., Ercit, T.S., Rossman, G.R., Sherriff, B.L., Fleet, M.E., Wicks, F.J., Ramik, R.A. & McCammon, C. (1991): Alpha-decay damage in natural titanites. *Am. Mineral.*, **76**:370–396.

Hawthorne, F.C., Burns, P.C. & Grice, J.D. (1996): The crystal chemistry of boron. In Grew, E.S. & Anovitz, L.M. (eds.): Boron mineralogy, petrology, geochemistry. /*Mineral. Soc. Am. Rev. Mineral.*, **33**/, 41–115.

Higgins, J.B. & Ribbe, P.H. (1977): The structure of malayaite, $CaSnOSiO_4$, a tin analogue of titanite. *Am. Mineral.*, **62**:801–806.

Hoffmann, R. (1988): *Solids and surfaces: a chemist's view of bonding in extended structures.* New York: VCH Publishers.

Hofmeister, W. & Tillmanns, E. (1978): Strukturelle Untersuchungen an Arsenbrackebuschit. *Tschermaks Mineral. Petrogr. Mitt.*, **25**:153–163.

Kampf, A.R. (1977): Minyulite: Its atomic arrangement. *Am. Mineral.*, **62**:256–262.

Kampf, A.R. & Moore, P.B. (1976): The crystal structure of bermanite, a hydrated manganese phosphate. *Am. Mineral.*, **61**:1241–1248.

Kampf, A.R. & Moore, P.B. (1977): Melonjosephite, calcium iron hydroxyphosphate: its crystal structure. *Am. Mineral.*, **62**:60–66.

Keller, P. & Hess, H. (1978): Die Kristallstruktur von Arthurit, $CuFe^{3+}_2[(H_2O)_4|(OH)_2|(AsO_4)_2]$. *Neues Jahrb. Mineral. Abh.*, **133**:291–302.

Keller, P. Hess, H. & Riffel, H. (1980): Die Kristallstruktur von Koritnigit, $Zn[H_2O|HOAsO_3]$. *Neues Jahrb. Mineral. Abh.*, **138**:316–322.

Khalilov, A.D., Khomyakov, A.P. & Makhmudov, S.A. (1977): Crystal structure of keldyshite, $NaZr(Si_2O_6OH)$. *Dokl. Akad. Nauk SSSR.*, **238**:573–577 (in Russian).

Khan, A.A. & Baur, W.H. (1972): Salt hydrates. VIII. The crystal structure of sodium ammonium orthochromate dihydrate and magnesium diammonium bis(hydrogen orthophosphate) tetrahydrate and a discussion of the ammonium ion. *Acta Crystallogr.*, **B28**:683–693.

Kitahama, K., Kiriyama, R. & Baba, Y. (1975): Refinement of the crystal structure of scorodite. *Acta Crystallogr.*, **B31**:322–324.

Kniep, R. & Mootz, D. (1973): Metavariscite: a redetermination of its crystal structure. *Acta Crystallogr.*, **B29**:2292–2294.

Kniep, R., Mootz, D. & Vegas, A. (1977): Variscite. *Acta Crystallogr.*, **B33**:263–265.

Kolesova, R.V. & Fesenko, E.G. (1968): Determination of the crystal structure of liroconite, $Cu_2Al[AsO_4](OH)_4{\cdot}4H_2O$. *Sov. Phys. Crystallogr.*, **13**:324–328.

Lewis, G.N. (1923): *Valence and the structure of atoms and molecules. Am. Chem. Soc. Mon. Ser.*, New York.

Liebau, F. (1985): *Structural chemistry of silicates.* Berlin: Springer-Verlag.

Lima-de-Faria, J. (1983): A proposal for a structural classification of minerals. *Garcia de Orta, Sér. Geol.*, **6**:1–14.

Lima-de-Faria, J. & Figueiredo, M.O. (1976): Classification, notation and ordering on a table of inorganic structure types. *J. Solid State Chem.*, **16**:7–20.

Lima-de-Faria, J., Hellner, E., Liebau, F., Makovicky, E. & Parthé, E. (1990): Nomenclature of inorganic structure types: Report of the IUCr Commission on Crystallographic Nomenclature Subcommittee on the Nomenclature of Inorganic Structure Types. *Acta Crystallogr.*, **A46**:1–11.

Lindberg, M.L. & Christ, C.L. (1959): Crystal structures of the isostructural minerals lazulite, scorzalite and barbosalite. *Acta Crystallogr.*, **12**:695–696.

McNear, E., Vincent, M.G., Parthé, E. (1976): The crystal structure of vuagnatite, $CaAl(OH)SiO_4$. *Am. Mineral.*, **61**:831–838.

Meagher, E.P. Gibbons, C.S. & Trotter, J. (1974): The crystal structure of jagowerite: $BaAl_2P_2O_8(OH)_2$. *Am. Mineral.*, **59**:291–295.

Mellini, M. (1981): Refinement of the crystal structure of låvenite. *Tschermaks Mineral. Petrogr. Mitt.*, **28**:99–112.

Mellini, M. & Merlino, S. (1979): Refinement of the crystal structure of wöhlerite. *Tschermaks Mineral. Petrogr. Mitt.*, **26**:109–123.

Menchetti, S. & Sabelli, C. (1976): The halotrichite group: the crystal structure of apjohnite. *Mineral. Mag.*, **40**:599–608.

Mereiter, K. (1974): Die Kristallstruktur von Rhomboklas, $H_5O_2^+\{Fe[SO_4]_2{\cdot}2H_2O\}^-$. *Tschermaks Mineral. Petrogr. Mitt.*, **21**:216–232.

Mongiorgi, R. & Riva di Sanseverino, L. (1968): A reconsideration of the structure of titanite. *Mineral. Petrogr. Acta*, **14**:123–141.

Moore, P.B. (1965): The crystal structure of laueite. *Am. Mineral.*, **50**:1884–1892.

Moore, P.B. (1966): The crystal structure of metastrengite and its relationship to strengite and phosphosilerite. *Am. Mineral.*, **51**:168–176.

Moore, P.B. (1970a): Structural hierarchies among minerals containing octahedrally coordinating oxygen. I. Steroisomerism among corner-sharing octahedral and tetrahedral chains. *Neues Jahrb. Mineral. Monatsh.*, 163–173.

Moore, P.B. (1970b): Crystal chemistry of the basic iron phosphates. *Am. Mineral.*, **55**:135–169.

Moore, P.B. (1971): Crystal chemistry of the alluaudite structure type: contribution to the paragenesis of pegmatitic phosphate giant crystals. *Am Mineral.*, **56**:1955–1975.

Moore, P.B. (1972): Octahedral tetramer in the crystal structure of leucophosphite, $K_2[Fe_4^{3+}(OH)_2(H_2O)_2(PO_4)_4]{\cdot}2H_2O$. *Am. Mineral.*, **57**:397–410.

Moore, P.B. (1973): Pegmatite phosphates: Mineralogy and crystal chemistry. *Mineral. Rec.*, **4**:103–130.

Moore, P.B. (1974): Structural hierarchies among minerals containing octahedrally coordinating oxygen: II. Systematic retrieval and classification of octahedral edge-sharing clusters: an epistemological approach. *Neues Jahrb. Mineral. Abh.*, **120**:205–227.

Moore, P.B. (1975a): Laueite, pseudolaueite, stewartite and metavauxite: a study in combinatorial polymorphism. *Neues Jahrb. Mineral. Abh.*, **123**:148–159.

Moore, P.B. (1975b): Brianite, $Na_2CaMg[PO_4]_2$: a phosphate analog of merwinite, $Ca_2CaMg[SiO_4]_2$. *Am. Mineral.*, **60**:717–718.

Moore, P.B. (1981): Complex crystal structures related to glaserite, $K_3Na(SO_4)_2$: evidence for very dense packings among oxysalts. *Bull. Soc. Fr. Minéral. Cristallogr.*, **104**:536–547.

Moore, P.B. (1982): Pegmatite minerals of P(V) and B(III). *Mineral. Assn. Can. Short Course*, **8**:267–291.

Moore, P.B. (1984): Crystallochemical aspects of the phosphate minerals. *In* Niagru, J.O. & Moore, P.B. (eds.): *Phosphate minerals*. Berlin: Springer-Verlag, 155–170.

Moore, P.B. & Araki, T. (1972): Atomic arrangement of merwinite, $Ca_2Mg[SiO_4]_2$, an unusual dense-packed structure of geophysical interest. *Am. Mineral.*, **57**:1355–1374.

Moore, P.B. & Araki, T. (1974a): Stewartite, $Mn^{2+}Fe_2^{3+}(OH)_2(H_2O)_6[PO_4]_2{\cdot}2H_2O$: its atomic arrangement. *Am. Mineral.*, **59**:1272–1276.

Moore, P.B. & Araki, T. (1974b): Jahnsite, $CaMn^{2+}Mg_2(H_2O)_8Fe_2^{3+}(OH)_2[PO_4]_4$: a novel stereoisomerism of ligands about octahedral corner-chains. *Am. Mineral.*, **59**:964–973.

Moore, P.B. & Araki, T. (1975): Palermoite, $SrLi_2[Al_4(OH)_4(PO_4)_4]$: its atomic arrangement and relationship to carminite, $Pb_2[Fe_4(OH)_4(AsO_4)_4]$. *Am. Mineral.*, **60**:460–465.

Moore, P.B. & Araki, T. (1977a): Overite, seglerite and jahnsite: a study in combinatorial polymorphism. *Am. Mineral.*, **62**:692–702.

Moore, P.B. & Araki, T. (1977b): Mitridatite, $Ca_6(H_2O)_6[Fe_2^{III}O_6(PO_4)_9]{\cdot}3H_2O$. A noteworthy octahedral sheet structure. *Inorg. Chem.*, **16**:1096–1106.

Moore, P.B. & Araki, T. (1977c): Holdenite, a novel cubic close-packed structure. *Am. Mineral.*, **62**:513–521.

Moore, P.B. & Ito, J. (1978): I. Whiteite, a new species, and a proposed nomenclature for the jahnsite–whiteite complex series. *Mineral. Mag.*, **42**:309–316.

Moore, P.B., Kampf, A.R. & Irving, A.J. (1974): Whitemoreite, $Fe^{2+}Fe_2^{3+}(OH)_2(H_2O)_4[PO_4]_2$, a new species: its description and crystal structure. *Am. Mineral.*, **59**:900–905.

Moore, P.B., Irving, A.J. & Kampf, A.R. (1975): Foggite, $CaAl(OH)_2(H_2O)[PO_4]$; goedkenite, $(Sr,Ca)_2Al(OH)[PO_4]_2$; and samuelsonite $(Ca,Ba)Fe^{2+}_2Mn^{2+}_2Ca_8Al_2(OH)_2[PO_4]_{10}$: three new species from the Palermo No. 1 pegmatite, North Groton, New Hamphsire. *Am. Mineral.*, **60**:957–964.

Moore, P.B., Araki, T., Kampf, A.R. & Steele, I.M. (1976): Olmsteadite, $K_2Fe^{2+}_2[Fe^{2+}_2(Nb,Ta)^{5+}_2O_4(H_2O)_2(PO_4)_4]$, a new species, its crystal structure and relation to vauxite and montgomeryite. *Am. Mineral.*, **61**:5–11.

Newnham, R.E. (1961): A refinement of the dickite structure and some remarks on polymorphism in kaolin minerals. *Mineral. Mag.*, **32**:683–704.

Nichols, M.C. (1966): The structure of tsumebite. *Am. Mineral.*, **51**:267.

Nikitin, A.V. & Belov, N.V. (1962): Crystal structure of batisite $Na_2BaTi_2Si_4O_{14} = Na_2BaTi_2O_2[Si_4O_{12}]$. *Dokl. Akad. Nauk SSSR.*, **146**:142–143.

Ohashi, Y. & Finger, L.W. (1976): The effect of a Ca substitution on the structure of clinoenstatite. *Carnegie Inst. Wash. Year Book*, **75**:743–746.

O'Keeffe, M. (1989): The prediction and interpretation of bond lengths in crystals. *Struct. Bond.* (Berlin), **71**:161–191.

O'Keeffe, M. (1990): A method for calculating bond valences in crystals. *Acta Crystallogr.*, **A46**:138–142.

O'Keeffe, M. & Brese, N.E. (1991): Atom sizes and bond lengths in molecules and crystals. *J. Am. Chem. Soc.*, **113**:3226–3229.

Otto, H.H. (1975): Die Kristallstruktur von Fleischerit, $Pb_3Ge[(OH)_6(SO_4)_2]\cdot 3H_2O$, sowie kristallchemische Untersuchungen an isotypen Verbindungen. *Neues Jahrb. Mineral Abh.*, **123**:160–190.

Pabst, A. (1950): A structural classification of fluoaluminates. *Am. Mineral.*, **35**:149–165.

Pajunen, A. & Lahti, S.I. (1985): New data on lacroixite, $NaAlFPO_4$. Crystal structure. *Am. Mineral.*, **70**:852–855.

Pauling, L. (1929): The principles determining the structure of complex ionic crystals. *J. Am. Chem. Soc.*, **51**:1010–1026.

Pauling, L. (1960): *The nature of the chemical bond.* 3rd ed. Ithaca, New York: Cornell University Press.

Perrault, G., Boucher, C., Vicat, J., Cannillo, E. & Rossi, G. (1973): Structure cristalline du nenadkevichite $(Na,K)_{2-x}(Nb,Ti)(O,OH)Si_2O_6\cdot 2H_2O$. *Acta Crystallogr.*, **B29**:1432–1438.

Protas, J. & Gindt, R. (1976): Structure cristalline de la brassite, $MgHAsO_4.4H_2O$, produit de deshydration de la roesslerite. *Acta Crystallogr.*, **B32**:1460–1466.

Pyatenko, Yu. A. (1973): Unified approach to analysis of the local balance of valences in inorganic structures. *Sov. Phys. Crystallogr.*, **17**:677–682.

Qurashi, M.M. & Barnes, W.H. (1963): The structures of the minerals of the descloizite and adelite groups: IV. The structure of conichalcite. *Can. Mineral.*, **7**:561–577.

Ribbe, P.H., Gibbs, G.V. & Hamil, M.M. (1977): A refinement of the structure of dioptase, $Cu_6[Si_6O_{18}]\cdot 6H_2O$. *Am. Mineral.*, **62**:807–811.

Robinson, P.D. & Fang, J.H. (1969): Crystal structures and mineral chemistry of double-salt hydrates: I. Direct determination of the crystal structure of tamarugite. *Am. Mineral.*, **54**, 19–30.

Robinson, P.D., Fang, J.H. & Ohya, Y. (1972): The crystal structure of kainite. *Am. Mineral.*, **57**:1325–1332.

Sabelli, C. (1985a): Refinement of the crystal structure of jurbanite, $Al(SO_4)(OH)\cdot 5H_2O$. *Z. Kristallogr.*, **173**:33–39.

Sabelli, C. (1985b): Uklonskovite, $NaMg(SO_4)F\cdot 2H_2O$: new mineralogical data and structure refinement. *Bull Minéral.*, **108**:133–138.

Scordari, F. (1978): The crystal structure of hohmannite, $Fe_2(H_2O)_4[(SO_4)_2O]\cdot 4H_2O$ and its relationship to amarantite, $Fe_2(H_2O)_4[(SO_4)_2O]\cdot 3H_2O$. *Mineral. Mag.*, **42**:144–146.

Scordari, F. (1980): Structural considerations of some natural and artificial iron hydrated sulphates. *Mineral. Mag.*, **43**:669–673.

Scordari, F. (1981a): Fibroferrite: a mineral with a $\{Fe(OH)(H_2O)_2SO_4\}$ spiral chain and its relationship to $Fe(OH)SO_4$, butlerite and parabutlerite. *Tshermaks Mineral. Petrogr. Mitt.*, **28**:17–29.

Scordari, F. (1981b): Sideronatrite: a mineral with a $\{Fe_2(SO_4)_4(OH)_2\}$ guildite type chain. *Tschermaks Mineral. Petrogr. Mitt.*, **28**:315–319.

Shannon, R.D. (1975): Systematic studies of interatomic distances in oxides. *In* Strens R.G.J. (ed.): *The physics and chemistry of minerals and rocks.* New York – London: Wiley – Interscience, 403–431.

Shannon, R.D. (1976): Revised ionic radii and systematic studies of interatomic distances in halides and oxides. *Acta Crystallogr.*, **A32**:751–767.

Shannon, R.D., Subramanian, M.A., Mariano, A.N., Gier, T.E. & Rossman, G.R. (1992): Dielectric constants of diaspore and B-, Be-, and P-containing minerals, the polarizabilities of B_2O_3 and P_2O_5, and the oxide additivity rule. *Am. Mineral.*, **77**:101–106.

Shen, J. & Moore, P.B. (1982): Törnebohmite, $RE_2Al(OH)[SiO_4]_2$: crystal structure and genealogy of RE(III)Si(IV) $\rightleftarrows$ Ca(II)P(V) isomorphisms. *Am. Mineral.*, **67**:1021–1028.

Shibaeva, R.P., Simonov, V.I. & Belov, N.V. (1964): Crystal structure of the Ca,Na,Zr,Ti silicate rosenbuschite, $Ca_{3.5}Na_{2.5}Zr(Ti,Mn,Nb)[Si_2O_7]_2F_2O(F,O)$. *Sov. Phys. Crystallogr.*, **8**:406–413.

Simonov, W.I. & Belov, N.V. (1958): Die Aufklärung der Struktur des Amblygonits mit Hilfe der Minimumfunktion. *Kristallografiya*, **3**:428–437.

Smyth, J.R. (1974): The high temperature crystal chemistry of clinohypersthene. *Am. Mineral.*, **59**:1069–1082.

Speer, J.A. & Gibbs, G.V. (1976): The crystal structure of synthetic titanite, and the domain structure of natural titanites. *Am. Mineral.*, **61**:238–247.

Srikanta, S., Sequeira, A. & Chidambaram, R. (1968): Neutron diffraction study of the space group and structure of manganese-leonite, $K_2Mn(SO_4)\cdot 4H_2O$. *Acta Crystalolgr.*, **B24**:1176–1182.

Stephens, J.S. & Cruickshank, D.W.J. (1970): The crystal structure of $(CrO_3)_\infty$. *Acta Crystallogr.*, **B26**:222–226.

Sturman, B.D. & Dunn, P.J. (1980): Gaitite, $H_2Ca_2Zn(AsO_4)_2(OH)_2$, a new mineral from Tsumeb, Namibia (South West Africa), *Can. Mineral.*, **18**:197–200.

Sueno, S., Cameron, M. & Prewitt, C.T. (1976): Orthoferrosilite: high-temperature crystal chemistry. *Am. Mineral.*, **61**:38–53.

Süsse, P. (1968a): The crystal structure of amarantite, $Fe_2(SO_4)_2O\cdot 7H_2O$. *Z. Kristallogr.*, **127**:261–275.

Süsse, P. (1968b): Die Kristallstruktur des Botryogens. *Acta Crystallogr.*, **B24**:760–767.

Sutor, D.J. (1967): The crystal and molecular structure of newberyite, $MgHPO_4\cdot 3H_2O$. *Acta Crystallogr.*, **23**:418–422.

Tillmanns, E. & Gebert, W. (1973): The crystal structure of tsumcorite, a new mineral from the Tsumeb mine, S.W. Africa. *Acta Crystallogr.*, **B29**:2789–2794.

Toraya, H., Iwai, S., Marumo, F. & Hirao, M. (1977): The crystal structure of taeniolite, $KLiMg_2Si_4O_{10}F_2$. *Z. Kristallogr.*, **144**:42–52.

Tossell, J.A. & Gibbs, G.V. (1977): Molecular orbital studies of geometries and spectra of minerals and inorganic compounds. *Phys. Chem. Minerals*, **2**:21–57.

Trinajstic, N. (1983): *Chemical graph theory*. Boca Raton: CRC Press. Vol. I.

Wan, C., Ghose, S. & Rossman, G.R. (1978): Guildite, a layer structure with a ferric hydroxy-sulphate chain and its optical absorption spectra. *Am. Mineral.*, **63**:478–483.

Wardle, R. & Brindley, G.W. (1972): The crystal structures of pyrophyllite, 1Tc, and of its dehydroxylate. *Am. Mineral.*, **57**:732–750.

Whitaker, A. & Jeffery, J.W. (1970): The crystal structure of struvite, $MgNH_4PO_4\cdot 6H_2O$. *Acta Crystallogr.*, **B26**:1429–1440.

Wood, M.M. (1970): The crystal structure of ransomite. *Am. Mineral.*, **55**:729–734.

Ya-hsien, K., Simonov, V.I. & Belov, N.V. (1963): Crystal structure of bafertisite, $BaFe_2TiO[Si_2O_7](OH)_2$. *Dokl. Akad. Nauk SSSR*, **149**:123–126.

Zahrobsky, R.F. & Baur, W.H. (1968): On the crystal chemistry of salt hydrates. V. The determination of the crystal structure of $CuSO_4\cdot 3H_2O$ (bonattite). *Acta Crystallogr.*, **B24**:508–513.

Zalkin, A. Ruben, H. & Templeton, D.H. (1962): The crystal structure of cobalt sulfate hexahydrate. *Acta Crystallogr.*, **15**:1219–1224.

Zalkin, A. Ruben, H. & Templeton, D.H. (1964): The crystal structure and hydrogen bonding of magnesium sulfate hexahydrate. *Acta Crystallogr.*, **17**:235–240.

Ziman, J. (1965): *Principles of the theory of solids*. Cambridge: Cambridge University Press.

Zoltai, T. (1960): Classification of silicates and other minerals with tetrahedral structures. *Am. Mineral.*, **45**:960–973.

Zvyagin, B.B. (1960): An electron-diffraction determination of the structure of kaolinite. *Sov. Phys. Crystallogr.*, **5**:32–42.

Appendix

Table I. $MT\phi_4$ and $MT_2\phi_n$ minerals based on isolated $M\phi_6$ octahedra and $T\phi_4$ tetrahedra

Mineral	Formula	*a* [Å]	*b* [Å]	*c* [Å]	β [°]	S.G.	Ref.
Bianchite	$[Zn(H_2O)_6][SO_4]$	10.096	7.201	24.492	98.3	$C2/c$	–
Ferrohexahydrite	$[Fe^{2+}(H_2O)_6][SO_4]$	10.08	7.28	24.59	98.4	$C2/c$	–
*Hexahydrite	$[Mg(H_2O)_6][SO_4]$	10.110(5)	7.212(4)	24.410(10)	98.30(5)	$C2/c$	[1]
Moorhouseite	$[Co(H_2O)_6][SO_4]$	10.032(4)	7.233(3)	24.261(10)	98.37(3)	$C2/c$	[2]
Nickel-hexahydrite	$[Ni(H_2O)_6][SO_4]$	9.895(2)	7.241(1)	24.188(5)	98.41(2)	$C2/c$	–
Retgersite	$[Ni(H_2O)_6][SO_4]$	6.776(3)	6.776(3)	18.249(9)	–	$P4_12_12_1$	[3]
Khademite	$[Al(H_2O)_5F][SO_4]$	11.181(4)	13.048(5)	10.885(4)	–	$Pcab$	[4]
*Epsomite	$[Mg(H_2O)_6][SO_4](H_2O)$	11.868(10)	11.996(10)	6.856(7)	–	$P2_12_12_1$	[5], [6]
Goslarite	$[Zn(H_2O)_6][SO_4](H_2O)$	11.779	12.050	6.822	–	$P2_12_12_1$	–
Morenosite	$[Ni(H_2O)_6][SO_4](H_2O)$	11.86	12.08	6.81	–	$P2_12_12_1$	–
Bieberite	$[Co(H_2O)_6][SO_4](H_2O)$	14.04	6.495	10.925	105.27	$P2_1/c$	–
Boothite	$[Cu(H_2O)_6][SO_4](H_2O)$	–	–	–	–	$P2_1/c$	–
Mallardite	$[Mn(H_2O)_6][SO_4](H_2O)$	14.15	6.5	11.06	105.6	$P2_1/c$	–
*Melanterite	$[Fe^{2+}(H_2O)_6][SO_4](H_2O)$	14.072(10)	6.503(7)	11.041(10)	105.57(8)	$P2_1/c$	[7]
Zinc-melanterite	$[Zn(H_2O)_6][SO_4](H_2O)$	–	–	–	–	$P2_1/c$	–
Phosphorrösslerite	$[Mg(H_2O)_6][PO_3(OH)](H_2O)$	6.6	25.36	11.35	95	$C2/c$	–
Rösslerite	$[Mg(H_2O)_6][AsO_3(OH)](H_2O)$	6.692(1)	25.744(2)	11.538(1)	95.15(1)	$C2/c$	[8]
Struvite	$NH_4[Mg(H_2O)_6][PO_4]$	6.941(2)	6.137(2)	11.199(4)	–	$Pmn2_1$	[9], [10]
*Amarillite	$Na[Fe^{3+}(SO_4)_2(H_2O)_6]$	–	–	–	–	$P2_1/a$	–
Tamarugite	$Na[Al(SO_4)_2(H_2O)_6]$	7.353(2)	25.225(5)	6.097(2)	95.2(1)	$P2_1/a$	[11]
*Mendozite	$Na[Al(SO_4)_2(H_2O)_6](H_2O)_5$	21.75(3)	9.11(10)	8.30(1)	92.47(8)	$C2/c$	[12]
Kalinite	$K[Al(SO_4)_2(H_2O)_6](H_2O)_5$	–	–	–	–	$C2/c$	–

Table I. (continued)

Mineral	Formula	*a* [Å]	*b* [Å]	*c* [Å]	β [°]	S.G.	Ref.
*Sodium alum	$Na[Al(SO_4)_2(H_2O)_6](H_2O)_6$	12.214(1)	–	–	–	*Pa*3	[13]
Potassium alum	$K[Al(SO_4)_2(H_2O)_6](H_2O)_6$	12.157(1)	–	–	–	*Pa*3	–
Tschermigite	$NH_4[Al(SO_4)_2(H_2O)_6](H_2O)_6$	12.240(1)	–	–	–	*Pa*3	–
Apjohnite	$Mn[Al(SO_4)_2(H_2O)_6]_2(H_2O)_{10}$	6.198(2)	24.347(4)	21.266(4)	100.28(3)	$P2_1/c$	[14]
Bilinite	$Fe^{2+}[Fe^{3+}(SO_4)_2(H_2O)_6]_2(H_2O)_{10}$	–	–	–	–	$P2_1/c$	–
Dietrichite	$Zn[Al(SO_4)_2(H_2O)_6]_2(H_2O)_{10}$	–	–	–	–	$P2_1/c$	–
*Halotrichite	$Fe^{2+}[Al(SO_4)_2(H_2O)_6]_2(H_2O)_{10}$	6.181	24.297	20.519	100.99	$P2_1/c$	–
Pickeringite	$Mg[Al(SO_4)_2(H_2O)_6]_2(H_2O)_{10}$	–	–	–	–	$P2_1/c$	–
Redingtonite	$Fe^{2+}[Cr(SO_4)_2(H_2O)_6]_2(H_2O)_{10}$	–	–	–	–	$P2_1/c$	–
Aubertite [1)]	$Cu^{2+}[Al(SO_4)_2(H_2O)_6]Cl(H_2O)_8$	6.282(3)	13.192(5)	6.260(3)	94.70(3)	$P\bar{1}$	[15]
Boussingaultite	$(NH_4)_2[Mg(SO_4)_2(H_2O)_6]$	6.211	12.597	9.324	107.22	$P2_1/c$	–
Cyanochroite	$K_2[Cu^{2+}(SO_4)_2(H_2O)_6]$	6.159(5)	12.131(7)	9.086(4)	104.45(5)	$P2_1/c$	[16]
Mohrite	$(NH_4)_2[Fe^{2+}(SO_4)_2(H_2O)_6]$	6.22	12.57	9.28	106.8	$P2_1/c$	–
*Picromerite	$K_2[Mg(SO_4)_2(H_2O)_6]$	6.121(3)	12.25(3)	9.09(1)	104.2(1)	$P2_1/c$	[17]
Despujolsite	$Ca_3[Mn^{4+}(SO_4)_2(OH)_6](H_2O)_3$	8.56(2)	–	10.76(4)	–	$P\bar{6}2c$	–
*Fleischerite	$Pb_3[Ge(SO_4)_2(OH)_6](H_2O)_3$	8.867(1)	–	10.875(1)	–	$P\bar{6}2c$	[18]
Schaurteite	$Ca_3[Ge(SO_4)_2(OH)_6](H_2O)_3$	8.529(1)	–	10.802(2)	–	$P\bar{6}2c$	–

References: [1] Zalkin *et al.* (1964); [2] Zalkin *et al.* (1962); [3] Beevers & Lipson (1932); [4] Bachet *et al.* (1981); [5] Ferraris *et al.* (1973); [6] Calleri *et al.* (1984); [7] Baur (1964b); [8] Ferraris & Franchini-Angela (1973); [9] Whitaker & Jeffery (1970); [10] Abbona *et al.* (1984); [11] Robinson & Fang (1969); [12] Fang & Robinson (1972); [13] Cromer *et al.* (1967); [14] Menchetti & Sabelli (1976); [15] Ginderow & Cesbron (1979); [16] Carapezza & Riva di Sanseverino (1968); [17] Carapezza & Riva di Sanseverino (1970); [18] Otto (1975)

* denotes the principal mineral of the group in Tables I–V.

[1)] aubertite: $\alpha = 91.85(3)°$, $\gamma = 82.46(3)°$

Table II. $MT\phi_4$ and $MT_2\phi_n$ minerals based on isolated clusters [1]

Mineral	Formula	*a* [Å]	*b* [Å]	*c* [Å]	β [°]	S.G.	Ref.
Jurbanite	$[Al(SO_4)(OH)(H_2O)_4](H_2O)$	8.3965(6)	12.479(2)	8.1549(9)	101.917(6)	$P2_1/n$	[1]
Aplowite	$[Co(SO_4)(H_2O)_4]$	5.937	13.546	7.888	90.55	$P2_1/n$	–
Boyleite	$[Zn(SO_4)(H_2O)_4]$	5.946	13.60	7.951	90.4	$P2_1/n$	–
Ilesite	$[Mn(SO_4)(H_2O)_4]$	5.94	13.76	8.01	90.8	$P2_1/n$	–
*Rozenite	$[Fe^{2+}(SO_4)(H_2O)_4]$	5.979(4)	13.648(4)	7.977(3)	90.4(2)	$P2_1/n$	[2]
Starkeyite	$[Mg(SO_4)(H_2O)_4]$	5.922(6)	13.604(4)	7.905(5)	90.9(2)	$P2_1/n$	[3]
Morinite	$Ca_2Na[Al_2(PO_4)_2F_4(OH)(H_2O)_2]$	9.454(3)	10.692(4)	5.444(2)	105.46(2)	$P2_1/m$	[4]
Anapaite[2]	$Ca_2[Fe^{2+}(PO_4)_2(H_2O)_4]$	6.447(1)	6.816(1)	5.898(1)	104.24(3)	$P\bar{1}$	[5]
Blödite	$Na_2[Mg(SO_4)_2(H_2O)_4]$	11.03	8.14	5.49	100.7	$P2_1/a$	[6]
Leonite	$K_2[Mg(SO_4)_2(H_2O)_4]$	12.03(3)	9.61(3)	9.98(4)	95.0(3)	$C2/m$	[7]
Schertelite	$(NH_4)_2[Mg(PO_3OH)_2(H_2O)_4]$	11.49(2)	23.66(6)	8.62(1)	–	$Pbca$	[8]
Römerite[3]	$Fe^{2+}[Fe^{3+}(SO_4)_2(H_2O)_4]_2(H_2O)_6$	6.463(8)	15.309(18)	6.341(8)	101.1(2)	$P\bar{1}$	[9]
Metavoltine	$K_2Na_6Fe^{2+}[Fe_3^{3+}(SO_4)_6O(H_2O)_3]_2(H_2O)_{12}$	9.575(5)	–	18.17(1)	–	$P3$	[10]

References: [1] Sabelli (1985a); [2] Baur (1962); [3] Baur (1964a); [4] Hawthorne (1979); [5] Catti *et al.* (1979); [6] Hawthorne, 1985(c); [7] Srikanta *et al.* (1968); [8] Khan & Baur (1972); [9] Fanfani *et al.* (1970a); [10] Giacovazzo *et al.* (1976b).

[1] In jurbanite, the structural unit is partly connected; in the remaining minerals, the structural units are completely connected.

[2] $\alpha = 101.64(3)°$, $\gamma = 70.76(4)°$

[3] $\alpha = 90.5(2)°$, $\gamma = 85.7(2)°$

Table III. $MT\phi_n$ and $M(TO_4)_2\phi_n$ minerals based on infinite chains

Mineral	Formula	*a* [Å]	*b* [Å]	*c* [Å]	α [°]	β [°]	γ [°]	S.G.	Ref.
*Chalcanthite	$[Cu(SO_4)(H_2O)_4](H_2O)$	6.105	10.72	5.949	82.4	107.3	102.6	$P\bar{1}$	[1]
Jokokuite	$[Mn(SO_4)(H_2O)_4](H_2O)$	6.37	10.77	6.13	81.2	110.0	105.0	$P\bar{1}$	–
Pentahydrite	$[Mg(SO_4)(H_2O)_4](H_2O)$	6.314(5)	10.505(18)	6.030(6)	81.1(2)	109.8(2)	105.08(5)	$P\bar{1}$	[2]
Siderotil	$[Fe^{2+}(SO_4)(H_2O)_4](H_2O)$	6.25	10.63	6.06	82.8	109.7	105.0	$P\bar{1}$	–
Liroconite	$Cu_2[Al(AsO_4)(OH)_4](H_2O)_4$	12.64	7.50	9.86	–	91.3	–	$I2/a$	[3]
Brassite	$[Mg(AsO_3(OH))(H_2O)_4]$	7.472(1)	10.891(1)	16.585(5)	–	–	–	$Pbca$	[4]
Butlerite	$[Fe^{3+}(SO_4)(OH)(H_2O)_2]$	6.50(1)	7.37(1)	15.84(1)	–	108.38(8)	–	$P2_1/m$	[5]
Parabutlerite	$[Fe^{3+}(SO_4)(OH)(H_2O)_2]$	7.38	20.13	7.22	–	–	–	$Pmnb$	[6]
*Childrenite	$Mn^{2+}[Al(PO_4)(OH)_2(H_2O)]$	10.395(1)	13.394(1)	6.918(1)	–	–	–	$Bbam$	[7]
Eosphorite	$Fe^{2+}[Al(PO_4)(OH)_2(H_2O)]$	10.52(4)	13.60(5)	6.97(3)	–	–	–	$Bbam$	[8]
Uklonskovite	$Na[Mg(SO_4)(OH)(H_2O)_2]$	7.202(1)	7.214(1)	5.734(1)	–	113.23(1)	–	$P2_1/m$	[9]
Fibroferrite	$[Fe^{3+}(SO_4)(OH)(H_2O)_2](H_2O)_4$	24.176	24.176	7.656	–	–	120	$R\bar{3}$	[10]
Chlorothionite	$K_2[Cu(SO_4)Cl_2]$	7.732(2)	6.078(1)	16.292(3)	–	–	–	$Pnma$	[11]
*Linarite	$Pb[Cu(SO_4)(OH)_2]$	9.81	5.65	4.70	–	104.7	–	$P2_1/m$	[12]
Schmiederite	$Pb_2[Cu_2(SeO_3)(SeO_4)(OH)_4]$	–	–	–	–	–	–	$P2_1/m$	–
Amarantite	$[Fe^{3+}_2(SO_4)_2O(H_2O)_4](H_2O)_3$	8.976(1)	11.678(2)	6.698(2)	95.65(2)	90.36(1)	97.20(2)	$P\bar{1}$	[13]
Hohmannite	$[Fe^{3+}_2(SO_4)_2O(H_2O)_4](H_2O)_4$	9.148(1)	10.922(1)	7.183(3)	90.29(6)	90.79(4)	107.36(2)	$P\bar{1}$	[14]
Brandtite	$Ca_2[Mn(AsO_4)_2(H_2O)_2]$	5.899(2)	12.968(4)	5.684(1)	–	108.05(2)	–	$P2_1/c$	[15]
*Kröhnkite	$Na_2[Cu(SO_4)_2(H_2O)_2]$	5.807(1)	12.656(2)	5.517(1)	–	108.32(1)	–	$P2_1/c$	[16]
Roselite	$Ca_2[Co(AsO_4)_2(H_2O)_2]$	5.801(1)	12.898(3)	5.617(1)	–	107.42(2)	–	$P2_1/c$	[15]
Cassidyite	$Ca_2[Ni(PO_4)_2(H_2O)_2]$	5.713(13)	6.730(15)	5.430(11)	96.7(2)	107.3(3)	104.7(2)	$P\bar{1}$	[17]
Collinsite	$Ca_2[Mg(PO_4)_2(H_2O)_2]$	5.734(1)	6.780(1)	5.441(1)	97.29(1)	108.56(1)	107.28(1)	$P\bar{1}$	[17,18]
Gaitite	$Ca_2[Zn(AsO_4)_2(H_2O)_2]$	5.915(5)	6.981(6)	5.572(6)	96.70(9)	108.76(6)	107.40(6)	$P\bar{1}$	[19]
Roselite-beta	$Ca_2[Co(AsO_4)_2(H_2O)_2]$	5.884(6)	6.963(8)	5.581(9)	97.72(8)	109.24(9)	107.5(1)	$P\bar{1}$	[18]
*Talmessite	$Ca_2[Mg(AsO_4)_2(H_2O)_2]$	5.884(4)	6.995(4)	5.564(4)	97.69(9)	109.7(1)	107.9(1)	$P\bar{1}$	[18]

Table III. (continued)

Mineral	Formula	*a* [Å]	*b* [Å]	*c* [Å]	α [°]	β [°]	γ [°]	S.G.	Ref.
*Fairfieldite	$Ca_2[Mn^{2+}(PO_4)_2(H_2O)_2]$	5.79(1)	6.57(1)	5.51(1)	102.3(3)	108.7(3)	90.3(3)	$P\bar{1}$	[20]
Messelite	$Ca_2[Fe^{2+}(PO_4)_2(H_2O)_2]$	5.95(2)	6.52(2)	5.45(2)	102.3(4)	107.5(4)	90.8(2)	$P\bar{1}$	[18]
Tancoite	$Na_2LiH[Al(PO_4)_2(OH)]$	6.948(2)	14.089(4)	14.065(3)	–	–	–	*Pbcb*	[21]
Sideronatrite [1)]	$Na_2[Fe^{3+}(SO_4)_2(OH)](H_2O)_3$	7.29(1)	20.56(2)	7.17(2)	–	–	–	*Pnn*2	[22]
*Jahnsite	$CaMnMg_2[Fe^{3+}(PO_4)_2(OH)]_2(H_2O)_8$	14.94(2)	7.14(1)	9.93(1)	–	110.16(8)	–	*P*2/*a*	[23]
Whiteite	$CaFe^{2+}Mg_2[Al(PO_4)_2(OH)]_2(H_2O)_8$	14.90(4)	6.98(2)	10.13(2)	–	113.11(9)	–	*P*2/*a*	[24]
Lun'okite	$Mn_2^{2+}Mg_2[Al(PO_4)_2(OH)]_2(H_2O)_8$	14.95	18.71	6.96	–	–	–	*Pbca*	–
Overite	$Ca_2Mg_2[Al(PO_4)_2(OH)]_2(H_2O)_8$	14.72(1)	18.75(2)	7.107(4)	–	–	–	*Pbca*	[25]
*Segelerite	$Ca_2Mg_2[Fe^{3+}(PO_4)_2(OH)]_2(H_2O)_8$	14.826(5)	18.751(4)	7.307(1)	–	–	–	*Pbca*	[25]
Wilhelmvierlingite	$Ca_2Mn_2^{2+}[Fe^{3+}(PO_4)_2(OH)]_2(H_2O)_8$	14.80(5)	18.50(5)	7.31(2)	–	–	–	*Pbca*	–
Guildite	$Cu^{2+}[Fe^{3+}(SO_4)_2(OH)](H_2O)_4$	9.786(2)	7.134(1)	7.263(1)	–	105.38(1)	–	$P2_1/m$	[26]
Yftisite	$Y_4[Ti(SiO_4)_2O](F,OH)_6$	14.949(4)	10.626(2)	7.043(2)	–	–	–	*Cmcm*	[27]
Arsen-brackebuschite	$Pb_2[Fe^{2+}(AsO_4)_2(H_2O)]$	7.763(1)	6.046(1)	9.022(1)	–	112.5(1)	–	$P2_1/m$	[28]
Arsentsumebite	$Pb_2[Cu(SO_4)(AsO_4)(OH)]$	7.84	5.92	8.85	–	112.6	–	$P2_1/m$	–
*Brackebuschite	$Pb_2[Mn(VO_4)_2(H_2O)]$	7.68	6.18	8.88	–	111.8	–	$P2_1/m$	[29]
Gamagarite	$Ba_2[(Fe^{3+},Mn)(VO_4)_2(OH,H_2O)]$	7.88(1)	6.17(1)	9.15(1)	–	112.7(1)	–	$P2_1/m$	–
Goedkenite	$Sr_2[Al(PO_4)_2(OH)]$	7.26(2)	5.74(2)	8.45(2)	–	113.7(1)	–	$P2_1/m$	[30]
Tsumebite	$Pb_2[Cu(PO_4)(SO_4)(OH)]$	7.85	5.80	8.70	–	111.5	–	$P2_1/m$	[31]
*Fornacite	$Pb_2[Cu(AsO_4)(CrO_4)(OH)]$	8.101(7)	5.892(11)	17.547(9)	–	110.00(3)	–	$P2_1/c$	[32]
Molybdofornacite	$Pb_2[Cu(AsO_4)(MoO_4)(OH)]$	8.100(5)	5.946(3)	17.65(1)	–	109.17(5)	–	$P2_1/c$	–
Törnebohmite	$(RE)_2[Al(SiO_4)_2(OH)]$	7.383(3)	5.673(3)	16.937(6)	–	112.04(2)	–	$P2_1/c$	[33]
Vauquelinite	$Pb_2[Cu(PO_4)(CrO_4)(OH)]$	13.754(5)	5.806(6)	9.563(3)	–	94.56(3)	–	$P2_1/n$	[34]
Ransomite	$Cu[Fe^{3+}(SO_4)_2(H_2O)]_2(H_2O)_4$	4.811(2)	16.217(4)	10.403(2)	–	93.02(3)	–	$P2_1/c$	[35]
Krausite	$K[Fe^{3+}(SO_4)_2(H_2O)]$	7.908(10)	5.152(5)	8.988(10)	–	102.75(8)	–	$P2_1/m$	[36]

Table III. (continued)

Mineral	Formula	*a* [Å]	*b* [Å]	*c* [Å]	α [°]	β [°]	γ [°]	S.G.	Ref.
*Botryogen	$Mg_2[Fe^{3+}_2(SO_4)_4(OH)_2(H_2O)_2](H_2O)_{10}$	10.47	17.83	7.11	–	100.3	–	$P2_1/n$	–
Zincbotryogen	$Zn_2[Fe^{3+}_2(SO_4)_4(OH)_2(H_2O)_2](H_2O)_{10}$	10.526(4)	17.872(7)	7.136(4)	–	100.13(4)	–	$P2_1/n$	[37]

References: [1] Bacon & Curry (1962); [2] Baur & Rolin (1972); [3] Burns *et al.* (1991); [4] Protas & Gindt (1976); [5] Fanfani *et al.* (1971); [6] Borene (1970); [7] Giuseppetti & Tadini (1984); [8] Hansen (1960); [9] Sabelli (1985b); [10] Scordari (1981a); [11] Giacovazzo *et al.* (1976a); [12] Bachmann & Zemann (1961);[13] Süsse (1968a); [14] Scordari (1978); [15] Hawthorne & Ferguson (1977); [16] Hawthorne & Ferguson (1975b); [17] Brotherton *et al.* (1974); [18] Catti *et al.* (1977); [19] Sturman & Dunn (1980), cell refined in reduced cell orientation; [20] Fanfani *et al.* (1970b); [21] Hawthorne (1983b); [22] Scordari (1981b); [23] Moore & Araki (1974b); [24] Moore & Ito (1978); [25] Moore & Araki (1977a); [26] Wan *et al.* (1978); [27] Balko & Bakakin (1975); [28] Hofmeister & Tillmanns (1978); [29] Donaldson & Barnes (1955); [30] Moore *et al.* (1975); [31] Nichols (1966); [32] Cocco *et al.* (1967); [33] Shen & Moore (1982); [34] Fanfani & Zanazzi (1968); [35] Wood (1970); [36] Graeber *et al.* (1965); [37] Süsse (1968b)

[1] structure not definitively established

Table IV. $MT\phi_n$ **and** $M(TO_4)_2\phi_n$ **minerals based on infinite sheets**

Mineral	Formula	*a* [Å]	*b* [Å]	*c* [Å]	α [°]	β [°]	γ [°]	S.G.	Ref.
octahedral-tetrahedral corner sharing and octahedral-octahedral corner sharing linkages									
Newberyite	$[Mg(PO_3OH)(H_2O)_3]$	10.215(2)	10.681(2)	10.014(2)	–	–	–	*Pbca*	[1]
Minyulite	$K[Al_2(PO_4)_2F(H_2O)_4]$	9.337(5)	9.740(5)	5.522(3)	–	–	–	*Pba*2	[2]
Gordonite	$Mg[Al_2(PO_4)_2(OH)_2(H_2O)_2]\cdot(H_2O)_4\cdot 2(H_2O)$	5.24	10.49	6.96	107.4	111.1	72.4	$P\bar{1}$	–
*Laueite	$Mn^{2+}[Fe^{3+}_2(PO_4)_2(OH)_2(H_2O)_2]\cdot(H_2O)_4\cdot 2(H_2O)$	5.28	10.66	7.14	107.9	111.0	71.1	$P\bar{1}$	[3]
Paravauxite	$Fe^{2+}[Al_2(PO_4)_2(OH)_2(H_2O)_2]\cdot(H_2O)_4\cdot 2(H_2O)$	5.233	10.541	6.962	106.9	110.8	72.1	$P\bar{1}$	[4]
Sigloite	$(Fe^{3+},Fe^{2+})[Al_2(PO_4)_2(OH)_2(H_2O)_2](H_2O, OH)_4\cdot 2(H_2O)$	5.26	10.52	7.06	106.97	111.50	69.50	$P\bar{1}$	[5]
Ushkovite	$Mg[Fe^{3+}_2(PO_4)_2(OH)_2(H_2O)_2]\cdot(H_2O)_4\cdot 2(H_2O)$	5.20	10.7	7.14	108.6	106.9	72.7	$P\bar{1}$	–
Stewartite	$Mn^{2+}[Fe^{3+}_2(PO_4)_2(OH)_2(H_2O)_2]\cdot(H_2O)_4\cdot 2(H_2O)$	10.398(2)	10.672(3)	7.223(3)	90.10(3)	109.10(2)	71.83(2)	$P\bar{1}$	[6]
Pseudolaueite	$Mn^{2+}[Fe^{3+}(PO_4)(OH)(H_2O)]_2(H_2O)_4\cdot 2(H_2O)$	9.647	7.428	10.194	–	104.63	–	$P2_1/a$	[7]
*Strunzite	$Mn^{2+}[Fe^{3+}(PO_4)(OH)(H_2O)]_2(H_2O)_4$	10.228(5)	9.837(5)	7.284(5)	90.17(5)	98.44(5)	117.44(5)	$P\bar{1}$	[8]
Ferrostrunzite	$Fe^{2+}[Fe^{3+}(PO_4)(OH)(H_2O)]_2(H_2O)_4$	10.23(2)	9.77(3)	7.37(1)	89.28(2)	98.3(1)	117.3(2)	$P\bar{1}$	–
Metavauxite	$Fe^{2+}[Al(PO_4)(OH)(H_2O)]_2(H_2O)_6$	10.22	9.56	6.94	–	97.9	–	$P2_1/c$	[9]

Table IV. (continued)

Mineral	Formula	*a* [Å]	*b* [Å]	*c* [Å]	α [°]	β [°]	γ [°]	S.G.	Ref.
	octahedral-tetrahedral corner sharing and octahedral-octahedral edge sharing linkages								
Tsumcorite	$Pb[(Zn,Fe^{3+})(AsO_4)(H_2O,OH)]_2$	9.124(3)	6.329(2)	7.577(2)	–	115.28(3)	–	*C2/m*	[10]
Bermanite	$Mn^{2+}[Mn^{3+}(PO_4)(OH)]_2(H_2O)_4$	5.446(3)	19.25(1)	5.248(3)	–	110.29(4)	–	$P2_1$	[11]
Foggite	$Ca[Al(PO_4)(OH)_2](H_2O)$	9.270(2)	21.324(7)	5.190(2)	–	–	–	$A2_122$	[12]
Arthurite	$Cu[Fe^{3+}(AsO_4)(OH)]_2(H_2O)_4$	10.189(2)	9.649(2)	5.598(1)	–	92.16(2)	–	$P2_1/c$	[13]
Earlshannonite	$Mn^{2+}[Fe^{3+}(PO_4)(OH)]_2(H_2O)_4$	9.910(13)	9.669(8)	5.455(9)	–	93.95(9)	–	$P2_1/c$	–
Ojuelaite	$Zn[Fe^{3+}(AsO_4)(OH)]_2(H_2O)_4$	10.247(6)	9.665(5)	5.569(4)	–	94.37	–	$P2_1/c$	–
*Whitmoreite	$Fe^{2+}[Fe^{3+}(PO_4)(OH)]_2(H_2O)_4$	10.00(2)	9.73(2)	5.471(8)	–	93.8(1)	–	$P2_1/c$	[14]
Krautite	$[Mn^{2+}(AsO_3OH)(H_2O)]$	8.012(2)	15.956(4)	6.801(2)	–	96.60(3)	–	$P2_1$	[15]
Fluckite	$[CaMn^{2+}(AsO_3OH)_2(H_2O)_2]$	8.459(2)	7.613(1)	6.968(1)	82.21(1)	98.25(1)	95.86(2)	$P\bar{1}$	[16]
Cobaltkoritnigite	$[Co(AsO_3OH)(H_2O)]$	7.95	15.83	6.67	90.9	96.6	90	$P\bar{1}$	–
*Koritnigite	$[Zn(AsO_3OH)(H_2O)]$	7.948(2)	15.829(5)	6.668(2)	90.86(2)	96.56(2)	90.05(2)	$P\bar{1}$	[17]
Kaolinite	$[Al_2Si_2O_5(OH)_4]$	5.139	8.932	7.371	91.6	104.8	89.9	*C*1	[18]
Dickite	$[Al_2Si_2O_5(OH)_4]$	5.15	8.94	14.763	–	103.58	–	*Cc*	[19]
Nacrite	$[Al_2Si_2O_5(OH)_4]$	8.909	5.146	15.697	–	113.70	–	*Cc*	[20]
Endellite [1)]	$[Al_2Si_2O_5(OH)_4](H_2O)_2$	5.15	8.92	d_{001}~10.0	–	–	–	–	–
Halloysite [2)]	$[Al_2Si_2O_5(OH)_4]$	5.14	8.90	d_{001}~7.2	–	–	–	–	–
Arseniosiderite	$Ca_2[Fe_3^{3+}(AsO_4)_3O_2](H_2O)_3$	17.76(4)	19.53	11.30	–	96.0	–	*Aa*	–
Kolfanite	$Ca_2[Fe_3^{3+}(AsO_4)_3O_2](H_2O)_2$	17.86	19.66	11.11	–	96.0	–	*Aa*	–
*Mitridatite	$Ca_2[Fe_3^{3+}(PO_4)_3O_2](H_2O)_3$	17.553(2)	19.354(3)	11.248(2)	–	95.84(1)	–	*Aa*	[21]
Robertsite	$Ca_2[Mn_3^{3+}(PO_4)_3O_2](H_2O)_3$	17.36(2)	19.53(5)	11.30(3)	–	96.0	–	*Aa*	–
Rhomboclase	$(H_5O_2)[Fe^{3+}(SO_4)_2(H_2O)_2]$	9.724(4)	18.333(9)	5.421(4)	–	–	–	*Pnma*	[22]
Olmsteadite	$KFe_2^{2+}[Nb(PO_4)_2O_2](H_2O)_2$	7.512(1)	10.000(3)	6.492(2)	–	–	–	$Pb2_1m$	[23]

Table IV. (continued)

Mineral	Formula	*a* [Å]	*b* [Å]	*c* [Å]	α [°]	β [°]	γ [°]	S.G.	Ref.
Brianite	$Na_2Ca[Mg(PO_4)_2]$	13.36(5)	5.23(2)	9.13(3)	–	91.2(2)	–	$P2_1/a$	[24]
*Merwinite	$Ca_3[Mg(SiO_4)_2]$	13.25(2)	5.293(9)	9.33(2)	–	91.9(2)	–	$P2_1/a$	[25]
Yavapaiite	$K[Fe^{3+}(SO_4)_2]$	8.152(5)	5.153(4)	7.877(5)	–	94.90(7)	–	$C2/m$	[26]
Bafertisite	$BaFe^{2+}[Ti(Si_2O_7)O_2]$	10.60	13.64	12.47	–	119.5	–	$C2/m$	[27]
Pyrophyllite	$[AlSi_2O_5(OH)]$	5.161(2)	8.958(2)	9.351(2)	91.03(2)	100.37(2)	89.75(2)	$C\bar{1}$	[28]
Dioctahedral micas	$(M^+,M^{2+})[(M^{3+},M^{2+})(Si,Al)_2O_5(OH)]_2$	~5.2	~9.0	~10.0	–	~100.0	–	$C2/m$	[29]
Ephesite	$NaLi[Al(Si,Al)_2O_5(OH)]_2$	5.27	9.13	10.25	–	100.0	–	$C2/m$	–
Dioctahedral smectites	$(M^+,H_2O)[(M^{3+},M^{2+})(Si,Al)_2O_5(OH)]_2$	~5.2	~9.0	variable	–	–	–	–	–
Brammallite	$(M^+,H_2O)_x\ [(Al,Mg,Fe)(Si,Al)_2O_5(OH)]_2$	–	–	–	–	–	–	–	–
Hydromica	$(M^+,H_2O)_x[Al(Si,Al)_2O_5(OH)]_2$	–	–	–	–	–	–	–	–
*Illite	$(M^+,H_2O)_x\ [(Al,Mg,Fe)(Si,Al)_2O_5(OH)]_2$	5.2	9.0	9.95	–	95.5	–	$C2/c$	–
Goldichite	$K_2[Fe_2^{3+}(SO_4)_4(H_2O)_4](H_2O)_4$	10.387(6)	10.486(6)	9.086(5)	–	101.68(7)	–	$P2_1/c$	[31]

References: [1] Sutor (1967); [2] Kampf (1977); [3] Moore (1965); [4] Baur (1969a); [5] Hawthorne (1988); [6] Moore & Araki (1974a); [7] Baur (1969b); [8] Fanfani *et al.* (1978); [9] Baur & Rama Rao (1967); [10] Tillmanns & Gebert (1973); [11] Kampf & Moore (1976); [12] Moore *et al.* (1975); [13] Keller & Hess (1978); [14] Moore *et al.* (1974); [15] Catti & Franchini-Angela (1979); [16] Catti *et al.* (1980); [17] Keller *et al.* (1980); [18] Zvyagin (1960); [19] Newnham (1961); [20] Blount *et al.* (1969); [21] Moore & Araki (1977b); [22] Mereiter (1974); [23] Moore *et al.* (1976); [24] Moore (1975b); [25] Moore & Araki (1972); [26] Graeber & Rosenzweig (1971); [27] Ya-hsien *et al.* (1963); [28] Wardle & Brindley (1972); [29] Bailey (1980); [30] Toraya *et al.* (1977); [31] Graeber & Rosenzweig (1971)

1) halloysite-10Å

2) halloysite-7Å

Table V. $MT\phi_n$ and $M(T_2)\phi_n$ minerals based on infinite frameworks

Mineral	Formula	*a* [Å]	*b* [Å]	*c* [Å]	β [°]	S.G.	Ref.
Bonattite	$[Cu(SO_4)(H_2O)_3]$	5.592(5)	13.029(10)	7.341(6)	97.1	*Cc*	[1]
Kolbeckite	$[Sc(PO_4)(H_2O)_2]$	5.44	10.22	8.92	~90	$P2_1/n$	–
*Metavariscite	$[Al(PO_4)(H_2O)_2]$	5.178(2)	9.514(2)	8.454(2)	90.35(2)	$P2_1/n$	[2]
Phosphosiderite	$[Fe^{3+}(PO_4)(H_2O)_2]$	5.30	9.77	8.73	90.6	$P2_1/n$	[3]
Mansfieldite	$[Al(AsO_4)(H_2O)_2]$	10.10	8.79	9.80	–	*Pbca*	–
*Scorodite	$\{Fe^{3+}(AsO_4)(H_2O)_2]$	10.278(2)	8.937(1)	9.996(2)	–	*Pbca*	[4], [5]
Strengite	$[Fe^{3+}(PO_4)(H_2O)_2]$	10.122(1)	8.723(1)	9.886(2)	–	*Pbca*	–
Variscite	$[Al(PO_4)(H_2O)_2]$	9.822(3)	8.561(3)	9.630(3)	–	*Pbca*	[6]
Kainite	$K_4[Mg_4(SO_4)_4(H_2O)_{11}]Cl_4$	19.72(2)	16.23(1)	9.53(1)	94.92(8)	*C*2/*m*	[7]
*Amblygonite [1)]	$Li[Al(PO_4)F]$	6.644(1)	7.744(2,	6.910(1)	117.33(2)	$C\bar{1}$	[8], [10]
Montebrasite [2)]	$Li[Al(PO_4)OH]$	6.713(1)	7.708(1)	7.019(1)	117.93(1)	$C\bar{1}$	[9], [10]
Natromontebrasite	$Na[Al(PO_4)(OH)]$	–	–	–	–	–	–
Tavorite	$Li[Fe^{3+}(PO_4)OH]$	–	–	–	–	–	–
Durangite	$Na[Al(AsO_4)F]$	6.69	8.66	7.27	115.8	–	–
Isokite	$Ca[Mg(PO_4)F]$	6.52(5)	8.75(5)	7.16	109.5	*C*2/*c*	–
Lacroixite	$Na[Al(PO_4)F]$	6.411(2)	8.210(2)	6.883(2)	115.43(3)	*C*2/*c*	[11]
Malayaite	$Ca[Sn^{4+}(SiO_4)O]$	6.66	8.906	7.149	113.3	*C*2/*c*	[12]
Panasqueiraite	$Ca[Mg(PO_4)OH]$	6.535(3)	8.753(4)	6.919(4)	112.33(4)	*C*2/*c*	–
Tilasite	$Ca[Mg(AsO_4)F]$	6.688(2)	8.944(2)	7.560(2)	121.17(2)	*Cc*	[13]
Titanite-$P2_1/c$	$Ca[Ti(SiO_4)O]$	6.562(1)	8.714(3)	7.068(1)	113.83	$P2_1/c$	[14]
*Titanite-*C*2/*c*	$Ca[(Ti,Al,Fe)(SiO_4)O]$	6.539(2)	8.681(4)	7.050(3)	113.90(3)	*C*2/*c*	[15], [16]
Dwornikite	$[Ni(SO_4)(H_2O)]$	6.839	7.582	7.474	117.85	*C*2/*c*	–
Gunningite	$[Zn(SO_4)(H_2O)]$	6.936(1)	7.587(1)	7.508(1)	116.25(1)	*C*2/*c*	–
*Kieserite	$[Mg(SO_4)(H_2O)]$	6.912(2)	7.624(2)	7.642(2)	117.70(2)	*C*2/*c*	[17]
Poitevinite	$[Cu(SO_4)(H_2O)]$	7.176(10)	7.426(10)	7.635(10)	116.15(3)	*C*2/*c*	–
Szmikite	$[Mn^{2+}(SO_4)(H_2O)]$	7.120(1)	7.666(1)	7.766(1)	115.85(1)	*C*2/*c*	–
Szomolnokite	$[Fe^{2+}(SO_4)(H_2O)]$	7.123	7.468	7.624	115.9	*C*2/*c*	–

Table V. (continued)

Mineral	Formula	*a* [Å]	*b* [Å]	*c* [Å]	β [°]	S.G.	Ref.
Adelite	$Ca[Mg(AsO_4)(OH)]$	7.525	8.895	5.850	–	$P2_12_12_1$	–
Austinite	$Ca[Zn(AsO_4)(OH)]$	7.506(6)	9.046(6)	5.932(6)	–	$P2_12_12_1$	–
*Conichalcite	$Ca[Cu(AsO_4)(OH)]$	7.40	9.21	5.84	–	$P2_12_12_1$	[18]
Duftite	$Pb[Cu(AsO_4)(OH)]$	7.778(4)	9.207(3)	6.000(5)	–	$P2_12_12_1$	–
Gabrielsonite	$Pb[Fe^{2+}(AsO_4)(OH)]$	7.86	8.62	5.98	–	$P2_12_12_1$	–
Vuagnatite	$Ca[Al(SiO_4)(OH)]$	7.055(6)	8.542(7)	5.683(5)	–	$P2_12_12_1$	[19]
Arsendescloizite	$Pb[Zn(AsO_4)OH]$	7.634	9.358	6.075	–	*Pnam*	–
Calciovolborthite	$Ca[Cu(VO_4)OH]$	7.45	9.26	5.91	–	*Pnam*	–
Čechite	$Pb[Fe^{2+}(VO_4)OH]$					*Pnam*	–
*Descloizite	$Pb[Zn(VO_4)OH]$	7.593(2)	9.416(2)	6.057(1)	–	*Pnam*	[20]
Mottramite	$Pb[Cu(VO_4)OH]$	7.682	9.278	6.034	–	*Pnam*	–
Pyrobelonite	$Pb[Mn(VO_4)OH]$	7.62	9.47	6.17	–	*Pnam*	–
Jagowerite $^{3)}$	$Ba[Al(PO_4)(OH)]_2$	6.049(2)	6.964(3)	4.971(2)	86.06(4)	$P\bar{1}$	[21]
Melonjosephite	$Ca[(Fe^{2+}Fe^{3+})(PO_4)_2(OH)]$	9.542(1)	10.834(1)	6.374(1)	–	*Pnam*	[22]
Bertossaite	$CaLi_2[Al(PO_4)(OH)]_4$	11.48(1)	15.73(2)	7.23(1)	–	*I*aa*	–
*Palermoite	$SrLi_2[Al(PO_4)(OH)]_4$	11.556(5)	15.847(7)	7.315(4)	–	*Imcb*	[23]
Carminite	$Pb[Fe^{3+}(AsO_4)(OH)]_2$	12.295(5)	16.595(5)	7.580(5)	–	*Amaa*	[24]
Leucophosphite	$K[Fe_2^{3+}(PO_4)_2(OH)(H_2O)](H_2O)_2$	9.782(9)	9.658(9)	9.751(9)	102.2(1)	$P2_1/n$	[25]
*Alluaudite	$(Na,Ca)[Fe^{2+}(Mn,Fe^{2+},Fe^{3+},Mg)_2(PO_4)_3]$	11.027(2)	12.533(4)	6.404(1)	97.5(1)	*I2/a*	[26]
Hagendorfite	$(Na,Ca)[Mn^{2+}(Fe^{2+},Mg,Fe^{3+})_2(PO_4)_3]$	10.933	12.594	6.515	97.98	*I2/a*	–
Maghagendorfite	$Na[Mn^{2+}(Mg,Fe^{2+},Fe^{3+})_2.(PO_4)_3]$	–	–	–	–	–	–
Varulite	$(Na,Ca)[Mn^{2+}(Mn,Fe^{2+},Fe^{3+})_2(PO_4)_3]$	–	–	–	–	–	–
Barbosalite	$Fe^{2+}[Fe^{3+}(PO_4)(OH)]_2$	7.25(2)	7.46(2)	7.49(2)	120.3(1)	$P2_1/c$	[27]
*Lazulite	$Mg[Al(PO_4)(OH)]_2$	7.144(1)	7.278(1)	7.228(1)	120.51(1)	$P2_1/c$	[27]
Scorzalite	$Fe^{2+}[Al(PO_4)(OH)]_2$	7.15(2)	7.31(2)	7.25(2)	120.7(1)	$P2_1/c$	[27]
Lawsonite	$Ca[Al_2(Si_2O_7)(OH)_2](H_2O)$	8.795(3)	5.847(1)	13.142(6)	–	*Ccmm*	[28]

Table V. (continued)

Mineral	Formula	*a* [Å]	*b* [Å]	*c* [Å]	β [°]	S.G.	Ref.
Dioptase	$[Cu_6(Si_6O_{18})(H_2O)_6]$	14.566	14.566	7.778	–	$R\bar{3}$	[29]
Veszelyite	$[Cu_2(ZnPO_4(OH))(OH)_2(H_2O)_2]$	9.828(3)	10.224(3)	7.532(2)	103.18(2)	*P*2₁/*a*	[30]
Holdenite	$[Mn_6^{3+}(Zn_3As_2SiO_{12}(OH)_8)]$	11.99(1)	31.46(4)	8.697(6)	–	*Abma*	[31]
Ferropumpellyite	$Ca_2[Al_2(Al,Fe^{2+})(SiO_4)(Si_2O_7)(OH)_2(OH,H_2O)]$	–	–	–	–	–	–
Julgoldite	$Ca_2[Fe_2^{3+}(Fe^{3+},Fe^{2+})(SiO_4)(Si_2O_7)(OH)_2(OH,H_2O)]$	8.922(4)	6.081(3)	19.432(9)	97.60(6)	*A*2/*m*	[32]
*Pumpellyite	$Ca_2[Al_2(Al,Mg)(SiO_4)(Si_2O_7)(OH)_2(OH,H_2O)]$	8.83(1)	5.90(1)	19.17(2)	97.12(8)	*A*2/*m*	[33]
Shuiskite	$Ca_2[Cr_2(Al,Mg)(SiO_4)(Si_2O_7)(OH)_2(OH,H_2O)]$	8.897	5.843	19.41	98.0	*A*2/*m*	–
Ardennite	$(Mn,Ca)_4[Al_4(Mg,Al)_2(SiO_4)_2(Si_3O_{10})(As,VO_4)(OH)_6]$	8.713(1)	5.811(1)	18.521(1)	–	*Pnmm*	[34]
Tiragalloite	$[Mn_4(AsSi_3O_{12}(OH))]$	6.66(1)	19.92(2)	7.67(1)	95.7(1)	*P*2₁/*n*	[35]
Medaite	$[Mn_6(VSi_5O_{18}(OH))]$	6.712(1)	28.948(8)	7.578(2)	95.4(2)	*P*2₁/*n*	[36]
Zoisite	$Ca_2[Al_3(SiO_4)(Si_2O_7)O(OH)]$	16.212(8)	5.559(6)	10.036(4)	–	*Pnma*	[37]
Allanite-(Ce)	$(Ce,Ca)_2[Al_3(SiO_4)(Si_2O_7)O(OH)]$	8.927(8)	5.761(6)	10.150(9)	114.77(5)	*P*2₁/*m*	[38]
Allanite-(Y)	$(Y,Ce,Ca)_2[Al_3(SiO_4)(Si_2O_7)O(OH)]$	–	–	–	–	*P*2₁/*m*	–
Clinozoisite	$Ca_2[Al_3(SiO_4)(Si_2O_7)O(OH)]$	8.879(5)	5.583(5)	10.155(6)	115.50(5)	*P*2₁/*m*	[37]
*Epidote	$Ca_2[Fe_3^{3+}(SiO_4)(Si_2O_7)O(OH)]$	8.914(9)	5.640(3)	10.162(9)	115.4(2)	*P*2₁/*m*	[38]
Hancockite	$(Pb,Ca)_2[Al_3(SiO_4)(Si_2O_7)O(OH)]$	8.958(20)	5.665(10)	10.304(20)	114.4(4)	*P*2₁/*m*	[38]
Piemontite	$Ca_2[Mn_3^{3+}(SiO_4)(Si_2O_7)O(OH)]$	8.878(10)	5.692(5)	10.201(10)	115.4(2)	*P*2₁/*m*	[39]
*Orthoenstatite	$[MgSiO_3]$	18.216(2)	8.813(2)	5.179(1)	–	*Pbca*	[40]
Hypersthene	$[(Mg,Fe^{2+})(SiO_3)]$	18.313(3)	8.912(2)	5.210(1)	–	*Pbca*	[41]
Orthoferrosilite	$[Fe^{2+}SiO_3]$	18.418(2)	9.078(1)	5.237(1)	–	*Pbca*	[42]
*Clinoenstatite	$[MgSiO_3]$	9.605(1)	8.813(1)	5.166(1)	108.46(1)	*P*2₁/*c*	[43]
Clinohypersthene	$[(Mg,Fe^{2+})SiO_3]$	9.691(3)	8.993(3)	5.231(2)	108.61(2)	*P*2₁/*c*	[44]
Clinoferrosilite	$[Fe^{2+}SiO_3]$	9.709(1)	9.087(1)	5.228(1)	108.43(1)	*P*2₁/*c*	[45]
Planchéite	$[Cu_8Si_8O_{22}(OH)_4(H_2O)]$	19.043(3)	20.129(5)	5.269(1)	–	*Pcnb*	[46]

Table V. (continued)

Mineral	Formula	*a* [Å]	*b* [Å]	*c* [Å]	β [°]	S.G.	Ref.
Keldyshite 4)	$(Na,H_3O)[ZrSi_2O_7]$	9.0(1)	5.34(2)	6.96(3)	116(1)	$P\bar{1}$	[47]
Parakeldyshite 5)	$Na[ZrSi_2O_7]$	9.31	5.42	6.66	115.3	$P\bar{1}$	[47]
Nenadkevichite	$Na_2[NbSi_2O_6(OH)](H_2O)_2$	7.408(2)	14.198(3)	7.148(2)	–	*Pbam*	[48]
Labuntsovite	$K_2[TiSi_2O_6(OH)](H_2O)_2$	14.18	13.70	7.74	117	*C2/m*	[49]
Batisite	$Na_2Ba[TiSi_2O_6O]_2$	10.40	13.85	8.10	–	*Ima*2	[50]
Shcherbakovite	$K_2Ba[(Ti,Nb)Si_2O_6O]_2$	10.55	13.92	8.10	–	*Ima*2	–
Alkali pyroxenes	$M^+[M^{3+}Si_2O_6]$	~9.7	~8.8	~5.25	~107.5	*C2/c*	[51]
Calcic pyroxenes	$Ca[M^{2+}Si_2O_6]$	~9.8	~8.9	~5.24	~105.5	*C2/c*	[51]
Låvenite	$(Na,Ca)_3[ZrSi_2O_7O]F$	10.83(1)	9.98(1)	7.174(5)	108.1(1)	$P2_1/a$	[52]
Wöhlerite	$Na_2Ca_4[ZrNb(Si_2O_7)_2O_2]F$	10.823(3)	10.244(3)	7.290(2)	109.00(4)	$P2_1$	[53]
Rosenbuschite 6)	$(Ca,Na)_2[Zr_2Ti_2(Si_2O_7)_4O_2F_2]F_4$	10.12(5)	11.29(5)	7.23(3)	99.7(5)	$P\bar{1}$	[54]

References: [1] Zahrobsky & Baur (1968); [2] Kniep & Mootz (1973); [3] Moore (1966); [4] Kitahama *et al.* (1975); [5] Hawthorne (1976); [6] Kniep *et al.* (1977); [7] Robinson *et al.* (1972); [8] Simonov & Belov (1958); [9] Baur (1959); [10] Groat *et al.* (1990); [11] Pajunen & Lahti (1985); [12] Higgins & Ribbe (1977); [13] Bladh *et al.* (1972); [14] Speer & Gibbs (1976); [15] Mongiorgi & Riva di Sanseverino (1968); [16] Hawthorne *et al.* (1991); [17] Hawthorne *et al.* (1987); [18] Qurashi & Barnes (1963); [19] McNear *et al.* (1976); [20] Hawthorne & Faggiani (1979); [21] Meagher *et al.* (1974); [22] Kampf & Moore (1977); [23] Moore & Araki (1975); [24] Finney (1963); [25] Moore (1972); [26] Moore (1971); [27] Lindberg & Christ (1959); [28] Baur (1978); [29] Ribbe *et al.* (1977); [30] Ghose *et al.* (1974); [31] Moore & Araki (1977c); [32] Allmann & Donnay (1973); [33] Galli & Alberti (1969); [34] Donnay & Allmann (1968); [35] Gramaccioli et al (1979); [36] Gramaccioli *et al.* (1981); [37] Dollase (1968); [38] Dollase (1971); [39] Dollase (1969); [40] Hawthorne & Ito (1977); [41] Ghose *et al.* (1975); [42] Sueno *et al.* (1976); [43] Ohashi & Finger (1976); [44] Smyth (1974); [45] Burnham (1966); [46] Evans & Mrose (1977); [47] Khalilov *et al.* (1977); [48] Perrault *et al.* (1973); [49] Golavastikov (1974); [50] Nikitin & Belov (1962); [51] Cameron & Papike (1981); [52] Mellini (1981); [53] Mellini & Merlino (1979); [54] Shibaeva *et al.* (1964).

1) $\alpha = 90.35(2)$, $\gamma = 91.01(2)$

2) $\alpha = 91.31(1)$, $\gamma = 91.77(1)$

3) $\alpha = 116.51(4)$, $\gamma = 112.59(3)$

4) $\alpha = 92(1)$, $\gamma = 88(1)$

5) $\alpha = 94.3$, $\gamma = 89.6$

6) $\alpha = 91.3(5)$, $\gamma = 111.8(5)$